

DISSERTATION

OPTIMIZING OPERATION AND DESIGN OF AQUIFER STORAGE AND RECOVERY
(ASR) WELLFIELDS

Submitted by

Abdulaziz Alqahtani

Department of Civil and Environmental Engineering

In partial fulfillment of the requirements

For the Degree of Doctor of Philosophy

Colorado State University

Fort Collins, Colorado

Fall 2019

Doctoral Committee:

Adviser: Tom Sale

Neil Grigg

Ryan Bailey

Michael Ronayne

Copyright by Abdulaziz Alqahtani 2019

All Rights Reserved

ABSTRACT

OPTIMIZING OPERATION AND DESIGN OF AQUIFER STORAGE AND RECOVERY (ASR) WELLFIELDS

Sustained production of groundwater from wells in wellfields can lead to declining water levels at production wells and concerns regarding the sustainability of groundwater resources.

Furthermore, minimizing energy consumption associated with pumping groundwater is a growing concern. Aquifer Storage and Recovery (ASR) is a promising approach for maintaining water levels in wells, increasing the sustainability of groundwater resources, and minimize energy consumption during groundwater pumping. Therefore, studying the importance of ASR in sustaining water levels and minimizing energy consumption is critical.

In the first part of this dissertation, an analytical model relying on superposition of the Theis equation is used to resolve water levels in 40 wells in three vertically stacked ASR wellfields. Fifteen years of dynamic recovery/recharge data are used to obtain aquifer and well properties. Estimated aquifer and well properties are used to predict water levels at production well. Close agreement between modeled and observed water levels support the validity of the analytical model for estimating water levels at ASR wells. During the study period, 45 million m³ of groundwater is produced and 11 million m³ is recharged leading to a net withdrawal of 34 million m³ of groundwater. Rates of changes in recoverable water levels in wells in the Denver, Arapahoe and Laramie-Fox Hill Aquifers are 0.20, -0.91, and -3.48 m per year, respectively. To quantify the benefits of recharge, the analytical model is applied to predicting water levels at wells absent the historical recharge. Results indicate that during recovery and no-flow periods, recharge has increased water levels at wells up to 60 m compared to the no-recharge scenario.

On average, the recharge increased water levels at wells during the study period by 3, 4, and 11 m in the Denver, Arapahoe, and Laramie Fox-Hills Aquifers, respectively. Overall, the analytical model is a promising tool for advancing ASR wellfields and ASR can be a viable approach to sustaining water levels in wells in wellfields.

In the second part of this dissertation, a simulation-optimization model (ASRSOM) is developed to optimize ASR wellfield operations. ASRSOM combines an analytical hydraulic model and a numerical optimization model to optimize wellfield operations. The objective function used to minimize energy consumption φ (L^4) is the temporal integral of the products of temporally varying total dynamic head values and pumping rates. Comparison of ASRSOM results to work by others for idealized aquifer operations supports the validity of ASRSOM. Four scenarios were simulated to evaluate the role that optimization of operations and aquifer recharge play in reducing the energy required to lift groundwater out of aquifer. A 10-year study period is considered using data from a municipal ASR wellfield. Optimization decreased φ by 19.6%, which yields an estimated reduction of 2,179 MW hours of power and 1,541 metric tons of atmospheric carbon. For the condition considered, recharge reduced power by 1%. The limited benefit of recharge is attributed to the small recharge volume in the case study and the short duration of the analysis. Additional opportunities to address economic and environmental impacts associated with lifting groundwater out aquifer include optimizing the position of wells and factors controlling total pumping head.

In the third part of this dissertation, the sensitivity of well-spacing in ASR wellfields to critical parameters is studied. The parameters studied are aquifer transmissivity and storativity, wells flowrate and the frequency of recharge and recovery. It has been found that larger well-spacing are appropriate for lower transmissivity and storativity, and larger wells flowrate and frequency.

More work is needed to fully understand the optimal well-spacing of wells in ASR wellfields associated with more realistic storage and recovery schedules, and more complex wellfields.

Overall, work supported the possibility that wells in ASR wellfields can be spread more closely than wells in conventional production wellfields.

TABLE OF CONTENTS

ABSTRACT.....	ii
LIST OF TABLES.....	vi
LIST OF FIGURES.....	vii
Chapter 1 - Introduction.....	1
1.1 Research motivation.....	1
1.2 Hypotheses.....	7
1.3 Contents.....	7
Chapter 2 - Demonstration of Sustainable Development of Groundwater through Aquifer Storage and Recovery (ASR).....	9
2.1 Introduction.....	10
2.2 Methods.....	13
2.3 Results and Discussion.....	21
2.4 Summary.....	32
Chapter 3 - Optimizing ASR Wellfield Operations to Minimize Energy Consumption.....	34
3.1 Introduction.....	35
3.2 Methods.....	37
3.3 Results and discussion.....	47
3.4 Summary and conclusion.....	55
Chapter 4 - Factors Controlling Well-Spacing in ASR Wellfields.....	57
4.1 Introduction.....	57
4.2 Methods.....	59
4.3 Results and discussion.....	65
4.4 Summary and Conclusion.....	71
Chapter 5 - Summary and Conclusion.....	73
References.....	77
Appendix A.....	87

LIST OF TABLES

Table 1: Summary of the time periods used to estimate aquifer and well properties	19
Table 2: Well loss coefficients during recharge and recovery cycles for wells in the Laramie Fox-Hills Aquifer	25
Table 3: Residuals - mean and standard deviation for the three aquifers	28
Table 4: NSCE for Laramie Fox-Hills Aquifer wells	29
Table 5: Summary of the four scenarios simulated in this paper	44
Table 6: Wellhead elevation and calibrated properties for all wells in the LFH Aquifer	47
Table 7: Cumulative ϕ values for the four scenarios (scenarios number in parentheses)	54
Table 8: Seven scenarios simulated in this study. Differences from base scenarios are shaded. .	63
Table 9: Parameters used as inputs for the cost and hydraulic models and their values.	65
Table 10: Pipe sizes and cost for different flowrates. Pipe size based on maximum 5 ft/sec flow. Pipe unit cost represent total cost include costs involved in installing one unit of piping	65

LIST OF FIGURES

Fig. 1: Flow chart illustrating the parameter estimation workflow. Shaded boxes represent the key steps of parameter. Adapted from (Lewis et al. 2016).	5
Fig. 2: Main components of drawdown in groundwater wells.	6
Fig. 3: Location of Centennial Water & Sanitation District wells. The red line on state of Colorado inset map indicates the extent of Denver Basin Aquifer system. Well names are provided for the Laramie-Fox Hills (LFH) wells.	15
Fig. 4: Laramie Fox Hills Well LFH-11: a) raw data, and b) parsed data.	18
Fig. 5: Model (squares) and 72-hour aquifer test (diamonds) T and S values for the Denver, Arapahoe, and Laramie-Fox Hills Aquifers.	22
Fig. 6: Contoured recoverable water level (h_0) values for the Laramie Fox Hills Aquifer indicate groundwater flow to the north-northeast and a gradient of 0.01.	24
Fig. 7: Observed water levels (black dots), and modeled water levels for ASR scenario (red solid line) for representative wells in the Larimer Fox-Hills Aquifer.	26
Fig. 8: a) Modeled versus observed water levels for the Laramie-Fox Hills wells; b) histogram of residuals.	28
Fig. 9: Observed (black dots), modeled with recharge (red solid line), and modeled without recharge (blue solid line) water levels for representative wells in LFH aquifer.	30
Fig. 10: Differences between modeled water levels with and without ASR during recovery and no-flow periods.	31
Fig. 11: Average of daily water level difference at wells with and without recharge for each aquifer (blue); all time average of water level difference at wells with and without recharge for each aquifer (red).	32
Fig. 12: Illustration of model workflow	42
Fig. 13: Location of Highlands Ranch wells in the Laramie-Fox Hills (LFH) Aquifer. The red line on state of Colorado inset map indicates the extent of the Denver Basin Aquifer system.	45
Fig. 14: Total daily wellfield stresses for all wells in the LFH Aquifer (recovery (+)/recharge (-)). Stresses prior to 2006 were used to precondition the model.	46
Fig. 15: Comparison of transient ASRSOM, transient Katsifarakis et al. (2018), and steady state (Katsifarakis 2008) objective function values through time.	48

Fig. 16: Cumulative daily ϕ values for historical and optimized scenarios for the 10-year study period.	50
Fig. 17: Daily differences between ϕ values for historical and optimized scenarios (historical ϕ minus optimized ϕ).	51
Fig. 18: Volume of water recovered (+) and recharged (-) from individual wells for the historical and optimized scenarios during the 10-year study period.	52
Fig. 19: Average water levels for historical and optimized scenarios at LFH wells.	53
Fig. 20: The three wells in an equilateral triangle layout that is used in this study. WTP is water treatment plant, l is the distance between wells “well-spacing”, and d is the length of pipe connects wells to WTP.	60
Fig. 21: Recovery (+) and recharge (-) stresses for individual ASR wells for different flow frequency, a) base b) 3-years c) 5-years scenario.	64
Fig. 22: Power, piping, and total variable costs for T equal to $30 \text{ m}^2/\text{day}$ in the base scenario ($S= 10^{-3}$, flow frequency of 1 year, $Q = 2725.5 \text{ m}^3/\text{day}$ for recovery and $-2180.4 \text{ m}^3/\text{day}$ for recharge).	66
Fig. 23: Total variable costs for different transmissivities for base scenario ($S= 10^{-3}$, flow frequency of 1 year, $Q = 2725.5 \text{ m}^3/\text{day}$ for recovery and $-2180.4 \text{ m}^3/\text{day}$ for recharge).	67
Fig. 24: Least cost well-spacing for base, 3-, and 5- years flow frequency scenarios as a function of transmissivity ($S= 10^{-3}$, $Q = 2725.5 \text{ m}^3/\text{day}$ for recovery and $-2180.4 \text{ m}^3/\text{day}$ for recharge). .	68
Fig. 25: Least cost well-spacing for base, high, and low flowrate scenarios as a function of transmissivity ($S= 10^{-3}$, flow frequency of 1 year)	69
Fig. 26: Least cost well-spacing for base, high, and low storativity scenarios as a function of transmissivity (flow frequency of 1 year, $Q = 2725.5 \text{ m}^3/\text{day}$ for recovery and $-2180.4 \text{ m}^3/\text{day}$ for recharge).	70

Chapter 1 - Introduction

1.1 Research motivation

Fresh water accounts for 2.5% of the total amount of water on earth ($1.4 \times 10^9 \text{ km}^3$). Most of fresh water (69.6%) is stored on glaciers and ice caps, which is difficult to access. Most of the remaining freshwater (30.1%) is stored as groundwater. The remaining 0.3% of world's freshwater is stored as surface water (Maidment 1993). Surface water is highly variable in space and time, often mismanaged, and often polluted. Traditional surface water storage techniques, such as surface reservoirs and dams, have become more difficult to build because of high cost and damage to the environment. Constraints to further development of surface water is driving growing interest in groundwater storage. This is particularly true in arid or semi-arid regions where surface water is limited and aquifers natural recharge is very low (Dillon 2005). The challenge with groundwater is that it needs to be managed efficiently to ensure long-term and cost-effective water supply for people and environmental needs (Mays 2013).

Currently, more than 1.5 billion people around the world, three quarters of the people in the countries of the European Union, approximately 70 percent of the population of China, and more than 50 percent of United States' population depend on groundwater as their primary source for municipal and irrigation purposes (Alley et al. 2002; Findikakis and Sato 2011). To meet municipal, agricultural, and industrial demand, the number of groundwater pumping wells are increasing at dramatic rates. With this, there is growing concerns regarding groundwater depletion (Konikow and Kendy 2005). "Groundwater depletion" can be defined as a rate of groundwater extraction in excess of recharge rate (Wada et al. 2010).

In the literature, groundwater depletion has been studied using different methods. For example, Konikow (2013) studied long-term groundwater depletion in 40 separate aquifers in the U.S. using different methods. These methods include: 1) water-level change and storativity, 2) Gravity Recovery and Climate Experiment (GRACE), 3) flow models, 4) confining unit (i.e. estimates of storage and thickness of the confining unit), 5) water budget, 6) pumpage fraction, 7) extraction, and 8) subsidence. The first three methods are the most reliable methods in estimating groundwater depletion. However, the error in calculating storage changes in the first three methods could reach up to 20%. Moreover, methods such as GRACE measures the monthly anomalies of earth's gravitational field at a scale of 10s kilometers, which means that the scale of such methods is very coarse that it cannot be used to estimate groundwater depletion at a wellfield scale.

Currently, groundwater depletion is leading to decline in water levels in many aquifers in different regions, including North Africa (Döll et al. 2012), Middle East (Konikow and Kendy 2005), India (Shankar et al. 2011), China (Feng et al. 2013), Australia (Khan et al. 2008; Wada et al. 2010), and North America (Konikow 2015 a & b). Decreasing water levels can have adverse effects on natural streamflow, groundwater-fed wetlands and critical ecosystems (Wada et al. 2010). Moreover, falling water levels can reduce well yields, drive the need to drill new wells, and increased pumping costs. In the United States, for example, the volume of groundwater stored in the subsurface decreased by almost 800 km³ during the 20th century, with the highest depletion rate in a single aquifer in the U.S. occurring in the High Plains (HP) aquifer (Konikow 2015a). By the end of 2008, the cumulative depletion has increased to 1000 km³, which indicates the accelerating rate of depletion. During the 20th century, the HP aquifer has undergone an estimated reduction of about 6% of the predevelopment volume of water in storage (McGuire et

al., 2003). Other studies estimate that the reduction at the HP aquifer by the end of 2007 was about 8% of the predevelopment volume of water (Scanlon et al. 2012).

Interestingly, the broad perception of the HP aquifer as a depleting aquifer focuses on local depletion, with the majority of the depletion occurring in the central and southern part of the aquifer. If the depletion were uniform, the decline of water level would be approximately 4 meters (Scanlon et al. 2012). Local depletion rates might indicate that the least expensive recoverable fresh groundwater has already been depleted and that the cost of future pumping will increase. Local depletion can be explained by the excessive pumping of groundwater to meet water demand. To mediate depletion problems, Konikow (2015) suggested that water managers should 1) reduce water demand by increasing efficiencies, changing land use, imposing tax or cost incentives, and 2) increase water supply through managed aquifer recharge, such as ASR, desalination, and developing other alternatives for water resources. The overall themes are 1) operating groundwater wellfields by considering long-term drawdown at wells, instead of considering wells flowrates, and 2) artificially recharging aquifers to sustain water levels in wellfields.

Artificial recharge is an important groundwater management practice that is emerging as a key tool for the sustainable use of groundwater (Bouwer 1994, 2002). Water can be recharged artificially through infiltration ponds, drainage pipes, and aquifer storage and recovery (ASR) systems (Bouwer 2002; Dillon 2005; Pyne 2005). The main application of artificial recharge is to store surplus water for seasonal, long-term, or emergency storage. According to Pyne (2005), additional applications include, increasing the water-table level, preventing saltwater intrusion, remediating soil and groundwater, deferring expansion of water facilities, and enhancing well-field production, to name a few.

Groundwater models have been used in the past decades to support the development and management of groundwater (Zhou and Li 2011). Different groundwater models have been developed to minimize energy consumption (Ahlfeld and Lavery 2011, 2015) and to minimize power cost (Katsifarakis 2008; Katsifarakis and Tselepidou 2009). Different artificial recharge models have been used to assess and simulate the hydraulics of the wellfield (Ringleb et al. 2016), biological and chemical processes (Rinck-Pfeiffer et al. 2000), cost and feasibility (Khan et al. 2008), water quality (Ward et al. 2007, 2008, 2009; Dillon et al. 2016), planning (Uddameri 2007), and recovery efficiency (Lowry and Anderson 2006).

Most groundwater wellfield models have used numerical solutions because of their ability to solve the full transient, 3D, heterogeneous and anisotropic governing equation under complex boundary and initial conditions (Anderson et al. 2015). However, numerical solutions are limited in their ability to predict water levels at wells, wherein the governing equation using approximates discretization of time and space. As an alternative, an analytical solution provides a continuous solution that can be used to resolve water levels at wells. Specifically, analytical models can be used to analyze and predict water levels at wells, optimize ASR operational schedules to minimize power and cost, and optimize well spacing between ASR wells to minimize total cost.

The groundwater flow model used in this study is a modification of a Theis (1935) superposition model developed by (Lewis et al. 2016). Herein the model is referred to as the wellfield model.

The wellfield model is composed of two parts: 1) parameters estimation and 2) a forward mode. The model utilizes water level time series from groundwater wells to estimate aquifer properties, recoverable water level, well loss coefficients, and estimates water level through wellfield with different operation schedule. Then, the model uses estimated parameters in the forward mode to

predict water levels at wells using stresses applied at wells. Fig. 1 shows flow chart illustrating the parameter estimation workflow. Shaded boxes represent the key steps of parameter estimation.

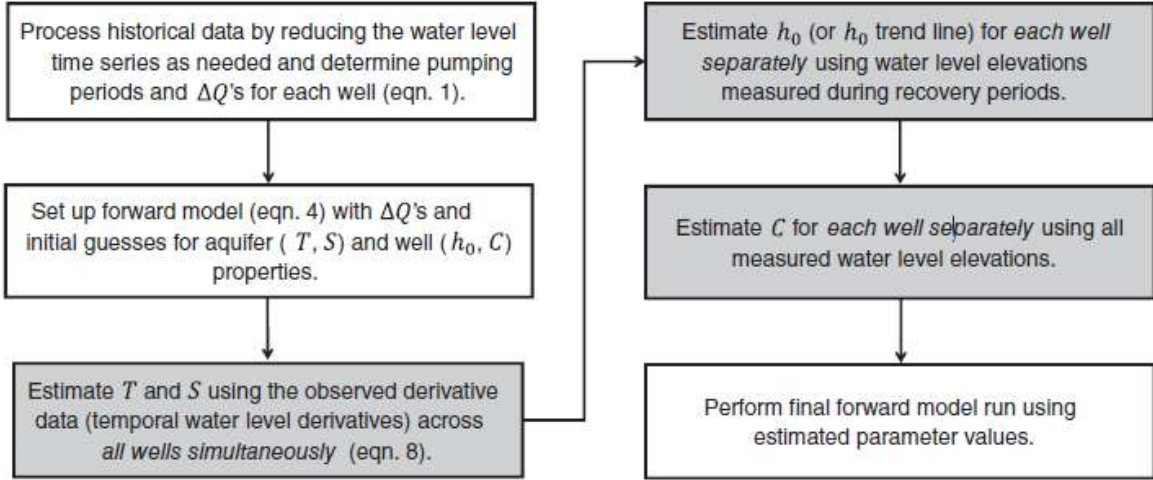


Fig. 1: Flow chart illustrating the parameter estimation workflow. Shaded boxes represent the key steps of parameter. Adapted from (Lewis et al. 2016).

The forward mode uses Theis superposition in time and space to calculate drawdown associated with historical groundwater recovery/recharge s_{aq} as follow:

$$s_{aq}(t) = \sum_{m=1}^M \left\{ \frac{Q_{m,0}}{4\pi T} W(u_{m,0}) + \sum_{n=1}^N \frac{\Delta Q_{m,n}}{4\pi T} W(u_{m,n}) \right\} \quad (1)$$

$$u_{m,n}(t) = \frac{r_m^2 S}{4T(t - t_{m,n})}$$

where T is aquifer transmissivity (L^2/T), S is storativity (dimensionless), $Q_{m,0}$ is the initial pumping rate at time $t_{m,0}$ (L^3/T), ΔQ_{mn} is the change in pumping rate (L^3/T) at well m at time increment n , N is the number of pumping rate changes before time t . W is the well function (dimensionless), and r_m is the radial distance from the point of interest to the individual pumped

locations (L), where r_m is equal to the radius of the well if drawdown is calculated at the pumped well. The main components of drawdown are presented at Fig. 2.

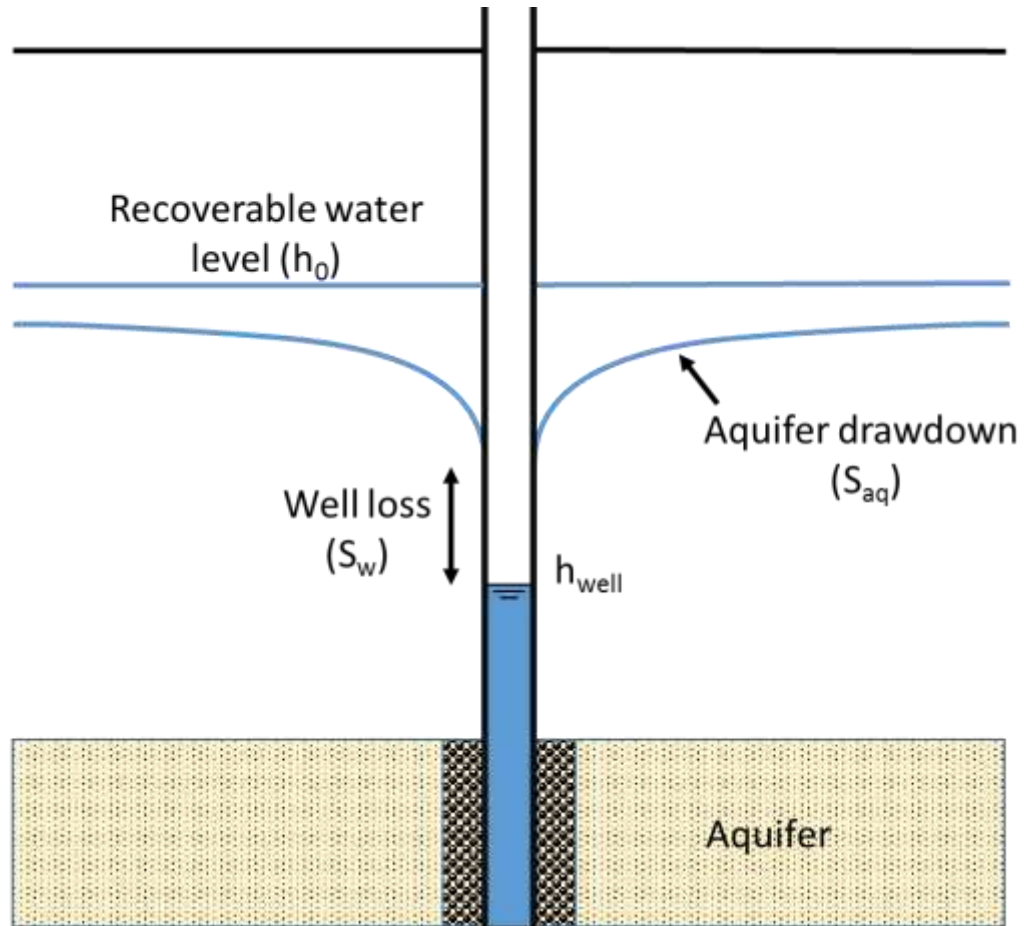


Fig. 2: Main components of drawdown in groundwater wells.

Total drawdown can be categorized in two different categories: Drawdown associated with aquifer response $s_{aq}(L)$ and well losses $s_w(L)$. Components of drawdown and head at well can be shown as follow:

$$s_{tot} = s_{aq} + s_w \quad (2)$$

$$h_{well} = h_0 - s_{aq} - s_w \quad (3)$$

where $h_{well}(L)$ is the head at well and $h_0(L)$ is recoverable water level.

1.2 Hypotheses

The hypotheses of this dissertation include making groundwater supplies more sustainable by examining that:

1a) The analytical model developed by Lewis et al. (2016) can be modified and used to predict water levels at wells in ASR wellfields.

1b) Artificial recharge through ASR wells can sustain water levels in wellfields.

2a) Optimization of recharge and recovery can reduce power consumption and carbon footprint in ASR wellfields.

2b) Artificial recharge can reduce power consumption and carbon footprint in ASR wellfields.

3) Small well-spacing are feasible for ASR wellfields.

1.3 Contents

This dissertation contains five chapters. This, the first chapter, states the significance of the problem and clarifies the research objectives. The second chapter describes the analytical model, its applicability to ASR wellfields, and estimate the role that ASR plays in sustaining water levels. The second chapter is a manuscript of a journal paper and was submitted to the Journal of Water Resources Management on December 2018. The third chapter addresses a methodology for minimizing operational cost by optimizing the wellfield recharge and recovery and evaluating the role that recharge plays in minimizing power consumption. The third chapter is a manuscript of a journal paper and was submitted to the Journal of Water Resources Planning and Management (June 2019). The fourth chapter addresses a sensitivity analysis of the most important parameters that effect well-spacing in ASR wellfields. The fourth chapter requires

further work and will be submitted as a journal paper in the near future. Lastly, Chapter 5 provides a summary of the dissertation.

Chapter 2 - Demonstration of Sustainable Development of Groundwater through Aquifer Storage and Recovery (ASR)¹

Chapter synopsis

Sustained production of groundwater from wells in wellfields can lead to declining water levels at production wells and concerns regarding the sustainability of groundwater resources. Aquifer Storage and Recovery (ASR) is a promising approach for maintaining water levels in wells and increasing the sustainability of groundwater resources. Herein, an analytical model relying on superposition of the Theis equation is used to resolve water levels in 40 wells in three vertically stacked ASR wellfields. Fifteen years of dynamic recovery/recharge data are used to obtain aquifer and well properties. Estimated aquifer and well properties are used to predict water levels at production well. Close agreement between modeled and observed water levels support the validity of the analytical model for estimating water levels at ASR wells. During the study period, 45 million m³ of groundwater is produced and 11 million m³ is recharged, leading to a net withdrawal of 34 million m³ of groundwater. Rate of changes in recoverable water levels in wells in the Denver, Arapahoe and Laramie-Fox Hill Aquifers are 0.20, -0.91, and -3.48 m per year. To quantify the benefits of recharge, the analytical model is applied to predicting water levels at wells absent the historical recharge. Results indicate that during recovery and no-flow periods, recharge has increased water levels at wells up to 60 m compared to the no-recharge scenario. On average, the recharge increased water levels at wells during the study period by 3, 4, and 11 m in the Denver, Arapahoe, and Laramie Fox-Hills Aquifers, respectively. Overall, the

¹ Authors are: Abdulaziz Alqahtani, Tom Sale, Michael J. Ronayne, and Courtney Hemenway

analytical model is a promising tool for advancing ASR wellfields and ASR can be a viable approach to sustaining water levels in wells in wellfields.

2.1 Introduction

Increasing global population, urbanization, and climate change are driving an ever-growing need for fresh water supplies (Bouwer 2002; Vanderzalm et al. 2010; Handel et al. 2014).

Unfortunately, meeting emerging water needs with surface water is increasingly difficult due to the historical development of the best alternatives, increasing environmental standards, concerns with seepage/evaporation losses, and costs for new surface water storage (Bouwer 1994). Given that groundwater represents more than 98% of all of the unfrozen fresh water on the planet (Maidment 1993), groundwater is an attractive option for new sources of fresh water.

To the positive, groundwater is often present in areas where water is needed, the quality of groundwater is commonly suited to needs, and initial development costs for groundwater can be low compared to surface water alternatives. To the negative, chronic use of groundwater often leads to concerns regarding aquifer depletion and debate as to the wisdom of developing what is often perceived as an “unsustainable resource” (Wada et al. 2010; Scanlon et al. 2012; Konikow 2015a). Aquifer storage and recovery (ASR) is a promising tool for advancing sustainable reliance on groundwater resources for water supply (Pyne 2005).

Public concern over aquifer depletion is common in areas where large-scale groundwater development has occurred and wells have been pumped over extended periods of time. Examples are found in Africa (Reddy 2002), the Middle East (Voss et al. 2013; Joodaki et al. 2014), India (Shankar et al. 2011; Thakur and Jayangondaperumal 2015), China (Feng et al. 2013), Australia (Döll et al. 2012) and North America (Konikow 2015a, b). Aquifer depletion has been studied at a regional-scale (Scanlon et al. 2012; Voss et al. 2013) and, to a far lesser degree, at a wellfield-

scale (Lewis et al. 2016). Herein, consideration is given to the sustainable use of wellfields in the Denver Basin Aquifers, immediately south of Denver, Colorado, USA, in the “South Metro Area.”

In the 1980s, projected population growth in the South Metro Area led to plans to build a 1.4 km³ surface water reservoir on the main stem of the South Platte River (Two Forks). Due to environmental concerns, permission to build the dam was denied (EPA 1990). Until recently, the projected urban water needs in the South Metro Area have been met, in large part, through the development of wellfields in the Denver Basin Aquifers. Concerns regarding sustainable use of the Denver Basin Aquifers have been advanced in local media (Topper and Reynolds 2007) and State of Colorado legislation (Senate Bill 5).

In the Denver Basin Aquifers, increasing depths to water (DTW) in wells in wellfields is a primary factor driving concerns regarding the sustainability of Denver Basin Aquifer groundwater supplies. Herein, a “wellfield” is defined as an area in which water levels in wells are influenced by pumping from a set of multiple wells. At wells in wellfields, depths to water are dependent on static water levels, drawdown associated with historical groundwater recovery/recharge, and well losses (Domenico and Schwartz 1998). As such,

$$DTW(t) = E - h_0(t) + s_{aq}(t) + s_w(t) \quad (4)$$

where E is the wellhead elevation (L), h_0 is the recoverable water level elevation (L) (i.e., the level to which the water level in a well would eventually recover if pumping were stopped), s_{aq} is drawdown in the aquifer caused by pumping/recharge from all wells in the wellfield (L), s_w is head loss associated with water entering the well (L), and t is time (T). Avoiding excessive depths to water in pumped wells is central to sustainable operations of wells in wellfields. On the

other hand, in areas influenced by groundwater recovery and recharge, DTW is not equivalent to water remaining in an aquifer as described by h_0 . Given the influences of groundwater recharge/recovery (both active and residual) and well efficiencies, care is needed to avoid misinterpreting DTW measured in wellfields as direct indicators of h_0 , and the amount of water present in aquifers.

Groundwater models provide a valuable tool for managing groundwater resources (Kabala 1994). Beginning in the 1970s, numerical models were employed in modeling wellfields (e.g., Prickett and Lonquist 1971). In early modeling efforts, both spatial and temporal discretization of modeled domains were insufficient to capture water levels at pumping wells. Since the 1970s, dramatic improvements in computational speed and numerical methods have led to vast improvements in numerical models, including highly flexible finite element grids (e.g., *MicroFEM* (Hemker 2004)) and embedded high-resolution grids and well packages (e.g., MODFLOW (Harbaugh 2005)). Unfortunately, approximations in numerical models including spatial and temporal discretization still constrain the ability of numerical models to resolve water levels at pumped wells.

Recognizing the need to resolve water levels at groundwater production wells, Lewis et al. (2016) developed an analytical model specifically for wellfield applications. The analytical model relies on the spatial and temporal superposition of the Theis solution for transient flow of groundwater to a well (Theis 1935). Model inputs include continuous water levels at wells, flow rates through time at wells, and the locations of wells. Model outputs include 1) aquifer transmissivity, T (L^2/T), and storativity, S (dimensionless) values for the wellfield aquifer and 2) recoverable water level, h_0 (L), and well loss coefficients, C (T^2/L^5), for individual wells in the wellfield. Critically, the analytical model is the only documented tool, to the authors' knowledge,

that estimates aquifer and well properties based on data from active wellfields, over extended periods of time, with varying rates of groundwater recovery and/or recharge.

The objectives of this research are to demonstrate the use of the analytical model developed by (Lewis et al. 2016) for ASR wellfields and to study the role of ASR in sustaining water levels at wells. The analytical model was applied to 15 years of operational data from three vertically stacked aquifers with ASR wellfields to estimate aquifer and well properties. Estimated aquifer and well parameters are used to simulate water levels using historical recovery and recharge flow rates. Lastly, the calibrated model is run without the historical groundwater recharge stresses. A comparison of water levels at wells, with and without recharge, is used to quantify the benefits of recharge.

2.2 Methods

The following sections present background information including the hydrogeology of the Denver Basin Aquifers, a description of the study wellfields and wells, employed water-level data, pumping data, and computational methods.

2.2.1 Hydrogeology of the Denver Basin Aquifers

The Denver Basin Aquifers include the Dawson, Denver, Arapahoe, and Laramie Fox-Hills Aquifers. Sediments were derived primarily from mass wasting off the Rocky Mountains during uplift 70-90 million years ago during the late Cretaceous and early Tertiary periods. Sediments were carried by gravity and water into the Denver Basin, a north-northeast trending down folded basin (forebay) located to the east of the Rocky Mountains (Raynolds 2003). Buried alluvial fans are encountered along the current mountain front in the study area. Examples include the Wildcat Mountain Alluvial Fan (Raynolds 2003) and the South Castle Rock Alluvial Fan (Sale et al.

2010). In addition, interbedded siltstones and shales in the formations were deposited as overbank deposits and as volcanic ash (Raynolds 2003; Barkmann et al. 2011).

The study area is the service district of Centennial Water and Sanitation, Highlands Ranch, Colorado, USA. The following description of the sediments in the study area is based on visual geologic logs of cuttings collected at 10-foot intervals from 40 wells collected by the authors in the study area. The Dawson Aquifer is 0 to 190 m thick. The Dawson is composed of poorly- to moderately-consolidated coarse-grained sandstones interbedded with conglomerate, siltstone, and claystone. The Denver Formation is 180 to 335 m in thickness. The Denver is composed of poorly- to moderately-consolidated sandstone, interbedded with siltstone and shale. Similarly, the Arapahoe Formation consists of 140 to 300 m of interbedded, sandstone, siltstone, and shale. The Laramie-Fox Hills Aquifer consists of 50 to 225 m of interbedded fine-grained sandstone, siltstone, and shale. The flow between the aquifers is constrained by low permeability siltstone and shale layers. Aquifer T values, S values, and natural groundwater flow are described in Results and Discussion.

2.2.2 Wellfields and wells

The Centennial Water and Sanitation service area is located immediately south of Denver, Colorado. Denver, Arapahoe, and Laramie-Fox Hills wellfields overlay each other (Fig. 3). This study considers 19, 10, and 11 wells completed in the Denver, Arapahoe, and Laramie Fox Hill Aquifers, respectively. The wells were drilled using reverse circulation mud rotary drilling techniques. Reverse circulation facilitates drilling large diameter holes needed for high capacity pumps and minimizes formation damage associated with overbalanced mud rotary drilling (Sterrett 2007).

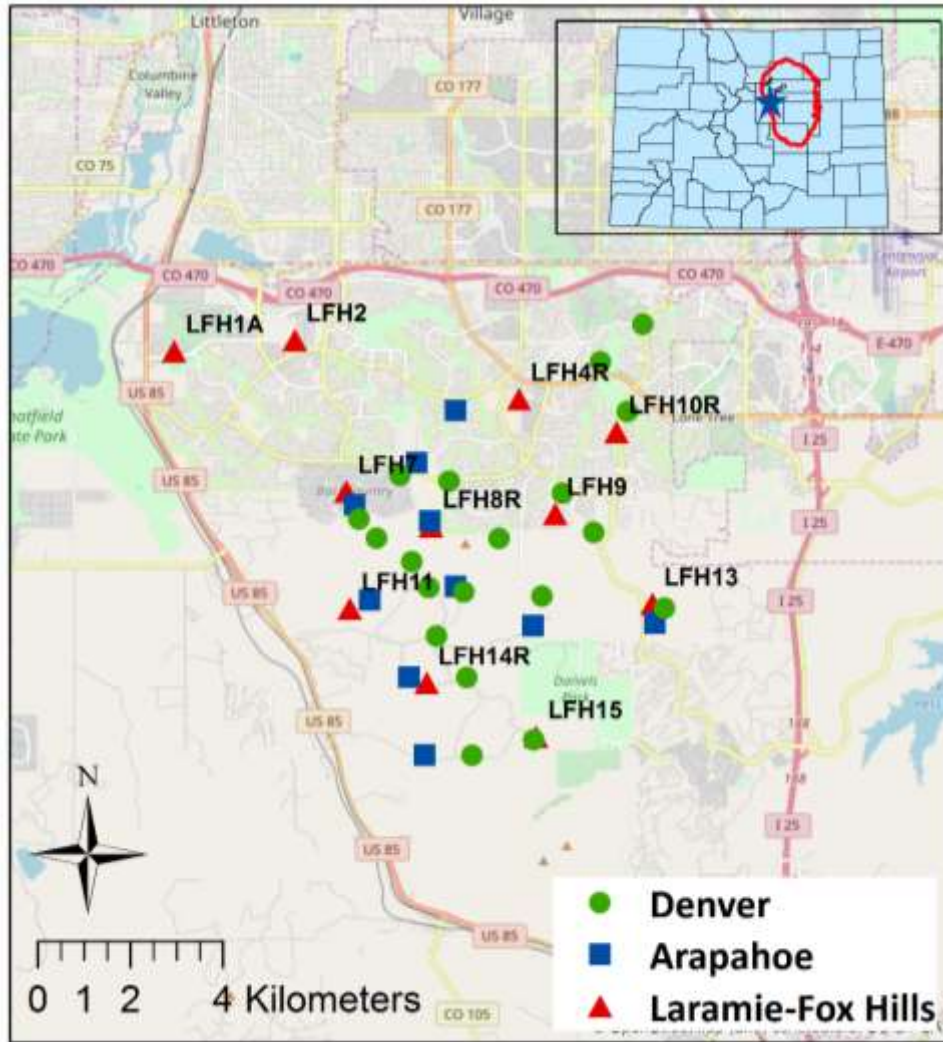


Fig. 3: Location of Centennial Water & Sanitation District wells. The red line on state of Colorado inset map indicates the extent of Denver Basin Aquifer system. Well names are provided for the Laramie-Fox Hills (LFH) wells.

Average total depths for Denver, Arapahoe, and Laramie-Fox Hills wells are 302, 443, and 665 m, respectively. Wells are completed with 200 to 300 mm ID low carbon steel casings and stainless-steel v-slot wire wrap screens. Well screens are located adjacent to sandstone beds based on downhole electric and gamma geophysical logs. Wells contain 40 to 150 m screened sections located through intervals adjudicated by the State of Colorado. Most of the wells are gravel packed with well-rounded quartz-feldspar (10-20 mesh). Gravel pack is placed from the bottom of the bore hole to above the top of the uppermost well screen. Neat cement is placed

from the top of the gravel pack to grade. Wells are developed by airlifting through screened intervals for total periods ranging from 24 to 48 hours. As required (approximately every 5 to 7 years), wells are redeveloped to address fouling of well screens and gravel pack.

Wells are equipped with multiple-stage submersible pumps sized to capacities based on step-drawdown tests and location-specific total dynamic head needed to move water from pumping level in wells to aboveground storage tanks. Pumps are equipped with variable frequency motor drives that are used to control groundwater recovery rates. By 2015, 24 of the wells were equipped with InFlex™ flow control valves (Baski Inc., Colorado). Flow control valves are located on the pump column immediately above the submersible pumps. The flow control valves allow a single pump column pipe to be used for recharge and recovery of groundwater. The key component of the flow control valves is a down-hole packer that regulates flow and maintains positive pressure in the riser pipe during groundwater recharge. During groundwater recharge, wells are pumped (backwashed) for approximately one hour every month to clear suspended solids from the well screens and gravel pack. Flow rates during recharge are limited to 80% of groundwater recovery to minimize irreversible plugging of wells during recharge.

2.2.3 Well water level and pumping data

Daily water-level and water-flow-rate data were acquired from pressure transducers and flow meters via a Supervisory Control and Data Acquisition (SCADA) system. The study data set extends from 2000 to 2015. Flow values and water levels were collected at midnight, and as a result, potential dynamic aspects of the operation that occur over the course of a single day can be missed. As an example, a well that is pumped for part of a day, but not at midnight, has a reported flow rate of zero. In addition, one-hour back-flushing events during recharge are typically not captured in the pumping records. Nevertheless, water levels and flow rate data from

40 active wells in three aquifers, over a period of 15 years, with both groundwater recharge and recovery provide a remarkable opportunity to evaluate the effects of Aquifer Storage and Recovery (ASR). During the study period, based on recorded flow rates and durations, 45 million m³ of groundwater is produced and 11 million m³ of groundwater is recharged, leading to a net withdrawal of 34 million m³ of groundwater. Notably, in the Denver Basin Aquifers, stored water can be used to increase allowable (water-rights based) groundwater production at individual well in drought years.

2.2.4 Parsing raw data

Parsing raw data is the primary task associated with applying the analytical model. Data were screened to remove periods from individual well records when either flow rate or water-level data were invalid. The basis for deleting select periods of record includes:

- Reported water levels or flows were outside of the plausible range of values
- Periods when water levels were anomalously constant, indicating problems with the measurement devices
- Early water levels that cannot be used to test the model due a need to capture the impact of antecedent pumping with at least one year of pumping stresses.

The automated data parser advanced in Lewis et al. (2016) was applied to the screened data. The parser transforms time-varying groundwater recharge and recovery rates into representative blocks of constant groundwater recharge and recovery rates. The analytical model relies on the superposition of the Theis Solution (Theis 1935) in time and space. Reducing varying flow-rate data to representative blocks of constant stresses enables practical prediction of water levels, given large numbers of wells with time-variant stress over extended periods of time. Raw and parsed datasets for a representative well (LFH-11) are presented in Fig. 4.

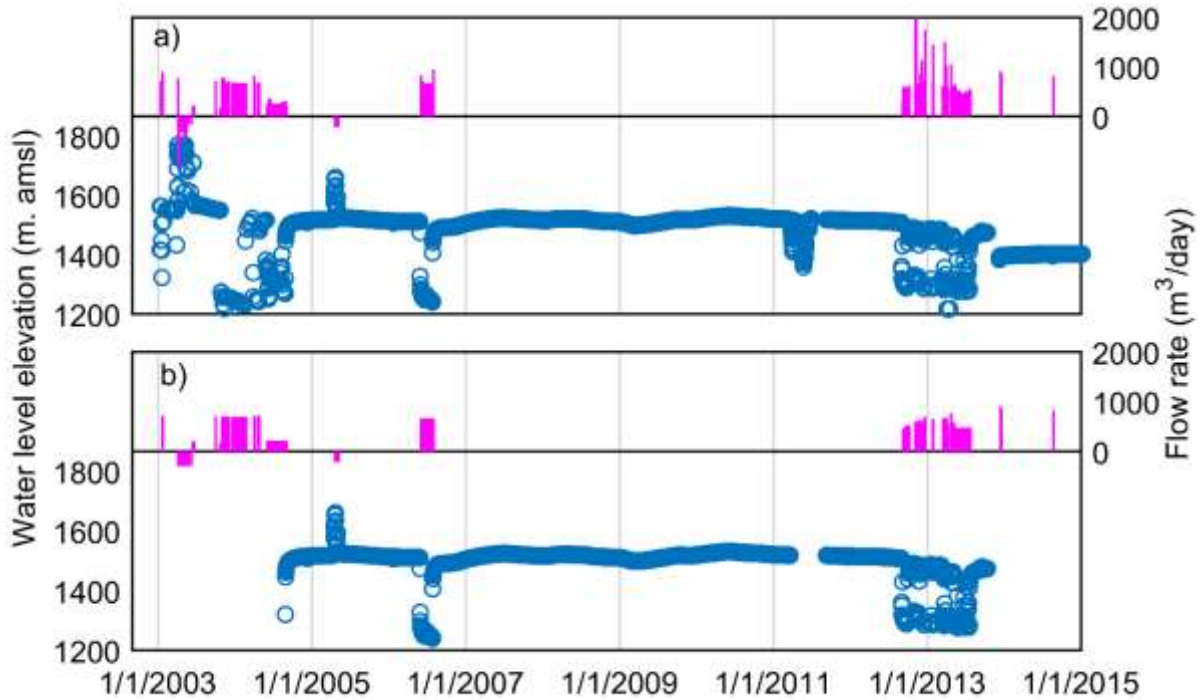


Fig. 4: Laramie Fox Hills Well LFH-11: a) raw data, and b) parsed data.

2.2.5 Parameter estimations

Using parsed data, the analytical model is used to estimate T and S for the wellfield aquifer and h_0 and C values (recharge (C_S), and recovery (C_R)) for individual wells. Briefly, the derivative of head values with respect to time, observed and modeled, is used in an iterative solver to obtain least-squares best-fit values for T and S for the aquifer. T and S values are obtained using data from periods when individual wells are recovering from prior groundwater recharge and recovery stresses.

The best-fit T and S values are used in the analytical model to estimate water levels at wells when there are no active stresses at individual wells. Values for h_0 at individual wells are iteratively tested to develop the least-squares best-fit between observed and modeling water levels at individual wells. Recognizing a tendency for h_0 values to drift through time, Lewis et al. (2016) reports h_0 as a time-dependent linear function:

$$h_0(t) = \alpha t + h_0(t_0) \quad (5)$$

where α (L/T) is the rate of change of the recoverable water level at individual wells, t is time (T), and t_0 (T) is zero for the first time in the data record.

Lastly, T , S , and h_0 values are used in the forward model to predict water levels at individual wells during periods of active groundwater recharge and recovery. The differences between predicted and observed water levels are used to estimate well losses s_w and best-fit well loss coefficients for individual wells. Following Domenico et al. (1998), well losses are modeled as:

$$s_w(t) = C[Q(t)]^2 \quad (6)$$

where C (T²/L⁵) is the well loss coefficient, and $Q(t)$ (L³/T) is the rate at which groundwater is placed into storage or recovered at a well during a blocked stress period.

Preliminary applications of the analytical model led to the realization that the well loss coefficients were higher during recharge versus recovery. Based on larger well loss coefficient values during recharge, the analytical model developed in Lewis et al. (2016) was modified to resolve loss coefficients for recharge (C_S), and recovery (C_R). A summary of parsed data blocks and derived parameters are provided in Table 1.

Table 1: Summary of the time periods used to estimate aquifer and well properties

Time periods	Estimated parameters
Selected periods when individual wells are recovering from prior groundwater recharge or recovery	T and S for the aquifer
All periods of no groundwater recharge or recovery	h_0 for individual wells

All periods of active groundwater recharge	Well loss coefficient for recharge (C_S) for individual wells
All periods of active groundwater recovery	Well loss coefficient for recovery (C_R) for individual wells

2.2.6 Forward model

Following Equation (4), the forward model predicts water levels at wells as a function of $h_0(t)$, $s_{aq}(t)$, and $s_w(t)$. Again, drawdown at wells, $s_{aq}(t)$ is based on the superposition of the Theis solution (Theis 1935) in space and time using the blocks of stresses (recharge and recovery) and estimated T and S values. s_{aq} as is calculated as follow:

$$s_{aq}(t) = \sum_{m=1}^M \left\{ \frac{Q_{m,0}}{4\pi T} W(u_{m,0}) + \sum_{n=1}^N \frac{\Delta Q_{m,n}}{4\pi T} W(u_{m,n}) \right\} \quad (7)$$

$$u_{m,n}(t) = \frac{r_m^2 S}{4T(t - t_{m,n})}$$

where T is aquifer transmissivity (L^2/T), S is storativity (dimensionless), $Q_{m,0}$ is the initial pumping rate at time $t_{m,0}$ (L^3/T), $\Delta Q_{m,n}$ is the change in pumping rate (L^3/T) at well m at time increment n , N is the number of pumping rate changes before time t . W is the well function (dimensionless), and r_m is the radial distance from the point of interest to the individual pumped locations (L), where r_m is equal to the radius of the well if drawdown is calculated at the pumped well.

Water levels, or hydraulic head, at any point in the wellfield are dependent upon all recharge/recovery imposed prior to the time of interest, from all wells in the wellfield. The forward model was used to estimate water levels at wells with historical groundwater recharge and recovery. Lastly, the model was used to estimate water levels at wells absent the historical groundwater recharge.

2.3 Results and Discussion

The following section advances 1) estimates of T and S values for the Denver, Arapahoe, and Laramie-Fox Hills Aquifers, 2) recoverable water levels (h_0), 3) well loss coefficients during recovery and recharge (C_R , and C_S) for all wells, 4) comparison of modeled and observed water levels, 5) statistical analysis of observed and modeled ASR water levels, and 6) comparison between water levels with and without recharge. Complementary information and results are presented in Supplementary Information (SI).

2.3.1 Aquifer properties (T and S)

Estimated T and S values for the Denver, Arapahoe, and Laramie Fox-Hills Aquifers and T and S obtained from 72-hour constant flow aquifer tests conducted in the same wellfields by the authors (Sale et al. 2010) are presented in Fig. 5. T and S values from the analytical model are in close agreement with the means of T and S values obtained from 72-hour aquifer tests. In addition, T and S values estimated by the analytical model are in agreement with data reported by other studies (Robson 1987; Robson and Banta 1995; Paschke et al. 2011).

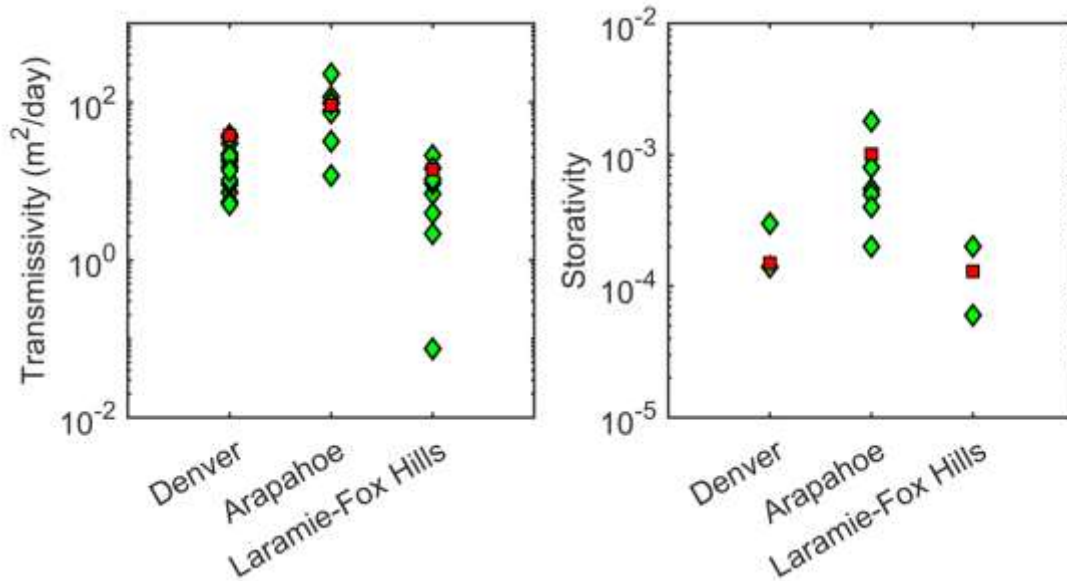


Fig. 5: Model (squares) and 72-hour aquifer test (diamonds) T and S values for the Denver, Arapahoe, and Laramie-Fox Hills Aquifers.

Differences between T and S for the individual wells and the analytical model are attributed to heterogeneity within each of the aquifers and the limited volume of the aquifer addressed in the 72-hour aquifer tests. Overall, the agreement between historical aquifer test T and S values and the analytical model supports the validity of using temporal ASR water-level derivatives to estimate T and S values. Furthermore, agreement between T and S values estimated immediately after construction of the wells (72-hour tests) and after extended periods of pumping suggests that historical pumping has not significantly affected the aquifer properties.

2.3.2 Recoverable water levels (h_0)

Median recoverable water levels from wells in the Denver, Arapahoe, and Laramie-Fox Hills Aquifers, over the study period, were 1,711, 1,497, and 1,503 m above sea level, respectively. Median recoverable water levels suggest a potential for upward flow of groundwater from the Laramie-Fox Hills Aquifer to the Arapahoe and downward flow of groundwater from the Denver

to the Arapahoe. This potential is consistent with the Arapahoe Aquifer having seen the greatest historical groundwater production in the study area.

Rates of change in the water levels in well in the Denver, Arapahoe, and Laramie-Fox Hills Aquifers (α) are 0.20, -0.91, and -3.48 m per year, respectively. Negative and positive α values reflect wellfield-scale aquifer depletion or accumulation, respectively. Further insights are obtained by developing a plan-view contour map of h_0 values. As an example, a contour map of h_0 values from wells in the Laramie-Fox Hills Aquifer is presented in Fig. 6. Consistent with the interpretation of the regional hydrogeology of the Denver Basin Aquifer (Robson 1987; Paschke et al. 2011), depicted regional groundwater flow is to the north-northeast at a gradient of 0.01. The ability to resolve regional groundwater flow through an active wellfield supports the interpretation of the best-fitting h_0 value as a meaningful recoverable water level elevation.

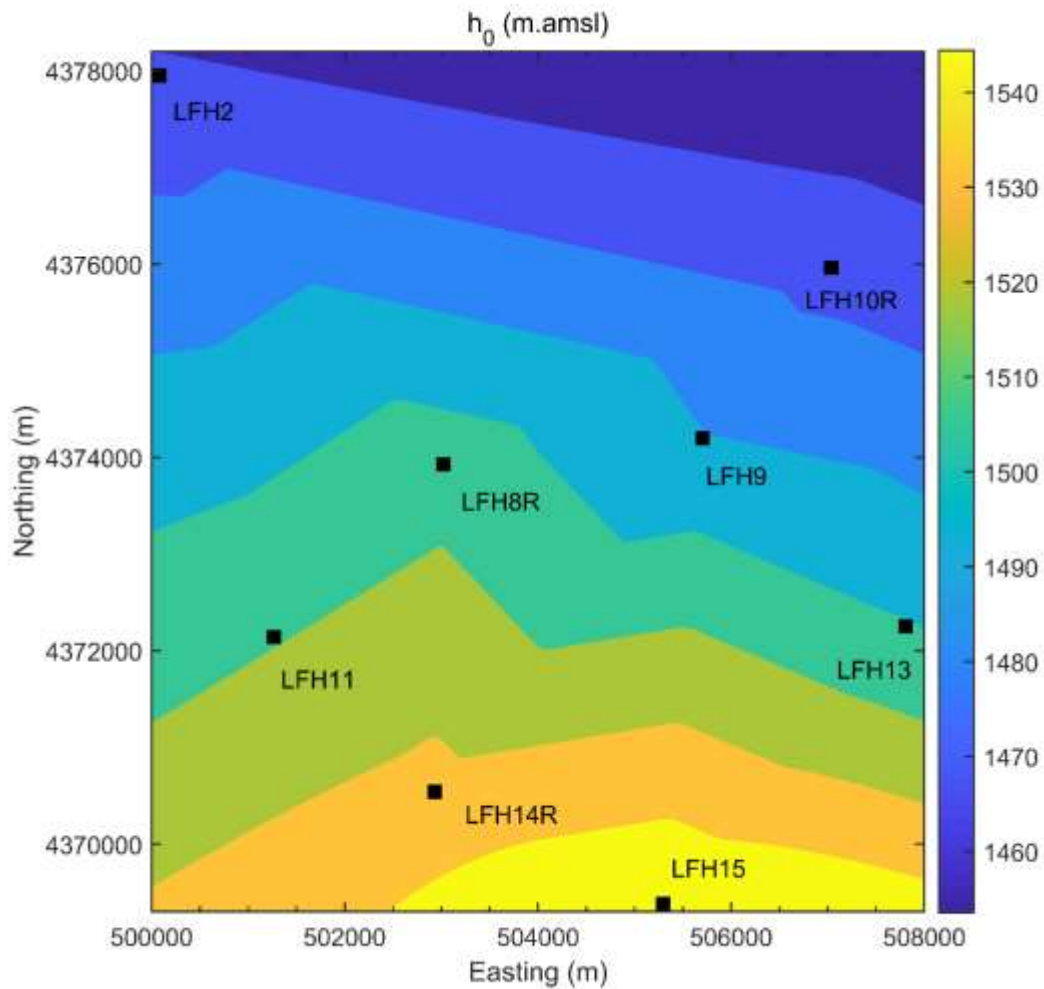


Fig. 6: Contoured recoverable water level (h_0) values for the Laramie Fox Hills Aquifer indicate groundwater flow to the north-northeast and a gradient of 0.01.

2.3.3 Recharge/recovery well loss coefficients (C_R and C_S)

Recharge and recovery well loss coefficients for Laramie-Fox Hills wells with C values greater than 10^{-4} days²/m⁵ are presented in Table 2. Considering Equation 6, a flow rate of 500 m³/day and a C value of 10^{-4} day²/m⁵ indicate well losses of 25 m. Correspondingly, C values less than 10^{-5} day²/m⁵ indicate well losses that are negligible (as compared to drawdown) and C values

greater than $10^{-4} \text{ day}^2/\text{m}^5$ suggest situations where remedies for near well head losses (e.g., well rehabilitation) may be needed.

Table 2: Well loss coefficients during recharge and recovery cycles for wells in the Laramie Fox-Hills Aquifer

Well	well loss coefficient (day^2/m^5)	
	Recovery	Recharge
LFH-8R	3.4 E-04	7.5 E-04
LFH-10R	NA	4.7 E-04
LFH-11	3.3 E-04	1.3 E-03
LFH-14R	0	3.0 E-03

Most recharge C_S values are greater than recovery values C_R . Given that well screens remain submerged throughout the study period, for the most part, blockage of groundwater flow during recharge, due to air entrainment, is an unlikely explanation for larger recharge C_S values.

Moreover, no correlation exists between wells with low 72-hour aquifer test T values. As such, a model bias for higher C_S values in wells with lower T values fails to resolve higher C_S values during recharge. The most probable explanation for higher C_S values during recharge seems to be solids from the wellfield distribution pipelines accumulating on and about the well screens. The hypothesis of distribution pipeline solids causing increased well losses is supported by suspended solids observed in the discharge from monthly recharge backwash events and a subsequent application of the analytical model to an ASR demonstration in the Denver and Arapahoe aquifers using new distribution pipelines in which well loss coefficients were equal during recharge and recovery and similar concerns with solids in distribution pipelines described by Bichara (1986). Recharge and recovery well loss coefficients for Denver and Arapahoe wells are presented in SI. Overall, estimates of C values from wells in active wellfields hold the promise as an important tool for sustainable management of wells in conventional and ASR in wellfields.

2.3.4 Comparison of modeled and observed water levels with groundwater recharge and recovery

Observed and modeled water levels using historical groundwater recharge and recovery stresses for four representative Laramie-Fox Hills wells are presented in Fig. 7. Similar plots for all wells in the study aquifers are presented in SI. Favorable agreement between observed and modeled water levels is seen with respect to water level elevations and the timing of responses to recharge and recovery.

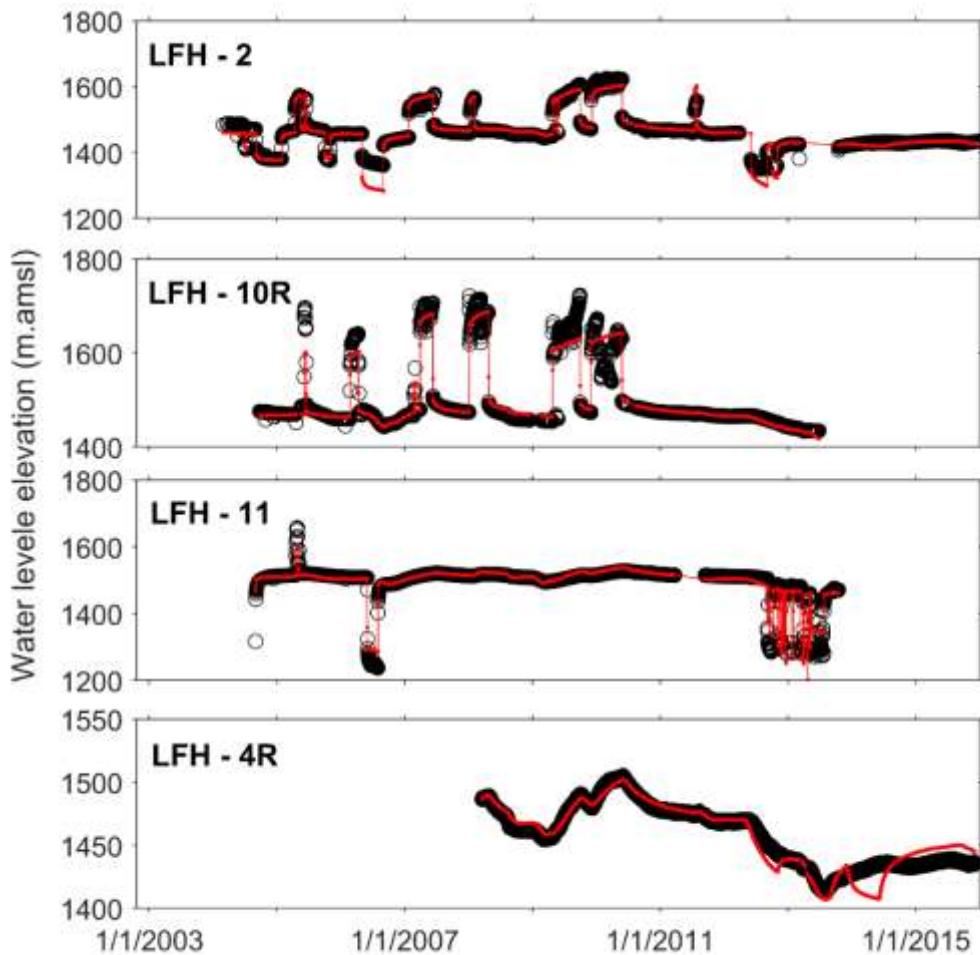


Fig. 7: Observed water levels (black dots), and modeled water levels for ASR scenario (red solid line) for representative wells in the Larimer Fox-Hills Aquifer.

With respect to individual wells in Fig. 7, LFH-2 experiences six recharge and six recovery cycles. A close fit between observed and modeled water levels for ASR scenario is seen except for the 2006 recovery cycle. During the 2006 recovery cycle at LFH-2, the model over-predicts drawdown by 100 m. A possible explanation for the 2006 anomaly may be errors in the reported flow rates or water levels. LFH 10R experiences six recharge and no recovery cycles. Favorable agreement is seen between observed and modeled water levels during stressed and unstressed periods. LFH-11 experiences one recharge cycle, six recovery cycles, and a 5-year period of no stresses (2007-2012). Close agreement is seen between observed and modeled water level, including the period of no stresses when water levels are governed by drawdown from distal wells in the wellfield. LFH-4R experiences no recharge/recovery stresses, effectively serving as a monitoring well within the active wellfield. As with the no-stress period for LFH-11, LFH-4R shows close agreement between observed and modeled water levels.

2.3.5 Statistical analysis of observed and modeled ASR water levels

Modeled versus observed water levels for the Laramie-Fox Hills Aquifer are presented in Fig. 8a. The histogram in Fig. 8b shows the frequency of residuals (observed water level elevation minus modeled water level elevation for a given observation time). Modeled versus observed water levels were plotted to show that the model is not under- or overestimated water level. A limitation of Fig. 8a is that many of the data points close to the 1:1 line overly one another. As such, Fig. 8a is misleading with respect to the fit of the actual versus modeled water levels. The mean and standard deviations of the residual values for the Laramie-Fox Hills Aquifer are 2.96 m and 33.2m, respectively. Residual means, Standard deviations, Absolute Value Error (AVE), Nash-Sutcliffe efficiency coefficient (NSCE), and Root Mean Square Error (RMSE) were

obtained for wells in the Denver, Arapahoe, and LFH Aquifers (Table 3). Brief description of AVE, NSCE, and RMSE is provided at SI.

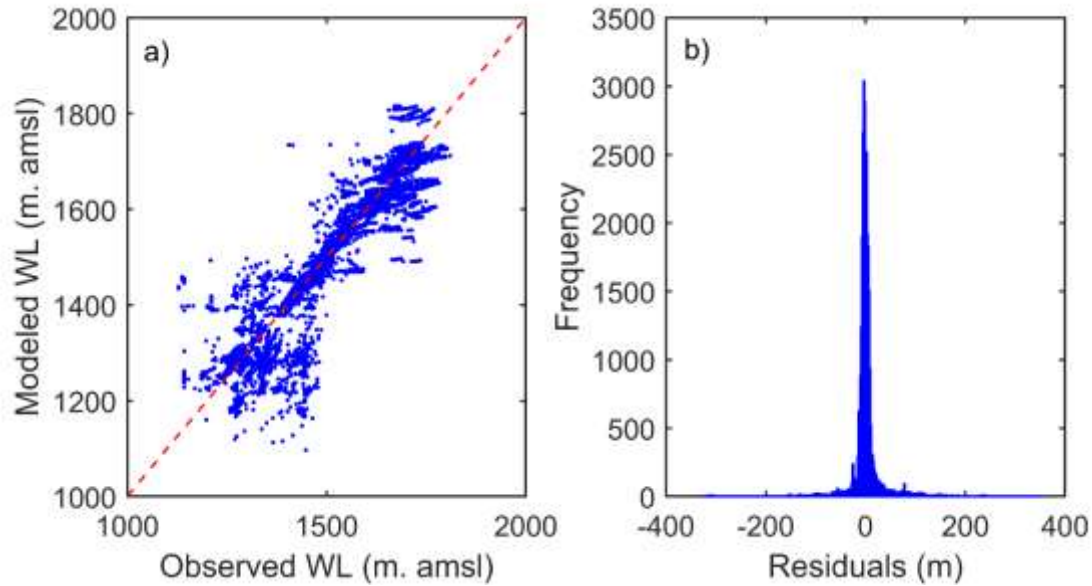


Fig. 8: a) Modeled versus observed water levels for the Laramie-Fox Hills wells; b) histogram of residuals.

Table 3: Residuals – mean, standard deviation, Absolute Value Error (AVE), Nash-Sutcliffe efficiency coefficient (NSCE), and Root Mean Square Error (RMSE) for the three aquifers

Aquifer	μ (m)	σ (m)	AVE	NSCE	RMSE
Denver	-0.74	15.0	11.7	0.78	30.66
Arapahoe	0.40	18.4	9.6	0.77	15.77
Laramie-Fox Hills	3.0	33.2	1.6	0.79	18.03

Statistics shown at table 3 supports that the model can be used in modelling water levels at different hydrogeological settings. Nash-Sutcliffe efficiency coefficient (NSCE) values for individual Laramie Fox Hills wells are presented in Table 4. Similar data are presented in SI for the Denver and Arapahoe Aquifer wells. NSCE for individual wells range from 0.52 to 0.92 for the Laramie Fox-Hills wells. LFH 7 is an apparent outlier in the data set. Overall, the fit

supports the validity of using the analytical model to predict water levels in at pumping well in ASR well fields.

Table 4: NSCE for Laramie Fox-Hills Aquifer wells

Well	NSCE
LFH-1A	0.58
LFH-2	0.88
LFH-4	0.88
LFH-7	0.52
LFH-8R	0.81
LFH-9	0.89
LFH-10R	0.92
LFH-11	0.90
LFH-13	0.82
LFH-14R	0.84
LFH-15	0.90
All Wells	0.84

2.3.6 Comparison of modeled water levels with and without groundwater recharge

Observed (black dots), modeled with recharge (red solid line), and modeled without recharge (blue solid line) water levels for representative wells in LFH aquifer are presented in Fig. 9.

Comparisons between water levels with and without recharge, for chosen wells at Laramie Fox-Hills during recovery and no-flow period, are presented in Fig. 10. Water levels at individual wells show that water levels absent recharge would be up to 60 m lower at times immediately following groundwater recharge (2009-2011). However, the increase in recovery and the absence of recharge in the Laramie-Fox Hills Aquifer between 2012 and 2015 led to decrease in the difference between water levels with and without recharge scenarios. Water level differences of

~5 m at the end of the study period (e.g., 2015 at well LFH-4R) demonstrate that ASR sustains water levels at wells for many years after recharge stopped.

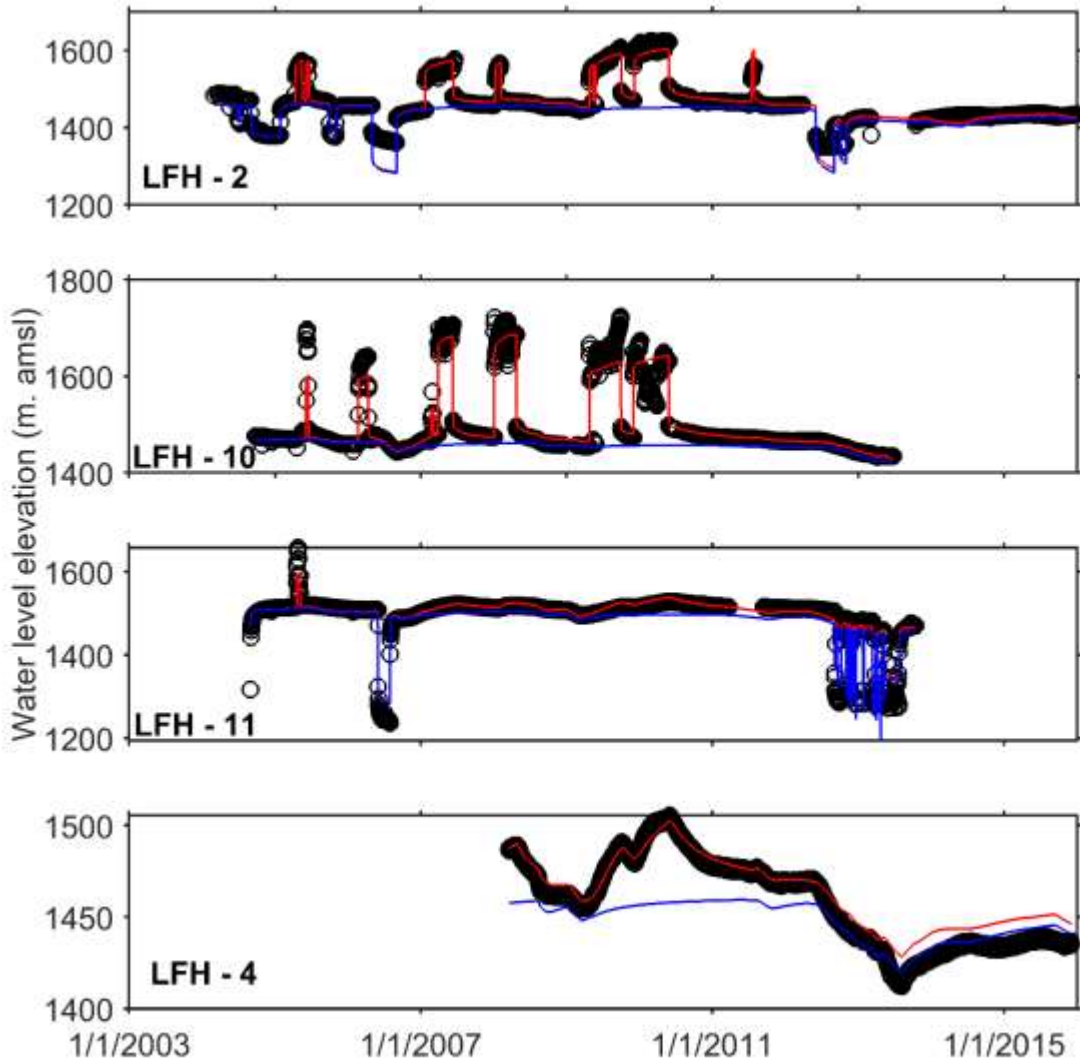


Fig. 9: Observed (black dots), modeled with recharge (red solid line), and modeled without recharge (blue solid line) water levels for representative wells in LFH aquifer.

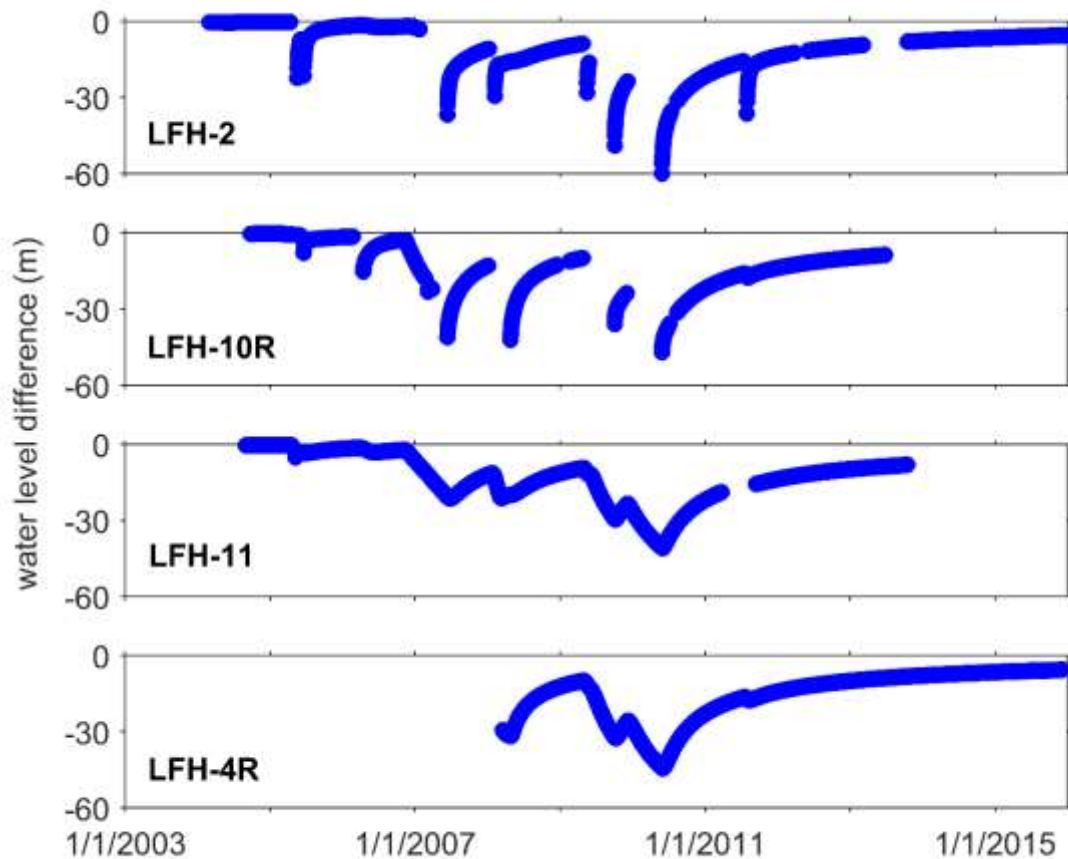


Fig. 10: Differences between modeled water levels with and without ASR during recovery and no-flow periods.

On average, historical recharge has increased average water levels by 3, 4, and 11 m in the Denver, Arapahoe, and Laramie Fox-Hills Aquifers, respectively (Fig. 11). Differences between water levels with and without recharge are smaller in the Denver and Arapahoe wells because of their higher recovery/recharge ratios and greater transmissivity values. The volumetric ratios of recovery to recharge are 8.9, 3.9 and 2 in the Denver, Arapahoe, and Laramie Fox-Hills Aquifers, respectively. Overall, groundwater recharge has helped sustain water levels in wells with the benefit of sustaining the aquifers' capacity to supply water and reducing the power cost associated with lifting groundwater out of the aquifers.

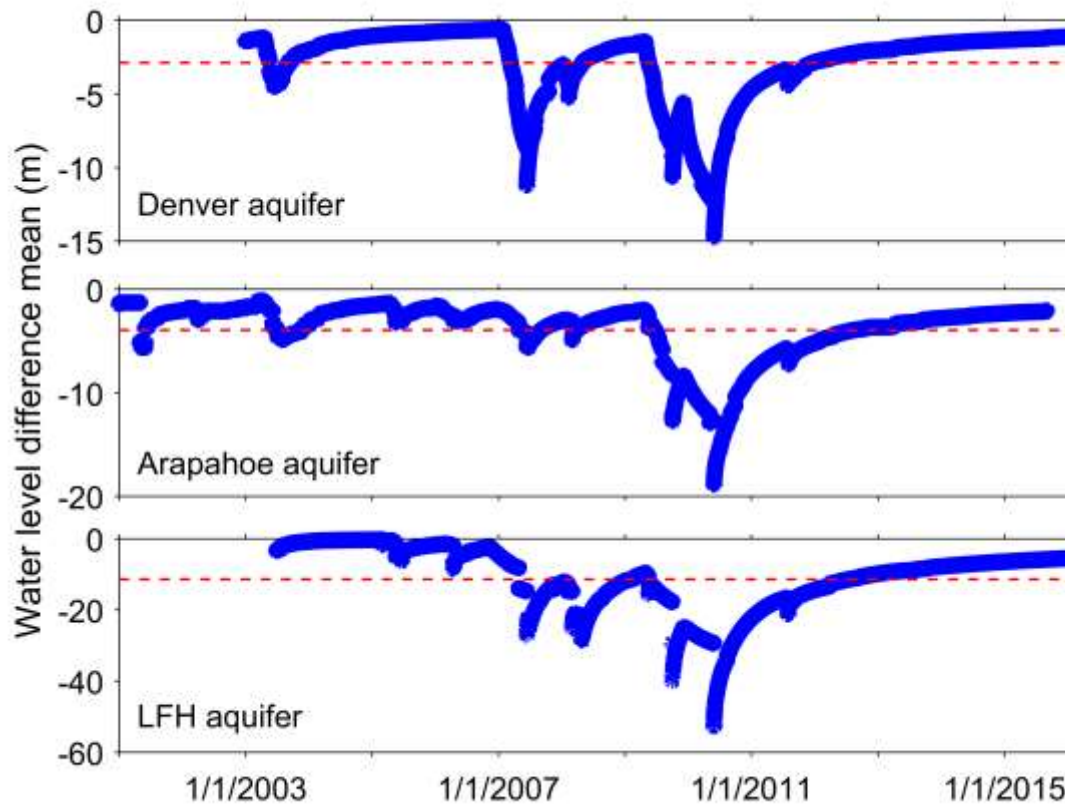


Fig. 11: Average of daily water level difference at wells with and without recharge for each aquifer (blue); all time average of water level difference at wells with and without recharge for each aquifer (red).

2.4 Summary

Extended production of groundwater from wellfields commonly leads to declining water levels at production wells and concern regarding the reliability of groundwater resources. ASR is a promising approach to sustaining water levels at production wells in wellfields. Herein, the analytical model of Lewis et al. 2016 is applied to three vertically stacked ASR wellfields using 15 years of pumping/recharge data, from 40 wells. During the study period, 45 million m^3 of groundwater is produced and 11 million m^3 is recharged, leading to a net withdrawal of 34 million m^3 of groundwater.

Dynamic water production and water-level data are used to resolve aquifer and well properties.

Close agreement between model best-fit and individual well aquifer test T and S values and

model and observed water levels supports the validity of using the analytical model for ASR wellfields. Rate of change in recoverable water levels in the Denver, Arapahoe and Laramie-Fox Hills wells are 0.20, -0.91, and -3.48 m per year, respectively. These modest rates of change, tied to a net withdrawal of 34 million m³, suggest the study aquifers can be a reliable source of water for many years to come. Estimated well loss coefficients for individual wells provide an important tool for scheduling well maintenance and provide insights regarding well losses during groundwater recharge and recovery.

Aquifer and well parameters derived from the analysis of dynamic pumping data are used to estimate water level absent the historical recharge. Water levels at individual wells shows that water levels absent recharge would be up to 60 m lower at times immediately following groundwater recharge. On average, historical recharge increased water levels by 3, 4, and 11 m in Denver, Arapahoe, and Laramie Fox-Hills aquifers, respectively. Benefits of sustaining water levels in wells include reduced energy requirements for lifting water out of aquifers, reduced well maintenance associated with keeping well screens submerged, and sustained well capacities. Critically, in the Denver Basin Aquifers, recharge enables groundwater extraction in excess of allowable annual allocations during periods of high demand including drought.

Overall, this work demonstrates the utility of the analytical model (Lewis et al. 2016) for the advancement of ASR. Furthermore, the benefits of ASR are documented with respect to sustaining water levels in wells in wellfields. Going forward, this manuscript sets a foundation for using the analytical model for optimizing operations and layout of ASR wellfields with respect to water levels at production wells.

Chapter 3 - Optimizing ASR Wellfield Operations to Minimize Energy Consumption²

Chapter synopsis

In a world that is ever more focused on energy efficiency and climate change, minimizing energy consumption associated with pumping groundwater is a growing concern. In this study, a simulation-optimization model (ASRSOM) is developed to optimize ASR wellfield operations. ASRSOM combines an analytical hydraulic model and a numerical optimization model to optimize wellfield operations. The objective function used to minimize energy consumption φ (L^4) is the temporal integral of the products of temporally varying total dynamic head values and pumping rates. Comparison of ASRSOM results to work by others for idealized aquifer operations supports the validity of ASRSOM. Four scenarios were simulated to evaluate the role that optimization of operations and aquifer recharge play in reducing the energy required to lift groundwater out of aquifer. A 10-year study period is considered using data from a municipal ASR wellfield. Optimization decreased φ by 19.6%, which yields an estimated reduction of 2,179 MW hours of power and 1,541 metric tons of atmospheric carbon. For the condition considered, recharge reduced power by 1%. The limited benefit of recharge is attributed to the small recharge volume in the case study and the short duration of the analysis. Additional opportunities to address economic and environmental impacts associated with lifting groundwater out aquifer include optimal positioning of ASR wells.

² Authors are: Abdulaziz Alqahtani, and Tom Sale

3.1 Introduction

The amount of energy required to lift groundwater out of aquifers can be substantial (Hansen et al. 2012; Ahlfeld and Lavery 2015). This is especially true in regions where groundwater is a primary water source. As an example, the state of California, USA, consumed 6,000 GWh of electricity to extract groundwater in 2010, (Bennett et al. 2010). Following USEPA (2019), this equates to an annual loading of 4.24 million metric tons of atmospheric carbon dioxide.

Moreover, the energy needed to lift groundwater out of aquifers tends to increase through time due to declining water levels associated with long-term pumping and increasing demands (Scott 2013). As such, both economic and environmental costs of groundwater extraction tend to increase with time. In a world that is ever more focused on energy efficiency and climate change, minimizing energy consumption associated with pumping groundwater is a growing concern.

Herein, consideration is given to the role that optimization of wellfield operations in aquifer storage and recovery (ASR) wellfields can play in minimizing energy needed to lift groundwater out of aquifers.

With respect to optimization of wellfield operations, Katsifarakis (2008) studied optimal flowrates for individual wells in a wellfield under steady-state conditions and concluded that pumping costs are minimized when hydraulic heads at all wells are the same. Furthermore, Ahlfeld and Lavery (2011 and 2015) evaluated optimal flowrates under 1) steady-state conditions and 2) transient-state conditions with constant flowrates. They concluded that pumping costs are minimized when “a stationarity condition” is met at all wells. Stationarity condition is defined as the condition where the value of $L + 2s_{aq}$ is the same at all wells at any point in time, where L (L) is the difference between elevation reference and recoverable water level, and s_{aq} (L) is the drawdown due to aquifer response. For transient conditions, Katsifarakis

et al. (2018) concluded that pumping cost at any instance in time is minimized when the instant differences between hydraulic head values at the locations of the wells are equal to half of the initial ones. Unfortunately, the pumping scheme considered by Katsifarakis (2008), Ahlfeld and Laverty (2011, 2015), and Katsifarakis et al. (2018) are highly idealized with respect to dynamic stresses typically found in water supply wellfields.

This manuscript advances the use of a groundwater simulation-optimization (GSO) model to minimize energy costs in dynamically pumped wellfields. GSO is an effective tool that has been used to satisfy single and multiple objectives including maximizing recharge and recovery rates from wellfields (Ebrahim et al. 2016), optimizing aquifers remediation (Ahlfeld 1990; Baú and Mayer 2006), conjunctive use of surface water and groundwater (Hernandez et al. 2014), planning new wellfields (Uddameri 2007; Arshad et al. 2014; Ebrahim et al. 2016), and controlling seawater intrusion (Abarca et al. 2006; Bray and Yeh 2008). Moreover, GSO can be used to minimize the energy/cost required to lift groundwater by optimizing wellfield operations. For example, by employing GSO, Bauer-Gottwein et al. (2016) optimized wellfield operations in a variable power price regime in Eastern Denmark by pumping water during times when energy was cheaper.

With respect to ASR, ASR is an artificial recharge technique that recharges available water through wells into aquifers and, subsequently, recovers the water when needed from the same wells (Pyne 2005). Common objectives for ASR include storing water for future use and sustaining water levels in aquifers. Alqahtani et al. (2019) studied ASR's role in sustaining water levels at wells in the Denver Basin and concluded that ASR is an effective approach for sustaining water levels and consequently reduces the power required to lift groundwater out of

aquifers. The effect of raising water level on minimizing energy consumption has yet to be studied.

A key challenge in minimizing energy associated with groundwater extraction is that production from water supply wellfield is commonly dynamic. Pumping rates at individual wells in water supply wellfields can vary on a daily basis, and annual demands can be highly dependent on yearly weather conditions. As such, optimizing pumping and recharge to minimize energy usage is a multi-period problem that requires dynamic solutions. In this paper, we introduce an ASR simulation-optimization model (ASRSOM) that uses an analytical model to simulate groundwater flow (Theis superposition) and a numerical optimization flowrate at wells through time. The objective of this paper is to advance novel modeling technique that minimize energy needed to lifting water out of aquifers by optimizing pumping and recharge rates in dynamic wellfields. Moreover, this paper evaluates the role that recharge and optimization of wellfield operations play in reducing the energy required to lift groundwater out of aquifers.

3.2 Methods

The following section describes a novel model developed in this study that is minimizing power consumption, tests used to evaluate the validity of the model, and four simulated scenarios used to demonstrate the merits of 1) optimization and 2) recharge in ASR wellfields.

3.2.1 Model

3.2.1.1 Objective function

The objective function used to minimize energy consumption φ (L^4) is the temporal integral of the products of temporally varying total dynamic head values and pumping rates:

$$\varphi = \int_{t_1}^{t_2} \sum_{m=1}^M TDH_m Q_m dt \quad (8)$$

where t_1 and t_2 (T) are the temporal bounds of the analysis, TDH (L) is total dynamic head, Q (L^3/T) is the well pumping or recharge rates, and M is the number of wells in a wellfield. TDH can be expanded as:

$$TDH(t, Q) = E_{dis} - h_0(t) + s_{aq}(t) + s_w(Q) + h_{lp}(Q) \quad (9)$$

where E_{dis} (L) is the elevation at which the well discharges to atmospheric storage, $h_0(t)$ is the time dependent recoverable water level in the aquifer, $s_{aq}(t)$ (L) is drawdown from the recoverable water level associated with pumping from all wells, and $s_w(Q)$ and $h_{lp}(Q)$ (L) are head losses associated with water moving from the aquifer into the well and water moving through conveyance piping to the atmospheric discharge point, respectively. Herein, it is assumed that E_{dis} can be treated as constant for all wells. Following Lewis et al. (2016) and Alqahtani et al. (2019), 1) $s_{aq}(t)$ is obtained via superposition of the Theis (1935) solution in space and time to account for temporally varying recovery or recharge stresses at all wells in a wellfield through time, and 2) $s_w(Q)$ is estimated as CQ^2 , where C is the well loss coefficient (T/L^5) with unique values for individual wells during recharge C_S and recovery C_R . Conveyance head losses $h_{lp}(Q)$ are treated as constant for all wells and correspondingly are neglected in the TDH value used in quantifying the objective function. Per Lewis et al. (2016) and Alqahtani et al. (2019), use of a continuous analytical solution for pumping-related drawdown, flow-dependent well losses, and temporally-varying recoverable water levels leads to rigorous predictions of water levels in wells in wellfields under complex, real-world pumping and recharge stresses.

Given the complexity of real-world recovery and recharge stresses, the temporal integral is estimated as follows:

$$\varphi = \int_{t_1}^{t_2} \sum_{m=1}^M TDH_m Q_m dt \approx \sum_{n=1}^{N_t} \sum_{m=1}^M \overline{TDH}_{m,n} \overline{Q}_{m,n} \Delta t_n \quad (10)$$

where N_t is the number of time increments at time t , $\overline{TDH}_{m,n}$ is total dynamic head, and $\overline{Q}_{m,n}$ is the pumping rate for individual wells over the period Δt_n (T).

3.2.1.2 Numerical optimization of operational rates

A built-in function (*fmincon*) in Matlab (MathWorks 2018) is used to iteratively solve for Q values for individual wells, in each time increment to minimize the objective function φ and correspondingly, power usage. *fmincon* is a nonlinear programming solver that optimizes certain parameters by minimizing the objective function considering specific constraints.

$$\varphi_{min} = fmincon\left(\sum_{n=1}^{N_t} \sum_{m=1}^M \overline{TDH}_{m,n} \overline{Q}_{m,n} \Delta t_n\right) \quad (11)$$

The components of \overline{TDH} governing the water levels in the pumped wells are $h_0(t)$, $s_{aq}(t)$, and $s_w(Q)$. Approaches for resolving $h_0(t)$ and $s_w(Q)$ are presented in Alqahtani et al. (2018). $s_{aq}(t)$ is resolved using:

$$s_{aq}(t) = s_{aq.N_t}(t) + s_{aq.N_{t+1}}(t) \quad (12)$$

$$s_{aq.N_t}(t) = \sum_{m=1}^M \left\{ \frac{Q_{m,0}}{4\pi T} W(u_{m,0}) + \sum_{n=1}^{N_t} \frac{\Delta Q_{m,n}}{4\pi T} W(u_{m,n}) \right\} \quad (13)$$

$$s_{aq.N_{t+1}}(t) = \sum_{m=1}^M \left\{ \frac{\Delta Q_{m,N_{t+1}}}{4\pi T} W(u_{m,N_{t+1}}) \right\} \quad (14)$$

$$u_{m,n}(t) = \frac{r_m^2 S}{4T(\Delta t_{m,n})}$$

where T is aquifer transmissivity (L^2/T), S is storativity (dimensionless), $Q_{m,0}$ is the initial pumping rate at time $t_{m,0}$ (L^3/T), ΔQ_{mn} is the change in pumping rate (L^3/T) at well m at time

increment n , W is the well function (dimensionless), and r_m is the radial distance from the point of interest to the individual pumped locations (L), where r_m is equal to the radius of the well if drawdown is calculated at the pumped well. Although recharge and recovery are optimized, objective function values are calculated for recovery only because there is no power needed for recharge.

Pumping/recharge rates at each time step are optimized within practical constraints, and, correspondingly, the objective function in Equation. 10 is minimized. Constraints include limiting head at wells, pump capacities, and total demand or recharge in a given time step. Head at wells are limited to upper and lower limits determined in advance (e.g., ground surface and half the saturated thickness of the aquifer):

$$h_{m.lower} \leq h_m \leq h_{m.upper} \quad (15)$$

where $h_{m.lower}$ and $h_{m.upper}$ (L) are the lower and upper limits of water level elevation at well m (h_m), respectively. Similarly, lower and upper pump capacities for each well ($Q_{m.lower}$ and $Q_{m.upper}$) (L³/T), for recharge and recovery, must be determined in advance. In this model, upper and lower pump capacities for each well are selected as the highest and lowest historical flowrate, respectively. Upper and lower pump capacities for individual wells are:

$$Q_{m.lower} \leq Q_m \leq Q_{m.upper} \quad (16)$$

The total stresses for all individual wells, in any time step n , must be equal to the total pumping or recharge stress on the aquifer.

$$\sum_{m=1}^M Q_{m,n} = D_n \quad (17)$$

where D_n is total demand or recharge (L^3/T) on the aquifer in a given time step.

3.2.1.3 Workflow

The workflow of the model is presented in Fig. 12. Steps include: 1) entering well locations, individual wells recharge/recovery stresses, and aquifer/well properties; 2) summing optimized recharge/recovery stresses from different wells to calculate the total temporal recharge/recovery stresses on the aquifer; 3) marching through time to estimate the hydraulic head at wells at the end of the current time increment (h_{N_t}); 4) optimizing wells flowrates for the next time increment $Q_{n=N_{t+1}}$; 5) repeating steps 3 and 4 to resolve flowrate until the last time increment N ; 6) summing daily φ value to obtain a final value of the objective function.

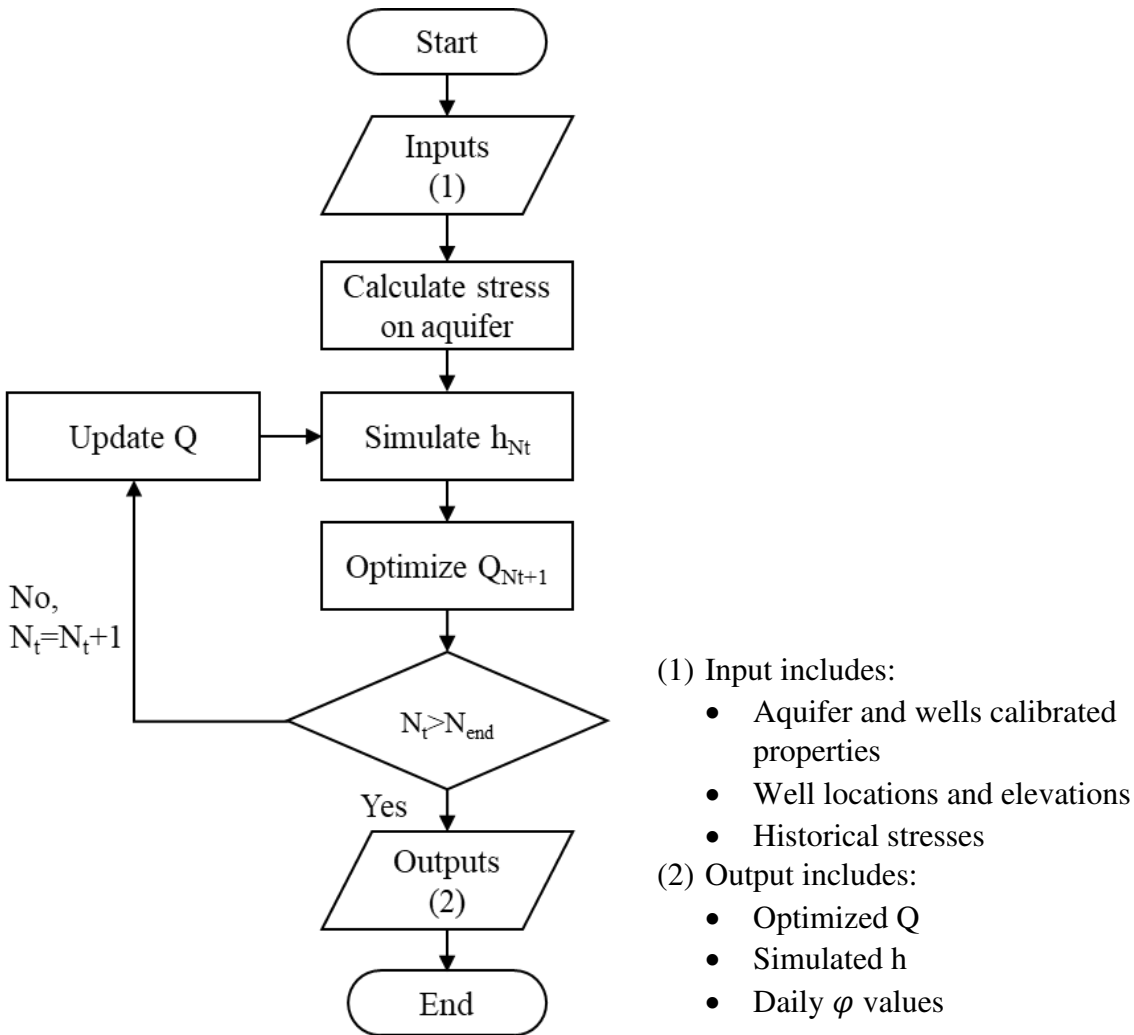


Fig. 12: Illustration of model workflow

3.2.1.4 Testing model validity

To test the validity of the mathematical approach and algorithms used in the model, the analytical model was applied to a hypothetical problem advanced by Katsifarakis et al. (2018). The hypothetical problem assumes an 8-well wellfield that is pumped for 18 hours with a total flowrate, for all wells, of 200 liter/second (86.4 m³/day). The goal of the hypothetical problem is to optimize individual well flowrates to minimize φ . Aquifer transmissivity and storativity are assumed to be 0.002 m²/second and 0.001, respectively. Full details of the example, including wells layout, are provided in Katsifarakis et al. (2018).

The hypothetical problem is solved using the steady-state solution derived in Katsifarakis (2008) and transient-state solution derived in Katsifarakis et al. (2018). Moreover, the problem is solved using the model proposed in this paper (ASRSOM). Comparisons of results from the models are used to evaluate the validity of ASRSOM in the results and discussion section.

3.2.1.5 Evaluation of operation optimization and recharge role in minimizing pumping energy

Data from an ASR wellfield in Highlands Ranch, Colorado, USA are used to demonstrate ASRSOM. Four scenarios are considered, including:

- Scenario #1 (historical): historical water levels and pumping data from the study ASR wellfield are used to calculate the objective function.
- Scenario #2 (optimized): the distribution of historical pumping and recharge stresses are optimized to minimize energy consumption using ASRSOM. Optimized pumping rates and modeled water levels in pumped wells are used to calculate the objective function. The difference between the objective function values for scenario #1 (historical) and scenario #2 (optimized) provides a basis for evaluating the benefits of optimizing wellfield operations.
- Scenario #3 (historical without recharge): historical recharge is removed from the historical stresses, water levels are predicted, and the objective function is calculated for historical water production only. The difference between the objective function values for scenario #3 (historical without recharge) and scenario #1 (historical) provides a basis for estimating reduction in energy consumption attributable to recharge.
- Scenario #4 (optimized without recharge): historical pumping without recharge is optimized using the model developed in this paper. Optimized pumping rates without

recharge and modeled water levels at pumped wells are used to calculate the objective function. The difference between the objective function values for scenario #3 (historical without recharge) and scenario #4 (optimized without recharge) provides a basis for evaluating the benefits of optimization of wellfield operations absent recharge.

A summary of the four scenarios simulated in this paper are presented in Table 5.

Table 5: Summary of the four scenarios simulated in this paper

Scenario	Historical Recovery	Historical Recharge	Optimized Flows
Scenario #1	Yes	Yes	No
Scenario #2	Yes	Yes	Yes
Scenario #3	Yes	No	No
Scenario #4	Yes	No	Yes

3.2.1.6 Study site

The study site is a municipal ASR wellfield operated by the Centennial Water and Sanitation, Highlands Ranch, Colorado, USA. Highlands Ranch is underlain by the Denver Basin Aquifers including, from shallow to deep, the Dawson, Denver, Arapahoe, and Laramie-Fox Hills (LFH) Aquifers. The aquifers are comprised of interbedded sandstones, siltstones, and shales. A detailed description of the hydrogeology of the Denver Basin Aquifers can be found in (Raynolds 2003; Barkmann et al. 2011). The Laramie-Fox Hills Aquifer, the aquifer studied in this paper, consists of 50 to 225 m of interbedded fine-grained sandstone, siltstone, and shale, based on visual geologic logs of cuttings collected at 3m intervals from 11 wells collected by the authors. Aquifer transmissivity and storativity from Alqahtani et al. (2019) are 14 m²/day and 1.3×10⁻⁴, respectively. The location of the wellfield and the locations of LFH well in the wellfield are presented in Fig. 13.



Fig. 13: Location of Highlands Ranch wells in the Laramie-Fox Hills (LFH) Aquifer. The red line on state of Colorado inset map indicates the extent of the Denver Basin Aquifer system.

Groundwater recovery and recharge from the Laramie Fox-Hills aquifer, during the 2003 to 2016 study period, were $5.31 \times 10^6 \text{ m}^3$ and $2.61 \times 10^6 \text{ m}^3$, respectively. The amount of recovered water is almost double the amount of recharged water, leading to net water withdrawal. Hydraulic stresses between 2006 and 2016 were optimized in this study. Hydraulic stresses prior to 2006 have been used to precondition the ground water flow model. For this case study, daily time step is chosen because of data availability. Full details about individual well's flowrates and water levels for all wells in the three aquifers are presented in Alqahtani et al. (2019). Total wellfield daily stresses for the LFH Aquifer are presented in Fig. 14.

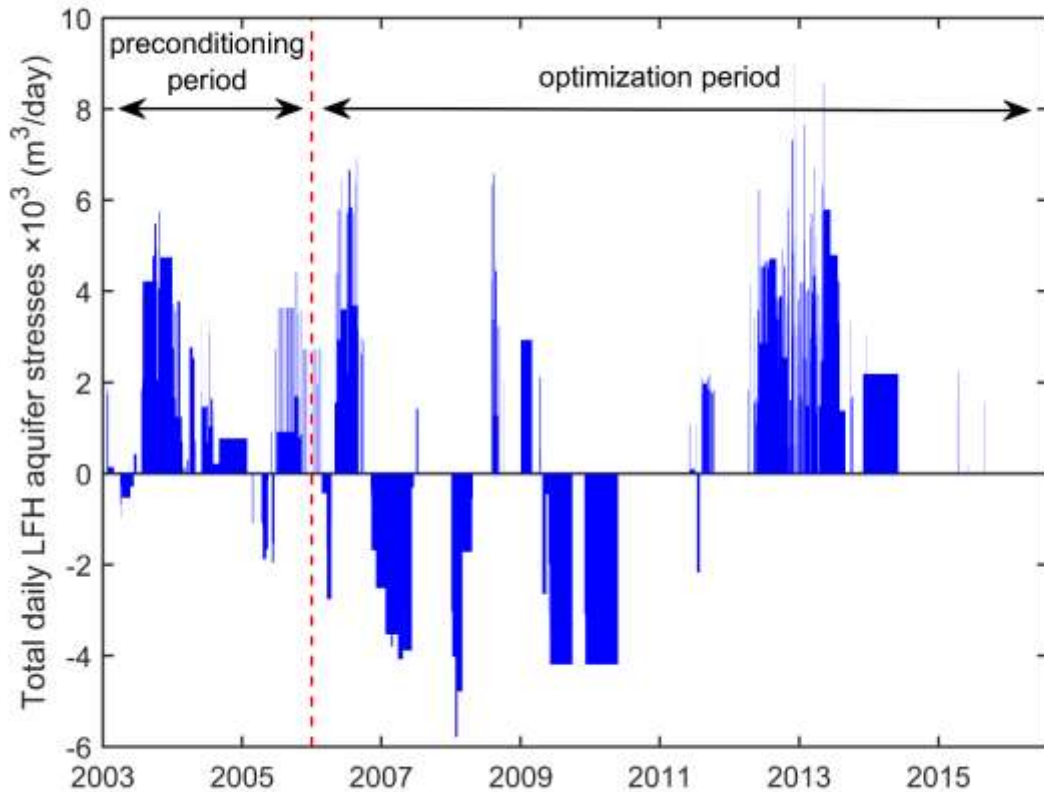


Fig. 14: Total daily wellfield stresses for all wells in the LFH Aquifer (recovery (+)/recharge (-)). Stresses prior to 2006 were used to precondition the model.

Wellhead elevation and calibrated properties for all wells in the LFH Aquifer from Alqahtani et al. (2019) are presented in Table 6. Calibrated properties include recoverable water levels (h_0), rate of change in recoverable water levels (α), well loss coefficients during recovery (C_R), and recharge (C_S). In this study, C values less than $10^{-5} \text{ day}^2/\text{m}^5$ were neglected by setting values to zero.

Table 6: Wellhead elevation and calibrated properties for all wells in the LFH Aquifer

Well	Wellhead elevation (m. amsl)	Recoverable water level		Well losses coefficient	
		h_0 (m. amsl)	α (m/year)	recovery (C_R) (days ² /m ⁵)	recharge (C_S) (days ² /m ⁵)
LFH-1A	1701.53	1483.78	-1.88	0	NA
LFH-2	1725.84	1486.34	-2.57	0	0
LFH-4R	1804.51	1475.39	-0.82	NA	NA
LFH-7	1793.48	1501.00	-3.51	0	0
LFH-8R	1864.64	1534.20	-3.15	3.43×10^{-4}	7.49×10^{-4}
LFH-9	1846.09	1516.97	-3.56	0	0
LFH-10R	1795.79	1493.93	-2.83	NA	4.67×10^{-4}
LFH-11	1774.94	1541.21	-3.49	3.3×10^{-4}	NA
LFH-13	1894.22	1530.96	-3.65	1.61×10^{-5}	0
LFH-14R	1848.44	1583.15	-7.07	0	3.05×10^{-3}
LFH-15	1907.18	1608.74	-7.80	NA	NA

As mentioned earlier, upper and lower pump capacities for each well were determined using historical flowrates. Assumed reasonable values were applied for wells that had insufficient historical data. For example, well LFH-10R has been used for recharge but not for recovery in the historical scenario. Therefore, LFH-10R was considered as an ASR well with recharge and recovery stresses. Moreover, LFH-1A and LFH-11 wells have not been used for recharge in the historical scenario, so they were considered as pumping wells only. LFH-4R and LFH-15 have not been used in either recharge or recovery. As such, they were categorized as observation wells with no active stresses.

The elevation of atmospheric discharge E_{dis} is assumed to be a constant for all wells in the wellfield (i.e., elevation of the storage tank). For this study, E_{dis} is set at the elevation of the highest wellhead, 1907.18 m amsl.

3.3 Results and discussion

3.3.1 Testing the validity of methods and computational algorithms

Fig. 15 presents the objective function φ versus time for the hypothetical 18-hour, 8-well test case advanced in Katsifarakis et al. (2018). Results are presented for the steady-state solution from (Katsifarakis 2008), the transient solution from Katsifarakis et al. (2018), and the transient ASRSOM advanced in this paper. Close agreement (within 0.1%) between the transient results supports the validity of the ASRSOM computational methods and the supporting algorithms. The limited differences between transient- and steady-state solutions can be attributed to steady water production over the brief (18-hour) period and the low stresses applied in the Katsifarakis et al. (2018) test scenario.

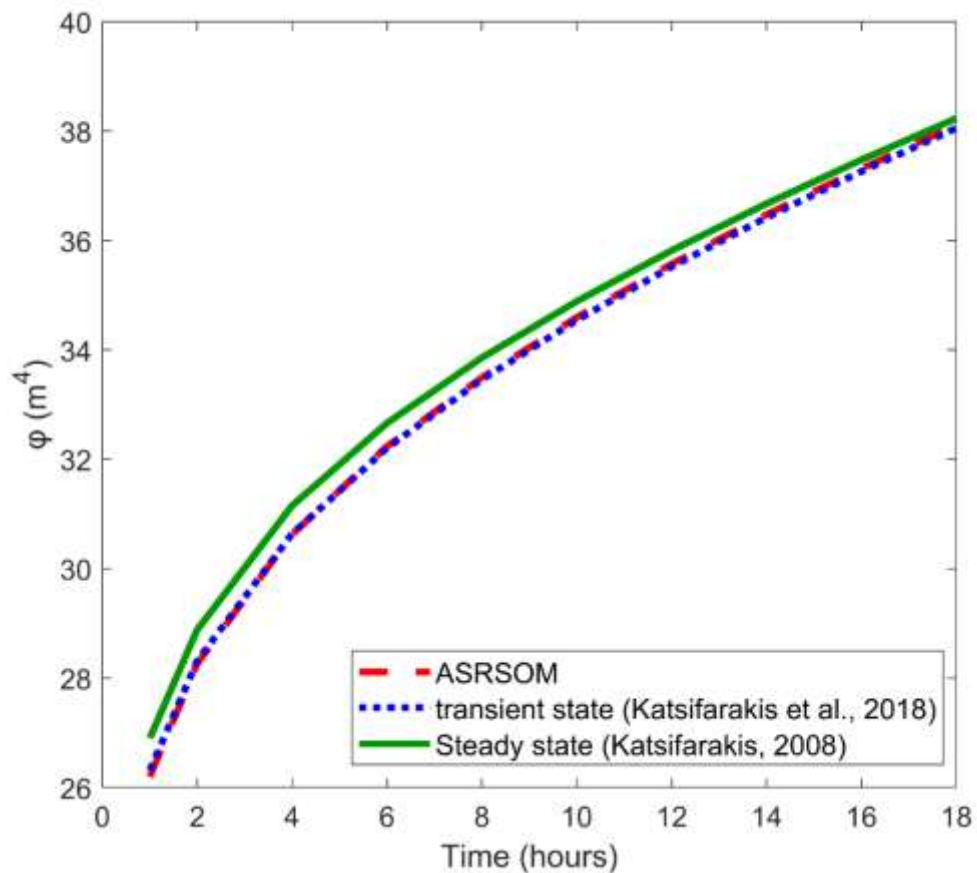


Fig. 15: Comparison of transient ASRSOM, transient Katsifarakis et al. (2018), and steady state (Katsifarakis 2008) objective function values through time.

3.3.2 Comparison of historical and optimized scenarios with recharge and recovery

The following section presents a comparison of historical and optimized scenarios (scenarios #1 and #2). First, consideration is given to how optimization reduced the objective function.

Secondly, consideration is given to how optimization altered the distribution of recovery and recharge and water levels.

3.3.2.1 Effect of optimization on the objective function

Fig. 16 presents cumulative daily φ values for historical and optimized scenarios for the 10-year study period. Cumulative objective function values are 2.04×10^9 and 1.64×10^9 m⁴ for historical and optimized scenarios, respectively. The cumulative φ value for optimized scenario is less than the cumulative φ value for historical scenario by 19.6%. Applying the gravitations coefficient, density of water, and an assumed pump-motor efficiency of 50% to the difference in the cumulative objective function values yields an estimated power saving, attributable to optimization, of 2,179 MW hours of power and 1,541 metric tons of atmospheric carbon. Actual operations of wellfields are constrained by additional factors not addressed in this paper, including the wellfields water treatment, water storage systems, and water distributions systems.

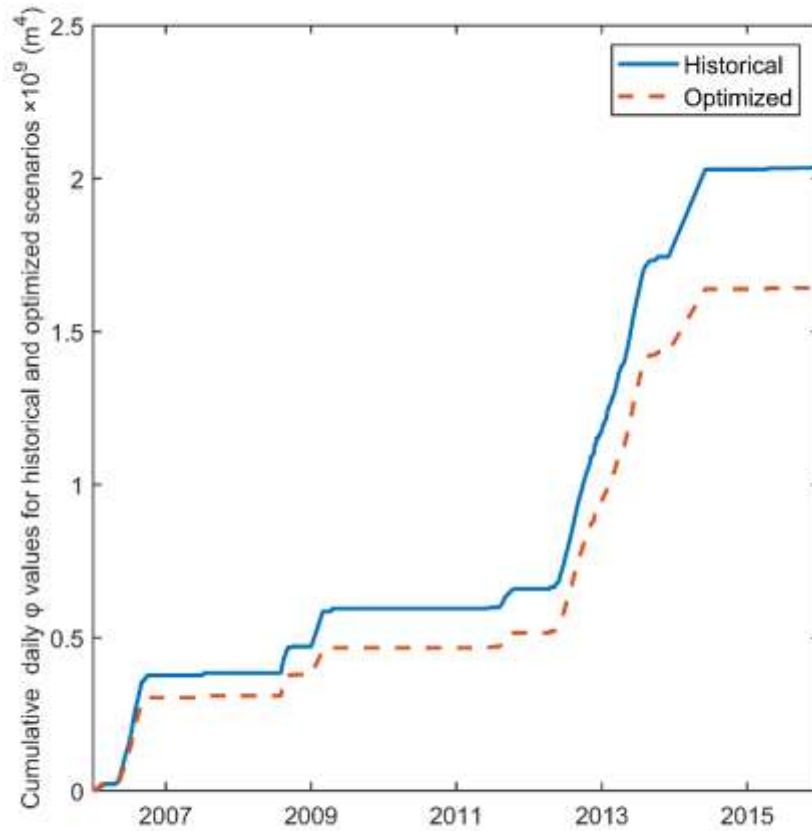


Fig. 16: Cumulative daily φ values for historical and optimized scenarios for the 10-year study period.

Fig. 17 presents daily differences between φ values for historical and optimized scenarios through time (historical φ minus optimized φ). The positive difference values describe the temporal variation in φ in the benefits of optimization. Periods with zero difference reflect times when no recovery occurred. During the 10-year study period, the φ value is negative for three days, showing that optimization succeeded in reducing the energy required to lift groundwater for all other days.

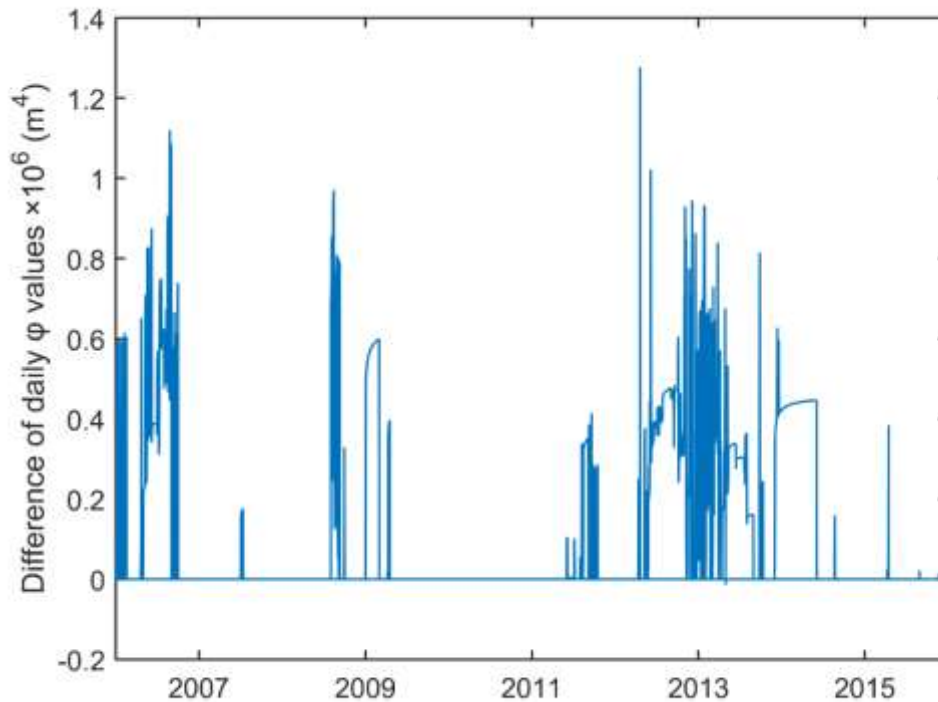


Fig. 17: Daily differences between ϕ values for historical and optimized scenarios (historical ϕ minus optimized ϕ).

3.3.2.2 Effect of optimization on distribution of recovery and recharge

Fig. 18 presents historical and optimized volumes of water stored and recovered from individual wells in the LFH Aquifer during the 10-year study period. The primary difference between historical and optimized scenarios is that optimized recovery and recharge is more uniformly distributed across all wells in the wellfield. In more detail, during the 10-year study historical analysis, 70% of the recovered groundwater came from three wells (LFH-7, LFH1A, and LFH-13), while the top three wells in the optimized scenario (LFH-13, LFH1A, and LFH-14R) account for only 30% of the recovered water.

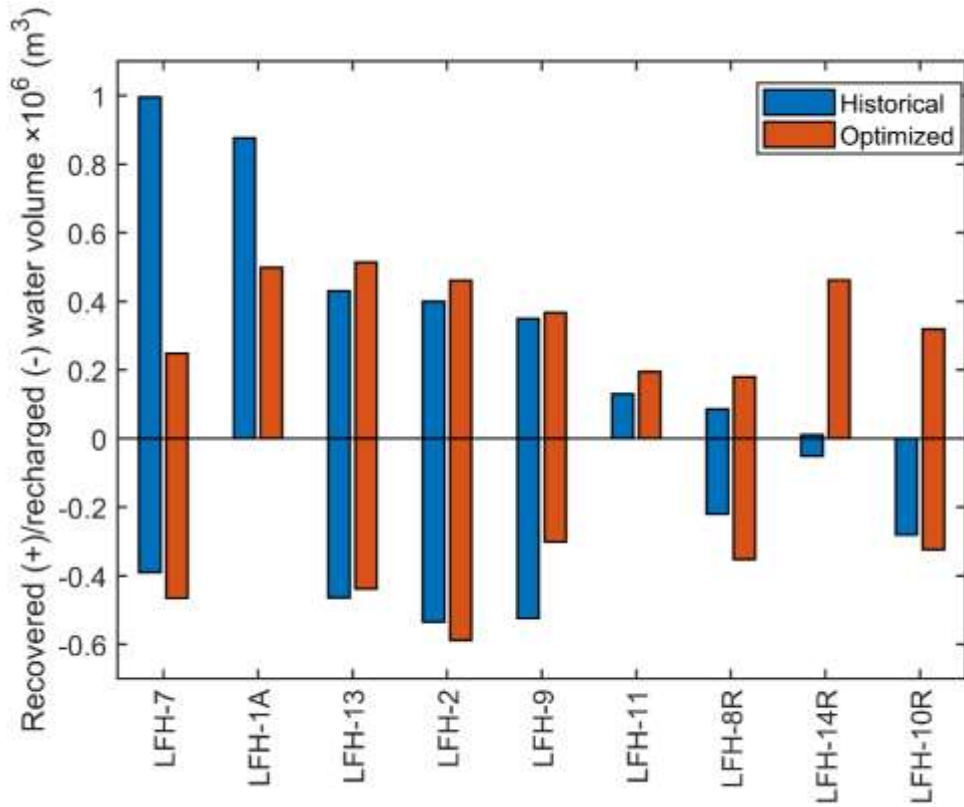


Fig. 18: Volume of water recovered (+) and recharged (-) from individual wells for the historical and optimized scenarios during the 10-year study period.

Furthermore, wells that have high well losses (LFH-8R and LFH-11) were among the least pumped wells in both scenarios. LFH-8R and LFH-11 were mostly avoided during recovery to minimize the energy required to overcome additional head losses from these wells' inefficiency. The inefficiency of some wells in the wellfield reduces the number of wells that could be used in recovery, thereby limiting the chance of reducing ϕ . Therefore, both constructing efficient wells and rehabilitating inefficient wells are important for minimizing energy consumption. It is noteworthy that including well losses during optimization is important to estimate actual *TDH* from different drawdown components.

3.3.2.3 Effect of optimization on water levels

Fig. 19 presents average water levels for historical and optimized scenarios for LFH wells.

Average water levels at the most pumped wells are lower than the average water levels at the least pumped wells. For example, wells LFH-7 and LFH-1A have the lowest average water levels among all other wells during historical scenario because they were the highest pumped wells. Moreover, the deviation of water levels from total average in the optimized scenario is less than the deviation in the historical scenario. The concept of reducing the variation between water levels at wells during operation is similar to the concept of stationarity (Ahlfeld and Laverty 2011, 2015) and to the optimal solutions derived by (Katsifarakis 2008; Katsifarakis et al. 2018).

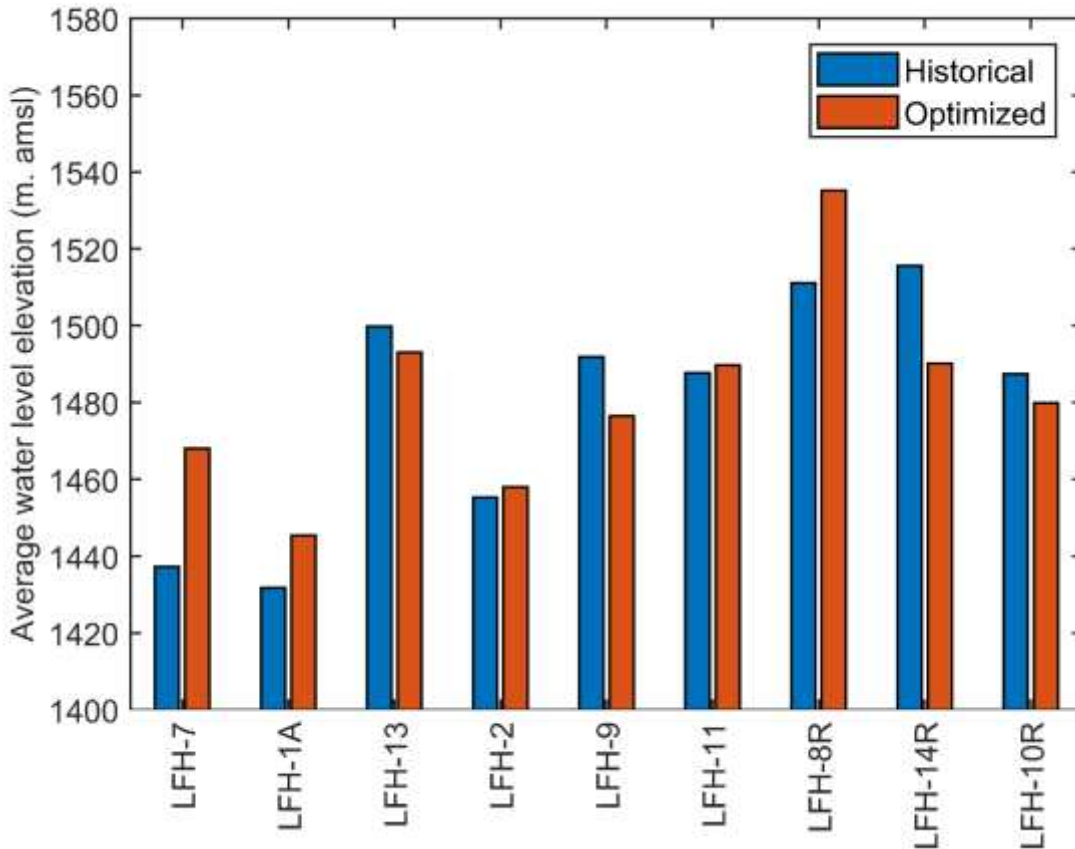


Fig. 19: Average water levels for historical and optimized scenarios at LFH wells.

3.3.3 Role of recharge in minimizing energy consumption

Table 7 presents the cumulative φ values for the four scenarios simulated in this paper.

Cumulative φ value for historical and historical without recharge scenarios (scenarios #1 and #3) are 2.04×10^9 and $2.06 \times 10^9 \text{ m}^4$, respectively. Similarly, cumulative φ values for optimized and optimized without recharge scenarios (scenarios #2 and #4) are 1.64×10^9 and $1.67 \times 10^9 \text{ m}^4$, respectively. The difference in cumulative φ between non-optimized scenarios (scenarios #1 and #3) of 1% and optimized scenarios (scenarios #2 and #4) of 1.8% shows that the importance of recharge is relatively small compared to operation optimization for this case study. The small effect of recharge on energy consumption is mainly due to the amount of water recovered from the aquifer being double the amount of water recharged, leading to net water withdrawal from the aquifer. The importance that recharge plays in reducing energy consumption is expected to increase with increasing recharge volumes and through extended periods of ASR operations.

Table 7: Cumulative φ values for the four scenarios (scenarios number in parentheses).

Cumulative φ value $\times 10^9 \text{ m}^4$	Non-optimized	Optimized	Optimization difference
Recharge	2.04 (#1)	1.64 (#2)	-19.6%
No recharge	2.06 (#3)	1.67 (#4)	-18.9%
Recharge difference	+1.0%	+1.8%	

3.3.4 Role of optimization in minimizing energy consumption in non-recharge scenarios

As discussed earlier, the difference in cumulative φ value between historical and optimized scenarios (scenarios #1 and #2) shows a reduction in the cumulative objective function by 19.6%. Similarly, optimization reduced the cumulative φ value of optimized without recharge scenario (scenario #4) by 18.9% compared to the cumulative φ value of historical without

recharge scenario (scenario #3). The difference between non-recharge scenarios (scenarios #3 and #4) of 18.9% provides further illustration of the utility of ASRSOM.

3.4 Summary and conclusion

In this study, a simulation-optimization model (ASRSOM) is developed to optimize ASR wellfield operations. ASRSOM combines an analytical hydraulic model and a numerical optimization model to optimize wellfield operations. The objective function used to minimize energy consumption φ (L^4) is the temporal integral of the products of temporally varying total dynamic head values and pumping rates. Comparison of ASRSOM results to work by others for idealized aquifer operations supports the validity of ASRSOM.

Four scenarios were simulated to evaluate the role that optimization of operations and aquifer recharge play in reducing the energy required to lift groundwater out of aquifers. Optimizing wellfields operation by distributing groundwater recovery among all available wells minimizes *TDH* and therefore φ . Cumulative objective function values are 2.04×10^9 and 1.64×10^9 m^4 for historical and optimized scenarios, respectively. The cumulative φ value for optimized scenario is less than the cumulative φ value for historical scenario by 19.6%, which indicates that the amount of energy consumed could be reduced by optimizing wellfield operations. The difference in the cumulative objective function values yields an estimated power saving, attributable to optimization, of 2,179 MW hours of power and 1,541 metric tons of atmospheric carbon.

During optimization, recharged and recovered water is uniformly distributed across all wells in the wellfield as compared to historical stresses. During the 10-year study historical analysis, 70% of the recovered groundwater came from three wells (LFH-7, LFH-1A, and LFH-13), while the top three well in the optimized scenario (LFH-13, LFH-1A, and LFH-14R) account for only 30%

of the recovered water. Moreover, avoiding or rehabilitating wells that have high well losses is important to minimize energy required to overcome such losses.

For this case study, recharge importance in minimizing energy consumption is relatively small compared to optimization of operation. The small effect of recharge on energy consumption is mainly due to the amount of water recovered from the aquifer being double the amount of water recharged, leading to net water withdrawal from the aquifer. The significance that recharge plays in reducing energy consumption is expected to increase with increasing volume and extended periods of recharge. Therefore, exploring such cases is required to assess the importance of higher recharge on water levels and reduction of energy consumption.

In conclusion, optimizing wellfield operations in ASR wellfields can substantially reduce the amount of energy required to lift groundwater out of aquifers. ASRSOM is a relatively simple model, since it adapts several assumptions (such as Theis' assumption) and neglects many operational factors (such as water rights and water quality). However, ASRSOM could be improved to fulfill the conditions of each case study separately. Additional opportunities to address economic and environmental impacts associated with lifting groundwater out aquifers include optimizing the position of ASR wells.

Chapter 4 - Factors Controlling Well-Spacing in ASR Wellfields³

Chapter synopsis

Over the past two decades, interest in Aquifer Storage and Recovery (ASR) has increased. The study of several factors that effects the design of ASR wellfields (well-spacing) is important to minimize cost. In this study, sensitivity analyses are performed on the main factors controlling ASR well-spacing and total variable cost. The main factors include aquifer transmissivity and storativity, wells flowrate, and frequency of recharge and recovery. The analysis is performed using a combination of hydraulic and cost models. The hydraulic model used to evaluate water levels at ASR wells is an analytical model relies on Theis superposition in time and space. The cost model is a simple model that calculates variables including cost of lifting groundwater out of the aquifer and piping cost needed for each well-spacing, and flowrate. It has been found that larger well-spacing is required for aquifers that has lower transmissivity and storativity, higher wells flowrate and frequency of recharge and recovery. However, because of the complexity of the problem, more work is needed to fully understand the optimal well-spacing of ASR wellfields under different conditions. In general, this work suggests that smaller well-spacing are plausible in ASR wellfields as compared to conventional production wellfields.

4.1 Introduction

Over the past two decades, interest in Aquifer Storage and Recovery (ASR) has increased. In the United States, for example, there were 25 ASR project that were operational in 1995. By 2016, there were more than 140 ASR wellfields with over than 500 ASR wells that operating in the U.S. (Pyne 2018; Dillon et al. 2019). Other countries embracing ASR include Australia, India,

³ Authors are: Abdulaziz Alqahtani, and Tom Sale

Canada and United Arab Emirates. ASR has proven to be economically efficient and can store a large amount of water with limited surface area (Pyne and Howard 2004; Zuurbier et al. 2013).

Different studies have evaluated the technical and economic potential of ASR wellfields.

Ebrahim et al. (2016), for example, evaluated the feasibility of managed aquifer recharge in Oman. The main goal of the study is to locate ASR wells to provide the maximum recharge and recovery rate in annual cycles.

ASR projects generally fit into the categories of 1) retrofits to existing wellfields and 2) development of new “Greenfield” wellfields. In the case of retrofits to existing wellfields, the spacing of wells is a given condition that was dictated by multiple factors including land use constraints, cost of transmission pipelines, and minimizing hydraulic interference between pumping wells. In the case of adding new ASR wells to an existing wellfield, or a Greenfield wellfield, the principles for spacing ASR wells in a wellfield are more complex. As an example, given similar volumes of storage and recovery, long-term drawdown interferences between wells can be reduced and, correspondingly spacing between ASR well can be reduced. Following the principles of the Theis equation (Theis 1935), appropriate spacings between ASR wells is a function of 1) targeted minimum and maximum water levels, 2) the frequency of storage and recovery, 3) well flow rates, 4) aquifer transmissivity, and to a lesser degree, aquifer storativity.

The principle factor guiding selection of spacing between ASR well is cost. According to Maliva et al., (2014), the major cost components for ASR wellfields can be divided into two main categories, capital cost and operational cost. Capital cost includes ASR wells, pipeline for water transmission, valves, land acquisition, ASR wells replacement cost, pipes replacement cost, feasibility and pilot studies, and engineering services. Operational cost includes power, labor, wells rehabilitation, Operational and maintenance (O&M) cost, pre- and post-water treatment,

and all other costs not included in the capital cost. Most of capital and operational costs are fixed costs for any well-spacing. However, piping and power costs are variable costs that change with the variation of well-spacing.

Piping and power required to lift groundwater out of aquifers are among the major cost elements in any ASR projects. As such, minimizing piping and power cost would minimize total project cost. Knowing best well-spacing for first installed wells in a wellfield, and parameters controlling well-spacing is helpful during preliminary studies and it could be adjusted for future wells after obtaining more data.

The main objective of this research is to evaluate the sensitivity of well-spacing to parameters controlling ASR well-spacing. Primary factors include aquifer parameter (transmissivity and storativity), well flowrate and the frequency of storage and recovery.

4.2 Methods

4.2.1 Hypothetical problem

A hypothetical situation is considered to evaluate the sensitivity of primary factors controlling well-spacing in ASR wellfields. Primary factors include aquifer transmissivity and storativity, wells flowrate, and frequency of storage and recovery. Fig. 20 shows three wells in an equilateral triangle layout that is used in this study. Well-spacing (l) ranging from 100 to 1500 m are considered in this study. Pipes length (d) that connects individual wells to water treatment plant (WTP) is calculated to estimate the cost of installing pipes for each well-spacing.

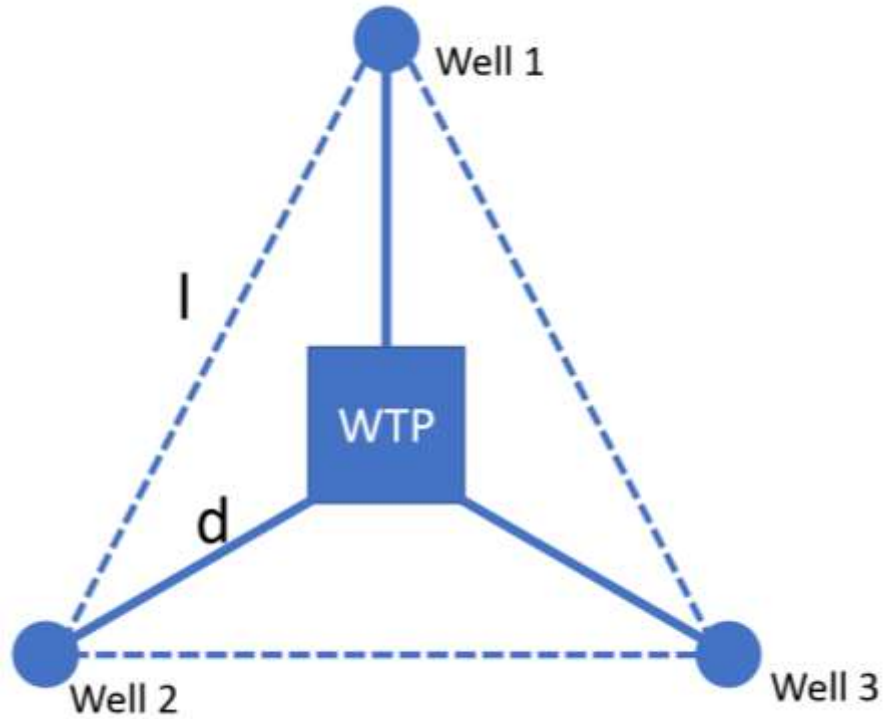


Fig. 20: The three wells in an equilateral triangle layout that is used in this study. WTP is water treatment plant, l is the distance between wells “well-spacing”, and d is the length of pipe connects wells to WTP.

4.2.2 Model

Cost and hydraulic models used in this study are presented in this section.

4.2.2.1 Cost Model

As discussed in the introduction, the major cost components of ASR wellfields can be divided into two main categories: capital cost and operational cost.

$$C_T = C_C + C_O \quad (18)$$

where C_T (USD) is total cost, C_C (USD) is capital cost and C_O (USD) is operational cost. Most of capital and operational costs are considered fixed costs for any well-spacing. However, piping and power costs are a variable costs that change with the variation of well-spacing. Herein, only variables cost (C_{va}) are considered during the sensitivity analyses.

$$C_{va} = C_{pi} + C_{po} \quad (19)$$

where piping cost C_p (USD) is calculated using the following equation:

$$C_{pi}(Q) = d \cdot C_{pu} \cdot \# \text{ of wells} \quad (20)$$

where d (L) is the distance between individual ASR wells and water treatment plant, C_{pu} (USD/L) is unit pipe cost and it include all costs involved in installing one unit of piping. Power cost can be calculated using the following equation:

$$C_{po}(Q) = \frac{Q \cdot TDH \cdot \rho \cdot g \cdot t \cdot C_{power}}{Eff} \quad (21)$$

where Q (L³/T) is the flowrate, TDH (L) is total dynamic head and will be calculated using the hydraulic model, ρ (M/L³) is water density, g (L/T²) is the acceleration of gravity, t (T) is the duration of pumping, C_{power} is the unit power price (USD/ PT), and Eff is the multiplication of pump and motor efficiencies and calculated using the following equation :

$$Eff = \text{pump efficiency} \cdot \text{motor efficiency} \quad (22)$$

Future power costs are discounted, using rate of return, to calculate present value. Present value is calculated using the following equation:

$$PV = \frac{FV}{(1 + i)^n} \quad (23)$$

where PV (USD) is the present value, FV (USD) is the future value, i is the rate of return (%), and n is the number of periods.

4.2.2.2 Hydraulic Model

The hydraulic model used in this study is an analytical model developed in Lewis et al. (2016). The model depends on the superposition of the Theis solution (Theis, 1935) in time and space to estimate drawdown at wells. The model was modified to include recharge stresses in ASR

wellfields in Alqahtani et al. (2019). In this study, the hydraulic model is used to calculate TDH that can be used to calculate power cost. Following Alqahtani et al. (2019), TDH can be expanded as:

$$TDH(t, Q) = E_{dis} - h_0(t) + s_{aq}(t) + s_w(Q) + h_{lp}(Q) \quad (24)$$

where E_{dis} (L) is the elevation at which the well discharges to atmospheric storage, $h_0(t)$ is the time dependent recoverable water level in the aquifer, $s_{aq}(t)$ (L) is drawdown from the recoverable water level associated with pumping from all wells, and $s_w(Q)$ and $h_{lp}(Q)$ (L) are head losses associated with water moving from the aquifer into the well and water moving through conveyance piping to the atmospheric discharge point, respectively. Herein, it is assumed that E_{dis} can be treated as constant for all wells. Moreover, $s_w(Q)$ and $h_{lp}(Q)$ are treated as constant for all wells and correspondingly are neglected in the TDH values.

4.2.3 Simulated scenarios

Table 8 shows the seven scenarios employed in this study. First scenario, the base scenario, has a flow frequency of 1-year and flowrates are 2725.5 and -2180.4 m³/day for recovery and recharge, respectively and aquifer storativity is 10⁻³. For the 3- and 5- years scenarios, flow frequency has changed to 3 and 5 years, from the base scenario, and all other parameters are kept the same. Fig. 21 shows the base, 3- and 5-years flow frequency recharge and recovery stresses for individual ASR wells. Comparison of the 3- and 5- years scenarios to the base scenario would help in understanding the sensitivity of total variable cost to different flow frequencies. For the high and low flowrate scenarios, flowrates are increased and decreased, compared to base scenario, by 1362.75 m³/day (250 gpm) and 1090.20 m³/day (200 gpm) for recovery and recharge, respectively. Comparison of high and low flowrate scenarios to the base scenario would help in understanding the sensitivity of total variable cost to different flowrates. For the

high and low S scenarios, aquifer storativity has increased and decreased, compared to base scenario, to 10^{-2} and 10^{-4} , respectively. Comparison of high and low S scenarios to the base scenario would help in understanding the sensitivity of total variable cost to different aquifer storativities. For all scenarios, transmissivity ranges from 10 to 100 m^2/day and well-spacing ranges from 100 to 1500 m.

Table 8: Seven scenarios simulated in this study. Differences from base scenarios are shaded.

Scenario	T (m^2/day)	Well-spacing (m)	Flow frequency	Recovery (m^3/day)	Recharge (m^3/day)	S
Base	10 to 100	100 to 1500	1- year	2725.5	-2180.4	10^{-3}
3- years	10 to 100	100 to 1500	3- years	2725.5	-2180.4	10^{-3}
5- years	10 to 100	100 to 1500	5- years	2725.5	-2180.4	10^{-3}
High flowrate	10 to 100	100 to 1500	1- year	4088.2	-3270.6	10^{-3}
Low flowrate	10 to 100	100 to 1500	1- year	1362.8	-1090.2	10^{-3}
High S	10 to 100	100 to 1500	1- year	2725.5	-2180.4	10^{-2}
Low S	10 to 100	100 to 1500	1- year	2725.5	-2180.4	10^{-4}

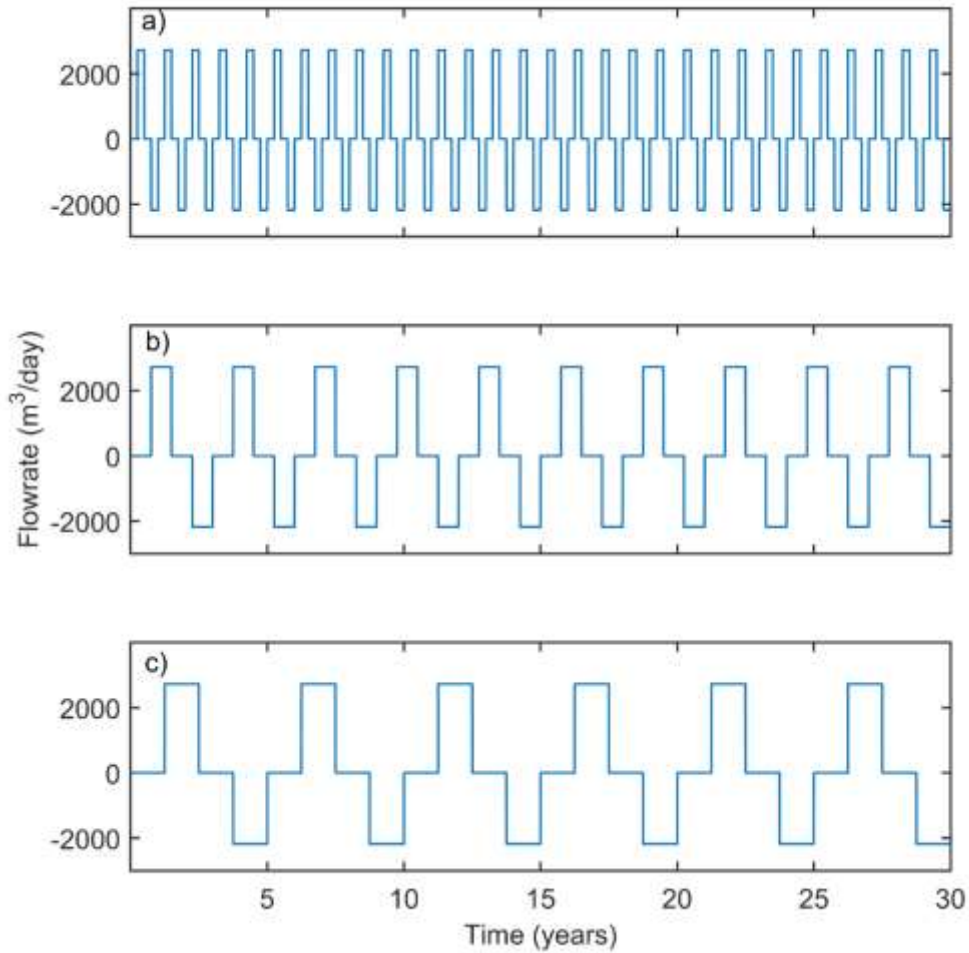


Fig. 21: Recovery (+) and recharge (-) stresses for individual ASR wells for different flow frequency, a) base b) 3-years c) 5-years scenario.

4.2.4 Parameters used in modelling

As stated in the introduction, this study evaluates the primary factors controlling well-spacing in ASR wellfields. Primary factors include aquifer properties (T and S), wells flow rates and frequency of recharge and recovery. Other parameters were considered constant for this analysis. Table 9 presents parameters used as inputs for the cost and hydraulic models and their values.

Table 9: Parameters used as inputs for the cost and hydraulic models and their values.

Parameters	Sensitivity Analysis?	Value
Transmissivity (T)	Yes	From 10 to 100 m ² /day
Storativity (S)	Yes	10 ⁻² , 10 ⁻³ or 10 ⁻⁴
Well-spacing	Yes	From 200 to 1800 m
Flow frequency	Yes	1,3, or 5 years
Flowrates	Yes	For each well: Recovery :2725.5 m ³ /day (500 gpm) ± 1362.75 m ³ /day (250 gpm) Recharge: 2180.4 m ³ /day (400 gpm) ±1090.20 m ³ /day (200 gpm)
Recoverable water level (h_0)	No	1500 m. amsl
Elevation at which the well discharges to atmospheric storage (E_{dis})	No	1700 m. amsl
Pump/Motor efficiency	No	0.7 for pump and 0.92 for motor (0.7*0.92=0.64) *
Power price to lift water	No	\$0.08 per kWh
Pipes cost per linear unit	No	Table 10
Rate of return	No	3%

* Based on mid-range for common pump and motor efficiencies from (Kauwale 2019)

Table 10: Pipe sizes and cost for different flowrates. Pipe size based on maximum 5 ft/sec flow. Pipe unit cost represent total cost include costs involved in installing one unit of piping

Flowrate (Recovery)	Pipe size (inch)	Unit total Cost
2725.5 m ³ /day (500 gpm)	8	213.25 USD/LM (65 USD/LF)
4088.24 m ³ /day (750 gpm)	8	213.25 USD/LM (65 USD/LF)
1362.75 m ³ /day (250 gpm)	6	193.5 USD/LM (59 USD/LF)

4.3 Results and discussion

The following present results for the base case scenario and variation from the base case scenario.

4.3.1 Base scenario

Fig. 22 shows power, piping, and total variable costs for T equal to $30 \text{ m}^2/\text{day}$ considering base scenario parameters. Well-spacing and power cost follow an exponential relationship. Especially, in well-spacing less than 600 m where the slope of the curve is steeper than the slope for well-spacing higher than 800 m . Higher drawdowns due to well interference occur with smaller well-spacing. The relationship between well-spacing and piping cost is a linear relationship. The total variable cost curve, combination of power and piping cost curves, shows how different well-spacing effect total variable cost. It can be seen that the lowest cost well-spacing is at 260 m for the assumed conditions. From that, we can see that small well-spacings are more feasible than wider well-spacing.

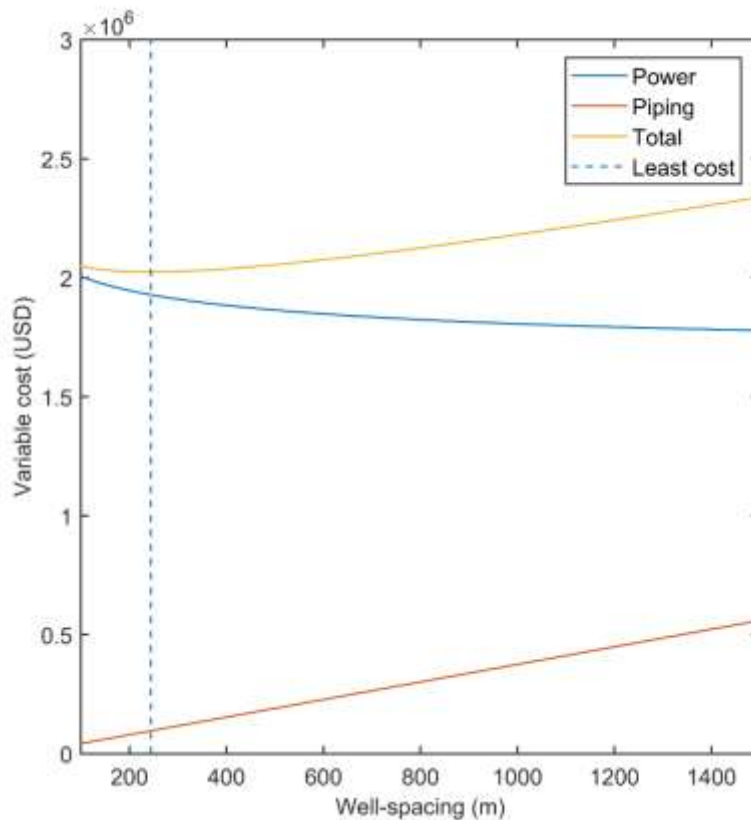


Fig. 22: Power, piping, and total variable costs for T equal to $30 \text{ m}^2/\text{day}$ in the base scenario ($S= 10^{-3}$, flow frequency of 1 year, $Q = 2725.5 \text{ m}^3/\text{day}$ for recovery and $-2180.4 \text{ m}^3/\text{day}$ for recharge).

Fig. 23 shows total variable costs for different transmissivities for base scenario. In general, total variable cost for low transmissivities is higher than total variable costs for low transmissivities. Moreover, least cost well-spacing in lower transmissivities is higher than least cost well-spacing in higher transmissivities. For example, least cost well-spacing for T equal to $10 \text{ m}^2/\text{day}$ is at 606 m, while the least cost well-spacing at T equal to $30 \text{ m}^2/\text{day}$ is at 260 m. The difference in total variable costs can be explained by higher drawdown in ASR wells in lower transmissivities which increase power cost. For high transmissivities, the difference between power cost, for different well-spacing, is lower than the difference between piping costs.

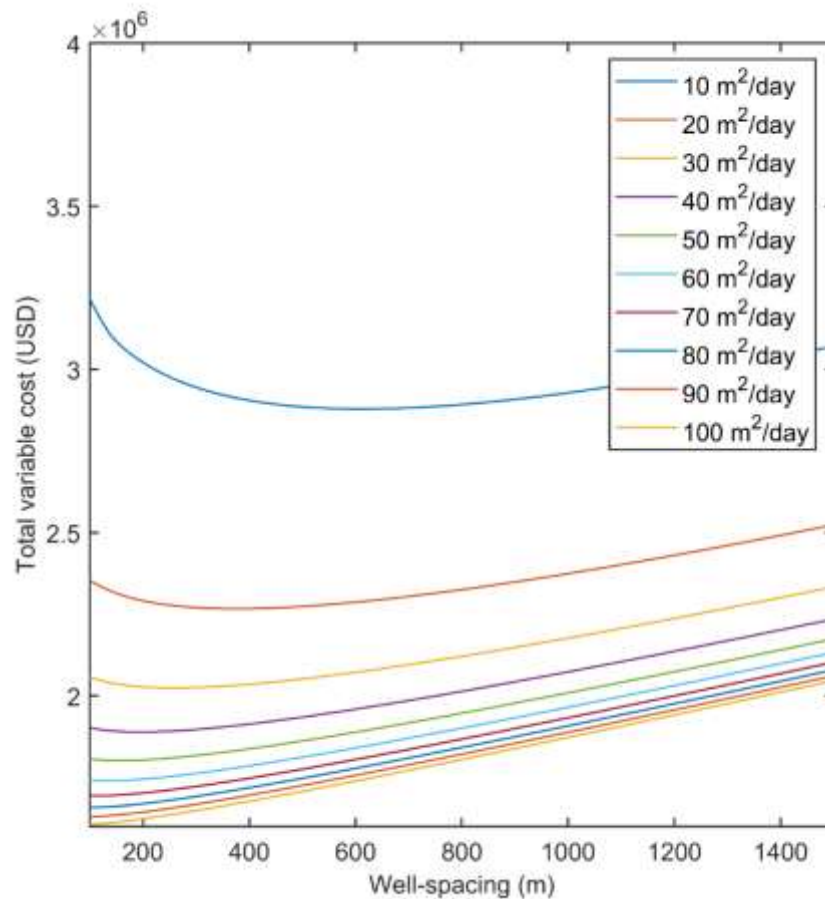


Fig. 23: Total variable costs for different transmissivities for base scenario ($S= 10^{-3}$, flow frequency of 1 year, $Q = 2725.5 \text{ m}^3/\text{day}$ for recovery and $-2180.4 \text{ m}^3/\text{day}$ for recharge).

4.3.2 Sensitivity analysis of well-spacing to flow frequency

Fig. 24 shows least cost well-spacing for base, 3-, and 5- years flow frequency scenarios as a function of transmissivity. Least cost well-spacing in 1 flow frequencies are larger than least cost well-spacing in base scenario. Especially in low transmissivities, where least cost well-spacing is larger than base case by more than 50%. The increase in well-spacing in higher flow frequency scenarios could be justified by greater well interference due to extended periods of recovery (pumping). It is worth mentioning that the difference between least well-spacing in 3- and 5- years scenario is small. Moreover, high flow frequency has minor effect on well-spacing in high transmissivities (higher than 60 m²/day).

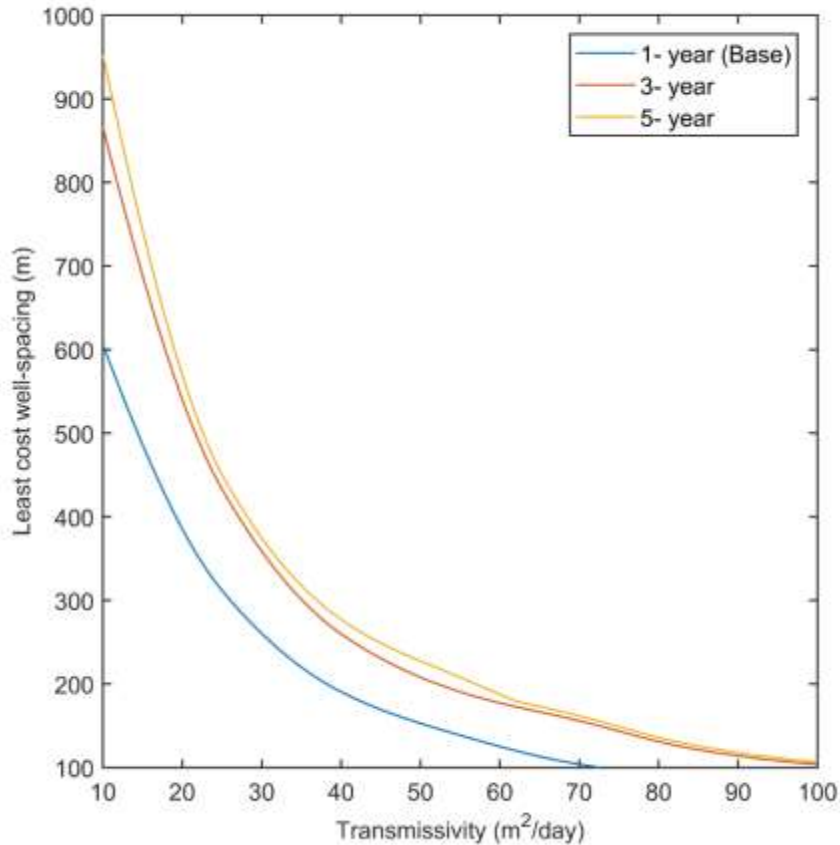


Fig. 24: Least cost well-spacing for base, 3-, and 5- years flow frequency scenarios as a function of transmissivity ($S = 10^{-3}$, $Q = 2725.5$ m³/day for recovery and -2180.4 m³/day for recharge).

4.3.3 Sensitivity analysis of well-spacing to wells flowrates

Fig. 25 shows least cost well-spacing for base, high, and low flowrate scenarios as a function of transmissivity. Least well-spacing cost for high flow frequency is higher than least cost well-spacing in base scenario in all transmissivities. The increase in flowrate by 50% has increased the least cost well-spacing by more than 80%, which shows the sensitivity of well-spacing to higher flowrates. Similarly, the decrease of flowrates by 50 % has decreased least cost well-spacing, compared to base scenario, by more than 100%.

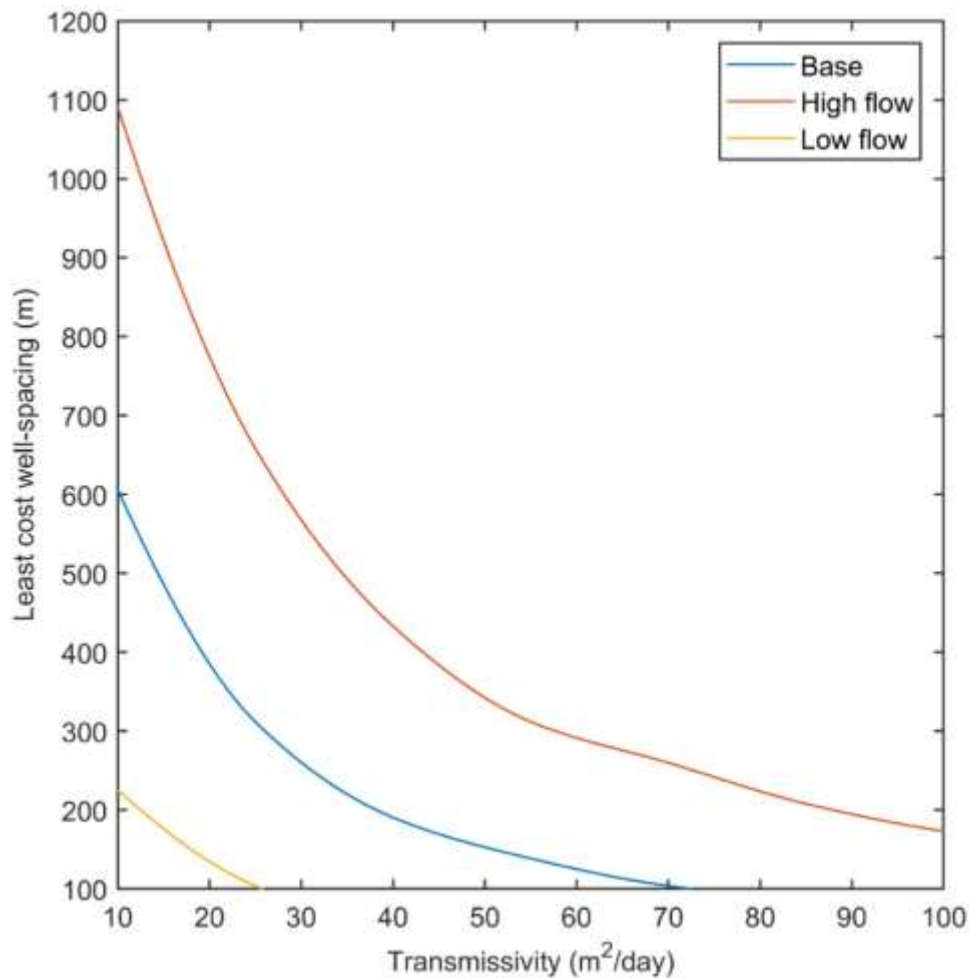


Fig. 25: Least cost well-spacing for base, high, and low flowrate scenarios as a function of transmissivity ($S= 10^{-3}$, flow frequency of 1 year)

4.3.4 Sensitivity analysis of well-spacing to S

Fig. 26 shows least cost well-spacing for base, high, and low storativity scenarios as a function of transmissivity. Least cost well-spacing for high transmissivity scenario is lower than base scenario. The lower well-spacing can be explained by lower drawdowns in ASR wells in aquifers that have higher storativities. Similarly, least cost well-spacing for low transmissivity scenario is higher than base scenario because of higher drawdowns. Small well-spacing (i.e. less than 40 m^2/day) is sensitive to storativity values. However, well-spacing in high transmissivities is relatively insensitive to storativity.

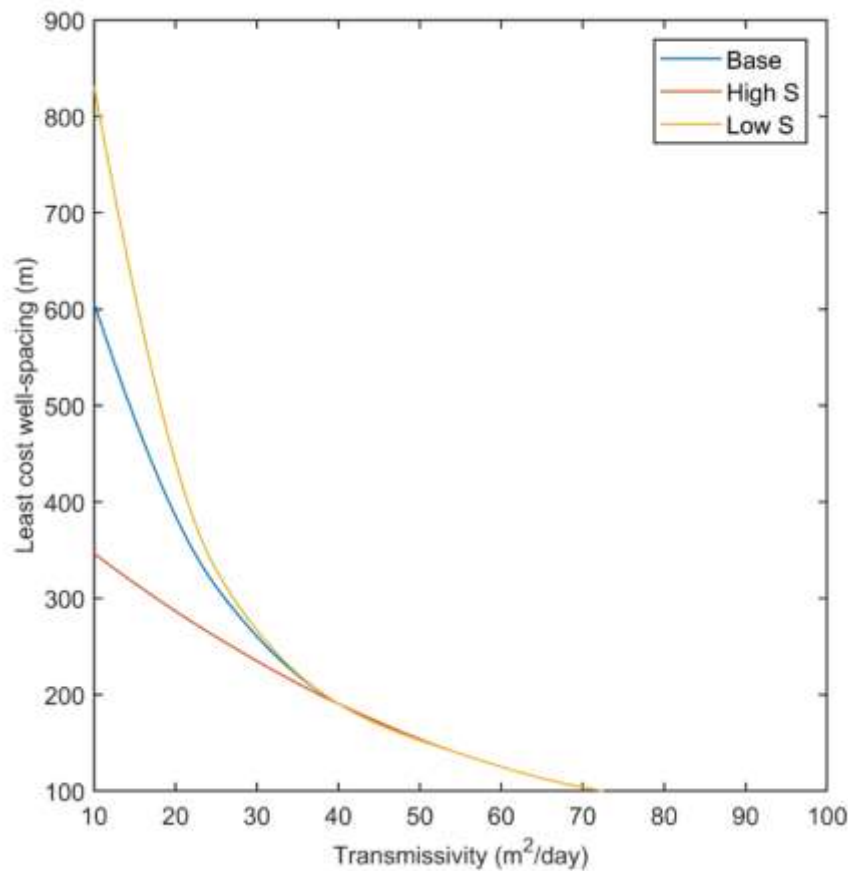


Fig. 26: Least cost well-spacing for base, high, and low storativity scenarios as a function of transmissivity (flow frequency of 1 year, $Q = 2725.5 \text{ m}^3/\text{day}$ for recovery and $-2180.4 \text{ m}^3/\text{day}$ for recharge).

4.4 Summary and Conclusion

In this study, sensitivity analyses are performed on the main factors controlling ASR well-spacing and total variable cost. The main factors include aquifer transmissivity and storativity, wells flowrate, and frequency of recharge and recovery. The analysis is performed using a combination of hydraulic and cost models. The hydraulic model used to evaluate water levels at ASR wells is an analytical model relies on Theis superposition in time and space. The cost model is a simple model that calculates variables including cost of lifting groundwater out of the aquifer and piping cost needed.

Seven scenarios were modeled to examine the sensitivity of ASR well spacing to multiple factors. Scenarios simulated include base scenario, where several assumptions were made, higher and lower aquifer storativity and wells flowrates, different timing of recharge and recovery. ASR well-spacing is sensitive to low aquifer transmissivity (lower than $50 \text{ m}^2/\text{day}$); which could be explained by high drawdowns in ASR wells in low transmissivities. On the other hand, ASR well-spacing is much less sensitive to high aquifer transmissivities (higher than $50 \text{ m}^2/\text{day}$). Moreover, ASR well-spacing is sensitive to high flow frequency of recharge and recovery as can be seen in the 3-year scenario. However, the sensitivity of ASR well-spacing to the 5-year flow frequency scenario is close to the 3-year scenario, which suggest that the relationship between ASR well-spacing and Flow frequency is not a linear relationship. For high flow scenario, ASR well-spacing increased for all transmissivities. Similarly with low flow transmissivity, where ASR well-spacing decreased for all transmissivities; which suggests that ASR well-spacing is sensitive to the change of flowrates for any transmissivity. From that, we can conclude that smaller well-spacings in ASR wellfields, compared to conventional wellfields, are promising and need to be considered during planning phase.

Current work can be expanded by including other parameters that were deterministic in this study. Additionally, including stochastic analysis in predicting water supply and demand using historical data would help narrowing the uncertainty and increase the reliability of the model outcomes. Moreover, including measures such as recovery efficiency, where other parameters such as water quality is considered, is important in planning new or expanding current wellfields. Other components of ASR wellfields, such as environmental aspects, should be considered during planning the location of new wells by performing cost benefit analysis to measure its benefits for all stakeholder. In conclusion, feasibility studies are a complicated process because of the variation between different case studies. Therefore, case by case detailed studies during planning ASR wellfields is advised.

Chapter 5 - Summary and Conclusion

In the first part of this study, the analytical model of Lewis et al. 2016 is modified and applied to three vertically stacked ASR wellfields using 15 years of pumping/recharge data, from 40 wells. Dynamic water production and water-level data are used to resolve aquifer and well properties. Close agreement between model best-fit and individual well aquifer test T and S values and model and observed water levels supports the validity of using the analytical model for ASR wellfields. Rate of change in recoverable water levels in the Denver, Arapahoe and Laramie-Fox Hills wells are 0.20, -0.91, and -3.48 m per year, respectively. These modest rates of change, tied to a net withdrawal of 34 million m³, suggest the study aquifers can be a reliable source of water for many years to come. Aquifer and well parameters derived from the analysis of dynamic pumping data are used to estimate water levels absent the historical recharge. Water levels at individual wells shows that water levels absent recharge would be up to 60 m lower at times immediately following groundwater recharge. On average, historical recharge increased water levels by 3, 4, and 11 m in Denver, Arapahoe, and Laramie Fox-Hills aquifers, respectively. Benefits of sustaining water levels in wells include reduced energy requirements for lifting water out of aquifers, reduced well maintenance associated with keeping well screens submerged, and sustained well capacities. Critically, in the Denver Basin Aquifers, recharge enables groundwater extraction in excess of allowable annual allocations during periods of high demand including drought.

In the second part of this study, a simulation-optimization model (ASRSOM) is developed to optimize ASR wellfield operations. ASRSOM combines an analytical hydraulic model and a numerical optimization model to optimize wellfield operations. The objective function used to

minimize energy consumption φ (L^4) is the temporal integral of the products of temporally varying total dynamic head values and pumping rates. Comparison of ASRSOM results to work by others for idealized aquifer operations supports the validity of ASRSOM. Four scenarios were simulated to evaluate the role that optimization of operations and aquifer recharge play in reducing the energy required to lift groundwater out of aquifers. Optimizing wellfields operation by distributing groundwater recovery among all available wells minimizes TDH and therefore φ . Cumulative objective function values are 2.04×10^9 and 1.64×10^9 m^4 for historical and optimized scenarios, respectively. The cumulative φ value for optimized scenario is less than the cumulative φ value for historical scenario by 19.6%, which indicates that the amount of energy consumed could be reduced by optimizing wellfield operations. The difference in the cumulative objective function values yields an estimated power saving, attributable to optimization, of 2,179 MW hours of power and 1,541 metric tons of atmospheric carbon.

During optimization, recharged and recovered water is uniformly distributed across all wells in the wellfield more than historical stresses. During the 10-year study historical analysis, 70% of the recovered groundwater came from three wells (LFH-7, LFH-1A, and LFH-13), while the top three well in the optimized scenario (LFH-13, LFH-1A, and LFH-14R) account for only 30% of the recovered water. Moreover, avoiding or rehabilitating wells that have high well losses is important to minimize energy required to overcome such losses. For this case study, recharge importance in minimizing energy consumption is relatively small compared to optimization of operation. The small effect of recharge on energy consumption is mainly due to the amount of water recovered from the aquifer being double the amount of water recharged, leading to net water withdrawal from the aquifer. The significance that recharge plays in reducing energy consumption is expected to increase with increasing volume and extended periods of recharge.

Therefore, exploring such cases is required to assess the importance of higher recharge on water levels and reduction of energy consumption.

In the third part of this study, sensitivity analysis is performed on the primary factors controlling spacing of wells in ASR wellfields. The main factors include aquifer transmissivity and storativity, wells flowrates, and the frequency of storage and recovery. Analyses are performed using a combination of hydraulic and cost models. The hydraulic model used to evaluate water levels at ASR wells is an analytical model relies on Theis superposition in time and space. The cost model is a simple model that calculate the cost of lifting groundwater out of the aquifer and calculate piping cost needed for each well-spacing.

Seven scenarios were modeled to examine the sensitivity of ASR well spacing to multiple factors. Scenarios simulated include base scenario, where several assumptions were made, higher and lower aquifer storativity and wells flowrates, different timing of recharge and recovery. ASR well-spacing is sensitive to low aquifer transmissivity (lower than $50 \text{ m}^2/\text{day}$); which could be explained by high drawdowns in ASR wells in low transmissivities. On the other hand, ASR well-spacing is much less sensitive to high aquifer transmissivities (higher than $50 \text{ m}^2/\text{day}$). Moreover, ASR well-spacing is sensitive to high flow frequency of recharge and recovery as can be seen in the 3-year scenario. However, the sensitivity of ASR well-spacing to the 5-year flow frequency scenario is close to the 3-year scenario, which suggest that the relationship between ASR well-spacing and Flow frequency is not a linear relationship. For high flow scenario, ASR well-spacing increased for all transmissivities. Similarly with low flow transmissivity, where ASR well-spacing decreased for all transmissivities; which suggests that ASR well-spacing is sensitive to the change of flowrates for any transmissivity. From that, we can conclude that

smaller well-spacings in ASR wellfields, compared to conventional wellfields, are promising and need to be considered during planning phase.

As discussed in the first chapter, this study examines several hypotheses to advance groundwater sustainability through ASR. These assumptions were tested in the second, third, and fourth chapters of this dissertation. In the second chapter, it was shown that the analytical model developed by Lewis et al. (2016) can be modified and used to predict water levels at wells in ASR wellfields. Moreover, it shows that artificial recharge through ASR wells can sustain water levels in wellfields. In the third chapter, it was shown that optimization of recharge and recovery can reduce power consumption and carbon footprint in ASR wellfields. Moreover, artificial recharge can reduce power consumption and carbon footprint in ASR wellfields. In the fourth chapter, it was shown that small well-spacing are feasible for ASR wellfields and should be considered during ASR wellfields design. However, the amount of assumptions were made suggests that more work is required to rigorously resolve the best spacing for wells in ASR wellfields.

To summarize, groundwater is the backbone of water supply systems for many countries around the world. Sustainable groundwater pumping can lead to groundwater depletion and decrease water levels at wells. Low water levels at wells would increase power consumptions to lift water out of aquifers and increase operational cost. Employing methods, such as artificial recharge through ASR wells and optimization of wells stresses, would help in sustaining water levels at wells and decrease power consumption and operational cost. Groundwater depletion can be mediated by storing water in aquifers (e.g. ASR) and decreasing demand on groundwater by operating wellfields to consider long-term drawdown at wells instead of meeting specific demand.

References

- Abarca E, Vázquez-Suñé E, Carrera J, Capino B, Gámez D, Batlle F (2006) Optimal design of measures to correct seawater intrusion. *Water Resour Res* 42:. doi: 10.1029/2005WR004524
- Ahlfeld D (1990) Two-stage ground-water remediation design. *J Water Resour Plan Manag* 116:517–529
- Ahlfeld D, Lavery M (2015) Field scale minimization of energy use for groundwater pumping. *J Hydrol* 525:489–495. doi: 10.1016/j.jhydrol.2015.03.065
- Ahlfeld DP, Lavery MM (2011) Analytical solutions for minimization of energy use for groundwater pumping. *Water Resour Res* 47:489–495. doi: 10.1029/2010WR009752
- Alley W, Healy R, LaBaugh J, Reilly T (2002) Flow and storage in groundwater systems. *Science* (80-) 296:1985–1990. doi: 10.1126/science.1067123
- Alqahtani A, Sale T, Ronayne MJ, Hemenway C (2019) Demonstration of Sustainable Development of Groundwater through Aquifer Storage and Recovery (ASR)- Manuscript submitted for publication
- Anderson MP, Woessner WW, Hunt RJ (2015) Forecasting and Uncertainty Analysis. In: *Applied Groundwater Modeling*. Elsevier, pp 443–491
- Arshad M, Guillaume J, Ross A (2014) Assessing the Feasibility of Managed Aquifer Recharge for Irrigation under Uncertainty. *Water* 6:2748–2769. doi: 10.3390/w6092748
- Barkmann PE, Dechesne M, Wickham ME, Carlson J, Formolo S, Oerter EJ (2011) Cross-

sections of the Fresh-water-bearing Strata of the Denver Basin between Greeley and Colorado Springs, Colorado. Denver

Baski Inc. C Baski Inflatable Packer, Downhole Flow Control Valves, Pitless Units and More.

<http://www.baski.com/>. Accessed 15 Mar 2018

Baú DA, Mayer AS (2006) Stochastic management of pump-and-treat strategies using surrogate functions. *Adv Water Resour* 29:1901–1917. doi: 10.1016/j.advwatres.2006.01.008

Bauer-Gottwein P, Schneider R, Davidsen C (2016) Optimizing Wellfield Operation in a Variable Power Price Regime. *Groundwater* 54:92–103. doi: 10.1111/gwat.12341

Bennett B, Park L, Sathe A, Rucker R, McBride W, Cannon L, Palermo E, Wang D, Gass M (2010) Embedded Energy in Water Studies Study 1 : Statewide and Regional Water-Energy Relationship Prepared by GEI Consultants / Navigant Consulting , Inc . California Public Utilities Commission Energy Division Managed by California Institute for Energy and Env. Energy

Bouwer H (2002) Artificial recharge of groundwater: Hydrogeology and engineering. *Hydrogeol J* 10:121–142. doi: 10.1007/s10040-001-0182-4

Bouwer H (1994) Role of groundwater and artificial recharge in future water resources management. *Futur Groundw Resour Risk* 491–497

Bray BS, Yeh WW-G (2008) Improving seawater barrier operation with simulation optimization in southern California. *J Water Resour Plan Manag* 134:171–180

Dillon P, Stuyfzand P, Grischek T, Lloria M, Pyne RDG, Jain RC, Bear J, Schwarz J, et al (2019) Sixty years of global progress in managed aquifer recharge. *Hydrogeol J* 27:1–30.

doi: 10.1007/s10040-018-1841-z

Dillon P, Vanderzalm J, Page D, Barry K, Gonzalez D, Muthukaruppan M, Hudson M (2016)

Analysis of ASR Clogging Investigations at Three Australian ASR Sites in a Bayesian Context. *Water* 8:442. doi: 10.3390/w8100442

Dillon PJ (2005) Future management of aquifer recharge. *Hydrogeol J* 13:313–316. doi:

10.1007/s10040-004-0413-6

Döll P, Hoffmann-Dobrev H, Portmann FT, Siebert S, Eicker A, Rodell M, Strassberg G,

Scanlon BR (2012) Impact of water withdrawals from groundwater and surface water on continental water storage variations. *J Geodyn* 59–60:143–156. doi:

10.1016/j.jog.2011.05.001

Domenico PA, Schwartz FW (1998) *Physical and chemical hydrogeology*. Wiley New York

Ebrahim GY, Jonoski A, Al-Maktoumi A, Ahmed M, Mynett A (2016) Simulation-Optimization

Approach for Evaluating the Feasibility of Managed Aquifer Recharge in the Samail Lower Catchment, Oman. *J Water Resour Plan Manag* 142:05015007. doi:

10.1061/(ASCE)WR.1943-5452.0000588

EPA (1990) Recommended Determination to Prohibit Construction of Two Forks Dam and

Reservoir Pursuant to Section 404 (c) of the Clean Water Act U . S . Environmental Protection Agency. 404:

Feng W, Zhong M, Lemoine JM, Biancale R, Hsu HT, Xia J (2013) Evaluation of groundwater

depletion in North China using the Gravity Recovery and Climate Experiment (GRACE) data and ground-based measurements. *Water Resour Res* 49:2110–2118. doi:

10.1002/wrcr.20192

Findikakis AN, Sato K (2011) Groundwater management practices. CRC Press

Handel F, Liu G, Dietrich P, Liedl R, Butler JJ, Haendel F, Liu G, Dietrich P, Liedl R, Butler JJ
(2014) Numerical assessment of ASR recharge using small-diameter wells and surface
basins. *J Hydrol* 517:54–63. doi: 10.1016/j.jhydrol.2014.05.003

Hansen AK, Madsen H, Bauer-Gottwein P, Falk AK V., Rosbjerg D (2012) Multi-objective
optimization of the management of a waterworks using an integrated well field model.
Hydrol Res 43:430. doi: 10.2166/nh.2012.142

Harbaugh AW (2005) MODFLOW-2005

Hemker CJ (2004) MicroFEM

Hernandez EA, Uddameri V, Arreola MA (2014) A multi-period optimization model for
conjunctive surface water-ground water use via aquifer storage and recovery in Corpus
Christi, Texas. *Environ Earth Sci* 71:2589–2604. doi: 10.1007/s12665-013-2900-3

Houben GJ (2015) Review: Hydraulics of water wells—head losses of individual components.
Hydrogeol J 23:1659–1675. doi: 10.1007/s10040-015-1313-7

Joodaki G, Wahr J, Swenson S (2014) Estimating the human contribution to groundwater
depletion in the Middle East, from GRACE data, land surface models, and well observations
Gholamreza. *Water Resour Res* 50:1–14. doi: 10.1002/2013WR014633. Received

Kabala ZJ (1994) Measuring distributions of hydraulic conductivity and specific storativity by
the double flowmeter test. *Water Resour Res* 30:685–690. doi: 10.1029/93WR03104

Karimi Askarani, K., Stockwell, E. B., Piontek, K. R., & Sale, T. C. (2018). Thermal Monitoring

- of Natural Source Zone Depletion. *Groundwater Monitoring & Remediation*, 38(3), 43-52.
<https://doi.org/10.1111/gwmr.12286>
- Katsifarakis KL (2008) Groundwater pumping cost minimization - An analytical approach.
Water Resour Manag 22:1089–1099. doi: 10.1007/s11269-007-9212-x
- Katsifarakis KL, Nikolettos IA, Stavridis C (2018) Minimization of Transient Groundwater
Pumping Cost - Analytical and Practical Solutions. *Water Resour Manag* 32:1053–1069.
doi: 10.1007/s11269-017-1854-8
- Katsifarakis KL, Tselepidou K (2009) Pumping cost minimization in aquifers with regional flow
and two zones of different transmissivities. *J Hydrol* 377:106–111. doi:
10.1016/j.jhydrol.2009.08.010
- Kauwale J (2019) Chilled Water Pump Design Guide. [https://www.engproguides.com/chilled-
water-pump-design.html](https://www.engproguides.com/chilled-water-pump-design.html)
- Khan S, Mushtaq S, Hanjra MA, Schaeffer J (2008) Estimating potential costs and gains from an
aquifer storage and recovery program in Australia. *Agric Water Manag* 95:477–488. doi:
10.1016/j.agwat.2007.12.002
- Konikow LF (2015a) Long-Term Groundwater Depletion in the United States. *Groundwater*
53:2–9. doi: 10.1111/gwat.12306
- Konikow LF (2015b) Long-Term Groundwater Depletion in the United States. *Groundwater*
53:2–9. doi: 10.1111/gwat.12306
- Konikow LF, Kendy E (2005) Groundwater depletion: A global problem. *Hydrogeol J* 13:317–
320. doi: 10.1007/s10040-004-0411-8

- Lewis AR, Ronayne MJ, Sale TC (2016) Estimating Aquifer Properties Using Derivative Analysis of Water Level Time Series from Active Well Fields. *Groundwater* n/a-n/a. doi: 10.1111/gwat.12368
- Lowry CS, Anderson MP (2006) An assessment of aquifer storage recovery using ground water flow models. *Ground Water* 44:661–667. doi: 10.1111/j.1745-6584.2006.00237.x
- Maidment DR (1993) *Handbook of Hydrology*. McGraw-Hill
- MathWorks (2018) Matlab (fmincon). <https://www.mathworks.com/help/optim/ug/fmincon.html>. Accessed 1 Jan 2018
- Mays LW (2013) Groundwater Resources Sustainability: Past, Present, and Future. *Water Resour Manag* 27:4409–4424. doi: 10.1007/s11269-013-0436-7
- McGuire V.L., Johnson M.R., Schieffer R.L., Stanton J.S., Sebree S.K., Verstraeten I.M. (2003) Water in Storage and Approaches to Ground-Water Management, High Plains Aquifer. 1243:
- Paschke SS, Banta ER, Capesius JP, W. Litke D (2011) Groundwater Availability of the Denver Basin Aquifer System, Colorado
- Prickett TA, Lonquist CG (1971) Selected digital computer techniques for groundwater resource evaluation
- Pyne D (2005) *Aquifer Storage Recovery: A Guide to Groundwater Recharge through Wells*, Second
- Pyne D (2018) GLOBAL INSIGHTS ON SUBSURFACE WATER STORAGE. In: *Subsurface Water Storage Symposium*. Fort Collins

- Pyne D, Howard JB (2004) Desalination/Aquifer Storage Recovery (DASR): a cost-effective combination for Corpus Christi, Texas. *Desalination* 165:363–367
- Raynolds RG (2003) Synopsis of the stratigraphy and paleontology of the uppermost Cretaceous and lower Tertiary strata in the Denver Basin, Colorado. *Rocky Mt Geol* 38:171–181. doi: 10.2113/gsrocky.38.1.171
- Reddy VR (2002) Water Security and Management: Lessons from South Africa. *Econ Polit Wkly* 37:2878–2881
- Rinck-Pfeiffer S, Ragusa S, Sztajn bok P, Vandavelde T (2000) Interrelationships between biological, chemical, and physical processes as an analog to clogging in aquifer storage and recovery (ASR) wells. *Water Res* 34:2110–2118. doi: 10.1016/S0043-1354(99)00356-5
- Ringleb J, Sallwey J, Stefan C (2016) Assessment of Managed Aquifer Recharge through Modeling—A Review. *Water* 2016, Vol 8, Page 579 8:579. doi: 10.3390/W8120579
- Robson SG (1987) Bedrock Aquifers in the Denver Basin, Colorado - A Quantitative Water-Resources Appraisal. *US Geol Surv* 73 p.
- Robson SG, Banta ER (1995) Ground-water atlas of the United States, segment 2, Arizona, Colorado, New Mexico, and Utah. U.S. Geological Survey Hydrologic Investigations Atlas HA-730C
- Sale T, Bailey A, Maurer A, Baker B, Hemenway C (2010) Studies Supporting Sustainable Use of the Denver Basin Aquifers in the Vicinity of Castle Rock Project report for the Town of Castle Rock
- Scanlon BR, Faunt CC, Longuevergne L, Reedy RC, Alley WM, McGuire VL, McMahon PB

- (2012) Groundwater depletion and sustainability of irrigation in the US High Plains and Central Valley. *Proc Natl Acad Sci* 109:9320–9325. doi: 10.1073/pnas.1200311109
- Scott CA (2013) Electricity for groundwater use: Constraints and opportunities for adaptive response to climate change. *Environ Res Lett*. doi: 10.1088/1748-9326/8/3/035005
- Shankar PSV, Kulkarni H, Krishnan S (2011) India's Groundwater Challenge and the Way Forward. *Econ Polit Wkly* xlvi:37–45. doi: 10.1061/41173(414)176
- Sterrett RJRRJ (2007) *Groundwater and Wells*, Third edit. Johnson Screens., New Brighton, MN
- Thakur VC, Jayangondaperumal R (2015) Seismogenic active fault zone between 2005 Kashmir and 1905 Kangra earthquake meizoseismal regions and earthquake hazard in eastern Kashmir seismic gap. *Curr Sci* 109:610–617. doi: 10.1038/nature08238
- Theis C V. (1935) The relation between the lowering of the Piezometric surface and the rate and duration of discharge of a well using groundwater storage. *Eos, Trans Am Geophys Union* 16:519–524. doi: 10.1029/TR016i002p00519
- Topper R, Raynolds B (2007) *Citizen's Guide to Denver Basin Groundwater*
- Uddameri V (2007) A dynamic programming model for optimal planning of aquifer storage and recovery facility operations. *Environ Geol* 51:953–962. doi: 10.1007/s00254-006-0458-z
- USEPA (2019) Greenhouse Gas Equivalencies Calculator. In: U.S. Environmental Prot. Agency. <https://www.epa.gov/energy/greenhouse-gas-equivalencies-calculator>. Accessed 2 Apr 2019
- Vanderzalm JL, Page DW, Barry KE, Dillon PJ (2010) A comparison of the geochemical response to different managed aquifer recharge operations for injection of urban stormwater in a carbonate aquifer. *Appl Geochemistry* 25:1350–1360. doi:

10.1016/j.apgeochem.2010.06.005

Voss KA, Famiglietti JS, Lo M, De Linage C, Rodell M, Swenson SC (2013) Groundwater depletion in the Middle East from GRACE with implications for transboundary water management in the Tigris-Euphrates-Western Iran region. *Water Resour Res* 49:904–914. doi: 10.1002/wrcr.20078

Wada Y, Van Beek LPH, Van Kempen CM, Reckman JWTM, Vasak S, Bierkens MFP (2010) Global depletion of groundwater resources. *Geophys Res Lett* 37:1–5. doi: 10.1029/2010GL044571

Ward JD, Simmons CT, Dillon PJ (2008) Variable-density modelling of multiple-cycle aquifer storage and recovery (ASR): Importance of anisotropy and layered heterogeneity in brackish aquifers. *J Hydrol* 356:93–105. doi: 10.1016/j.jhydrol.2008.04.012

Ward JD, Simmons CT, Dillon PJ (2007) A theoretical analysis of mixed convection in aquifer storage and recovery: How important are density effects? *J Hydrol* 343:169–186. doi: DOI 10.1016/j.jhydrol.2007.06.011

Ward JD, Simmons CT, Dillon PJ, Pavelic P (2009) Integrated assessment of lateral flow, density effects and dispersion in aquifer storage and recovery. *J Hydrol* 370:83–99. doi: 10.1016/j.jhydrol.2009.02.055

Zhou Y, Li W (2011) A review of regional groundwater flow modeling. *Geosci Front* 2:205–214. doi: 10.1016/j.gsf.2011.03.003

Zuurbier KG, Bakker M, Zaadnoordijk WJ, Stuyfzand PJ (2013) Identification de sites potentiels pour stockage en aquifère et récupération (ASR) dans les régions côtières en utilisant les

méthodes d'estimation de la performance de l'ASR. *Hydrogeol J* 21:1373–1383. doi:
10.1007/s10040-013-1003-2

Appendix A

Summary of aquifer properties for all wells based on 72-hour constant rates tests

Table A1

Transmissivity and storativity for the three aquifers

	Transmissivity (m ² /day)	Storativity	Transmissivity Range (m ² /day)		Storativity Range	
			Min	Max	Min	Max
Denver	38	1.50E-04	1.40E-04	3.00E-04	2.68E-01	3.96E+01
Arapahoe	91	1.01E-03	5.00E-05	1.49E-02	7.84E+01	2.30E+02
Laramie-Fox Hills	14	1.30E-04	6.00E-05	1.47E-02	7.45E-02	1.46E+01

Well properties for all Denver and Arapahoe Aquifer wells using the model of Lewis et al. (2016) modified for unique well loss coefficients for recovery and storage

Table A2

Denver wells properties

Well	h_0 (m. amsl)	α (m/year)	C_R (days²/m⁵)	C_S (days²/m⁵)
D4	1551.857	0.62	1.63E-05	NA
D8	1674.659	-1.70	3.40E-05	NA
D9	1656.44	2.44	0.00E+00	2.34E-14
D10A	1757.219	0.06	2.22E-14	NA
D11	1725.131	0.49	1.71E-04	NA
D12R	1692.582	-0.99	2.76E-05	NA
D13	1714.695	-2.34	1.47E-04	NA
D14	1712.479	3.40	1.70E-05	6.24E-06
D15	1711.463	-0.08	3.54E-05	NA
D16	1734.568	0.85	2.43E-14	NA
D17	1706.134	-1.07	7.88E-06	2.30E-14
D18	1725.294	-2.39	2.34E-14	NA
D19	1704.145	-0.47	2.23E-14	NA
D20	1685.692	6.63	2.22E-14	NA
TD5	1721.624	-1.39	5.29E-04	NA
TD6	1711.961	-4.16	5.44E-04	NA
TD7	1706.215	1.60	8.71E-07	NA
TD8	1702.262	-0.75	4.98E-05	NA
TD10	1726.697	-0.50	1.54E-04	NA

Table A3

Arapahoe wells properties

Well	h_0 (m. amsl)	α (m/year)	C_R (days²/m⁵)	C_S (days²/m⁵)
A1	1475.298	-0.19	2.34E-14	2.13E-05
A2	1494.462	-1.14	2.31E-14	1.77E-05
A3	1537.434	4.61	1.69E-04	1.00E-03
A5	1485.123	-0.15	7.73E-06	NA
A6	1507.092	-0.55	1.29E-05	5.07E-05
A7	1438.917	3.82	1.61E-06	3.99E-05
A8	1529.727	-1.41	2.92E-06	NA
A9	1491.93	-1.57	9.42E-06	2.88E-05
A10	1496.103	-2.77	2.34E-14	2.44E-06
A11	1518.27	-0.80	1.72E-06	7.61E-06
A12	1498.99	-1.02	2.22E-14	2.25E-05
A13	1496.684	-2.13	4.95E-06	NA

Comparison of modeled and observed water levels (with groundwater recharge) for all wells

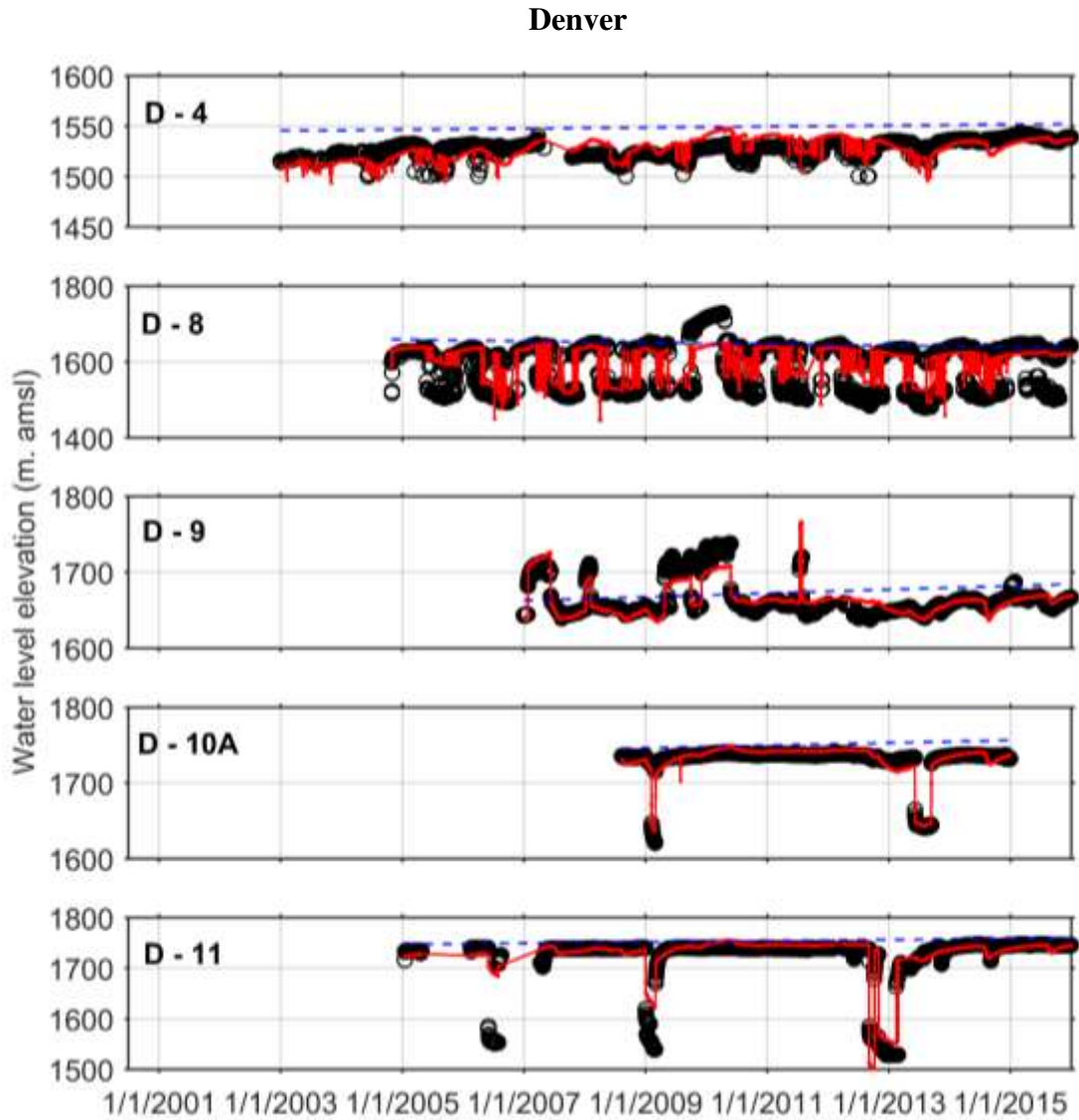


Fig. A1

Observed (black) and modeled (red) water levels and apparent recoverable water level (blue) for representative wells at the Denver Aquifer.

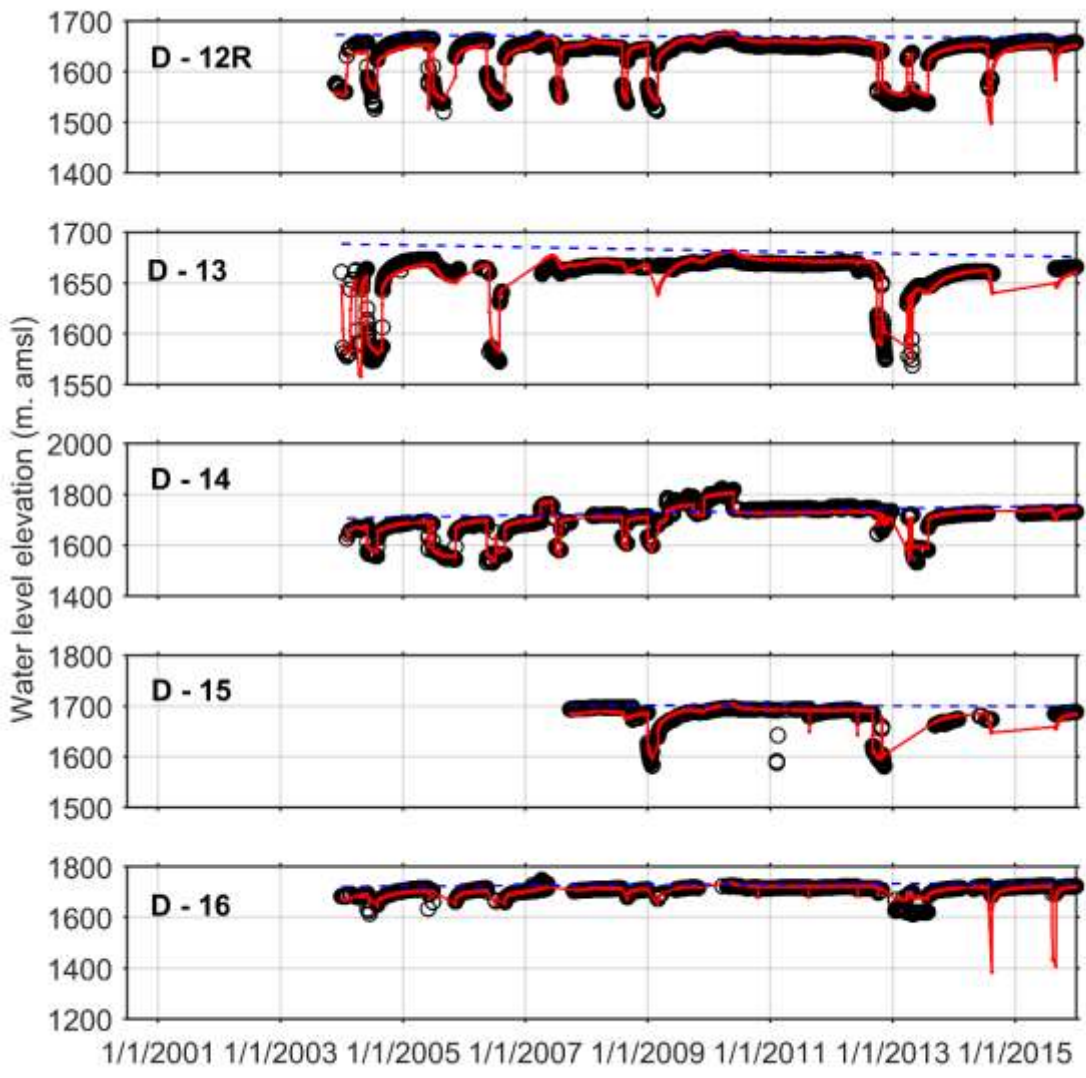


Fig. A2

Observed (black) and modeled (red) water levels and apparent recoverable water level (blue) for representative wells at the Denver Aquifer.

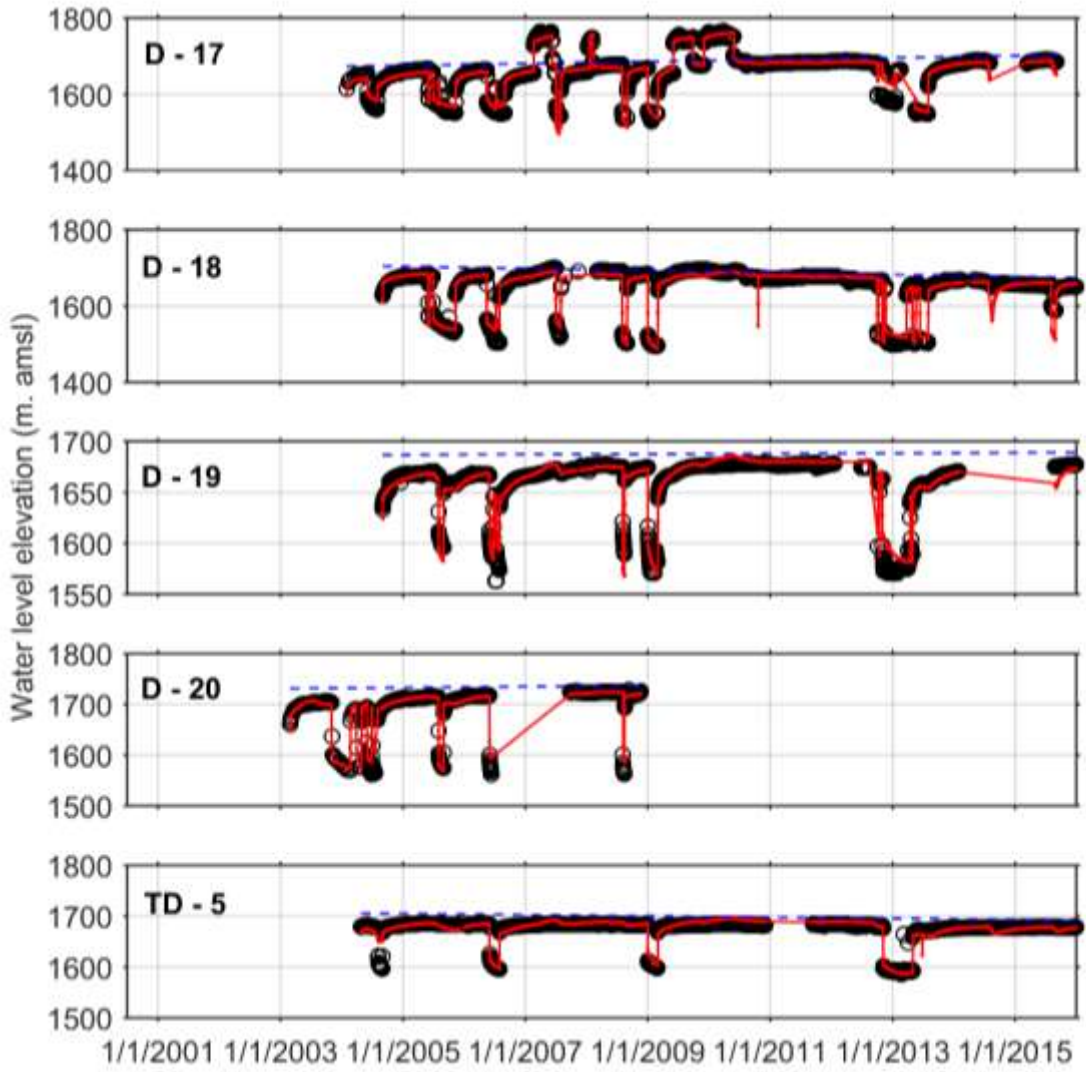


Fig. A3

Observed (black) and modeled (red) water levels and apparent recoverable water level (blue) for representative wells at the Denver Aquifer.

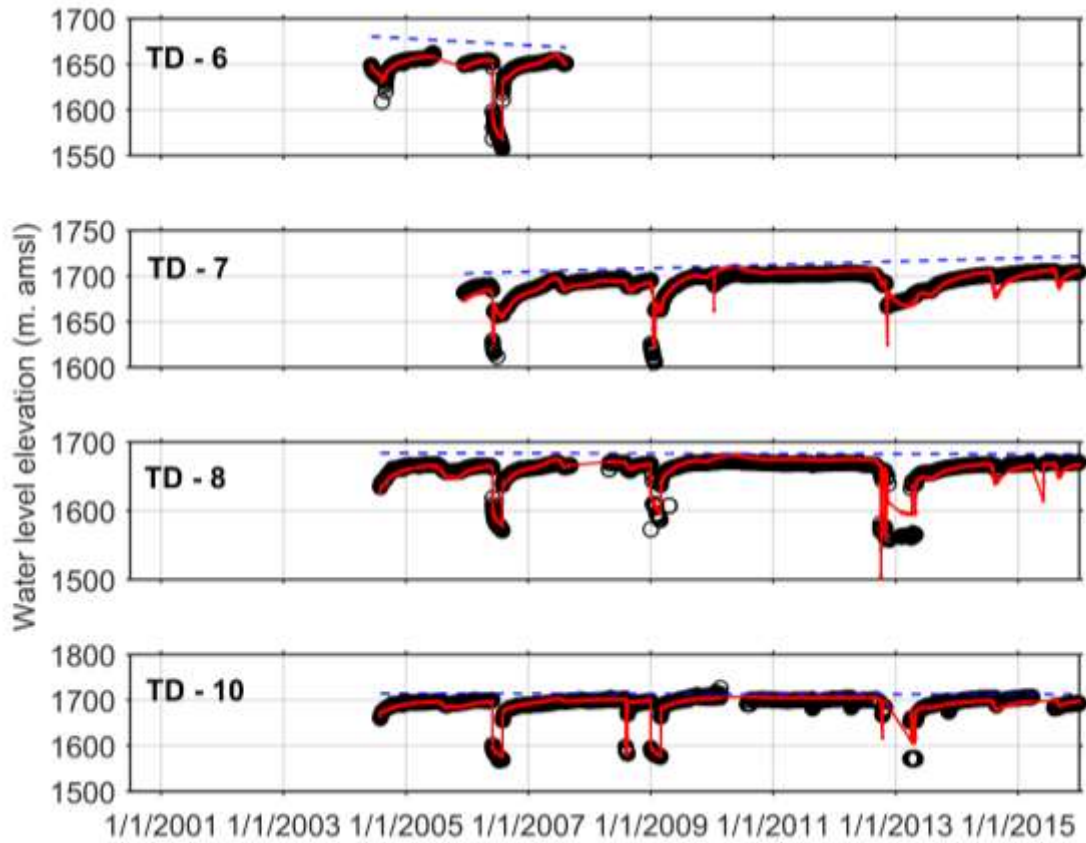


Fig. A4

Observed (black) and modeled (red) water levels and apparent recoverable water level (blue) for representative wells at the Denver Aquifer.

Arapahoe

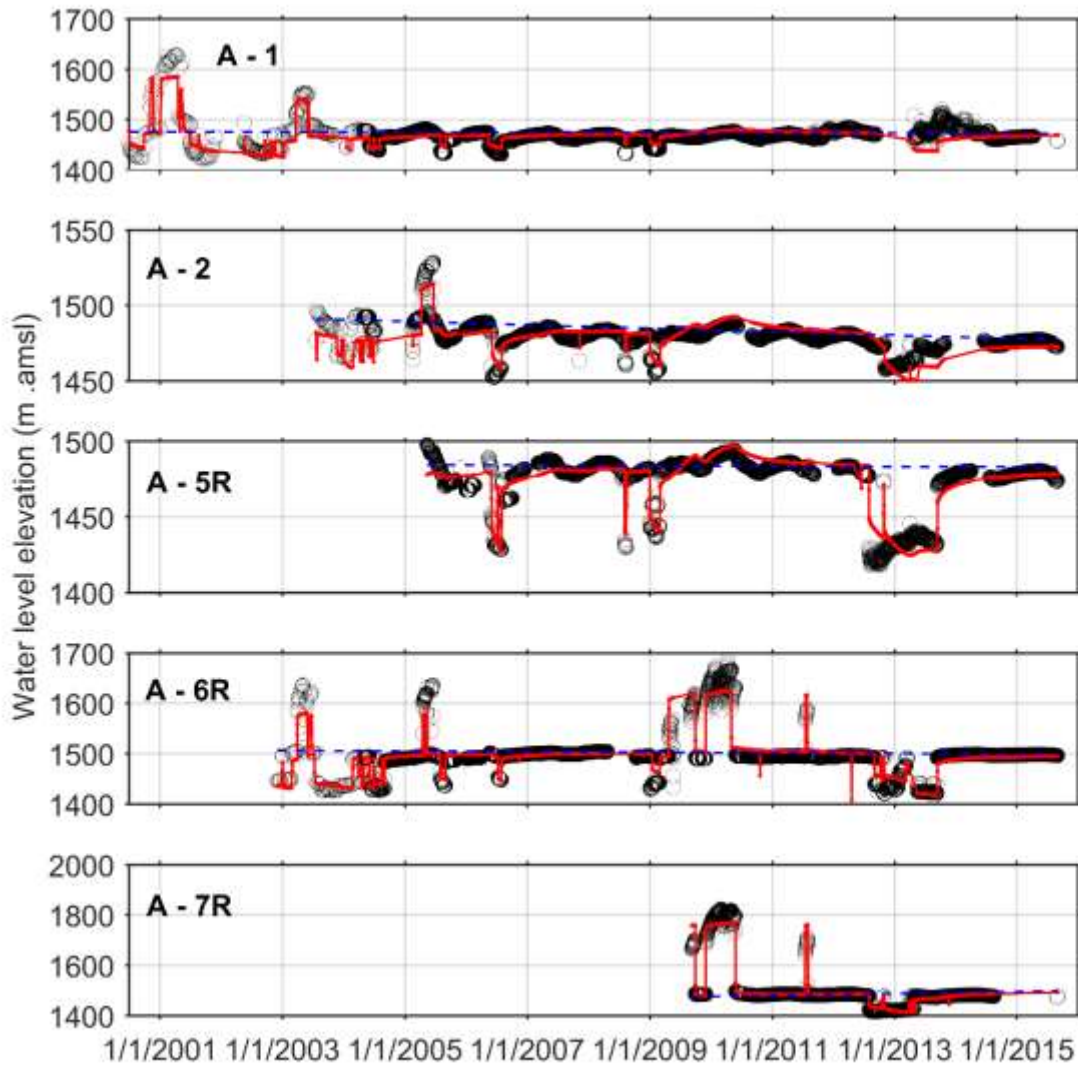


Fig. A5

Observed (black) and modeled (red) water levels and apparent recoverable water level (blue) for representative wells at the Arapahoe Aquifer.

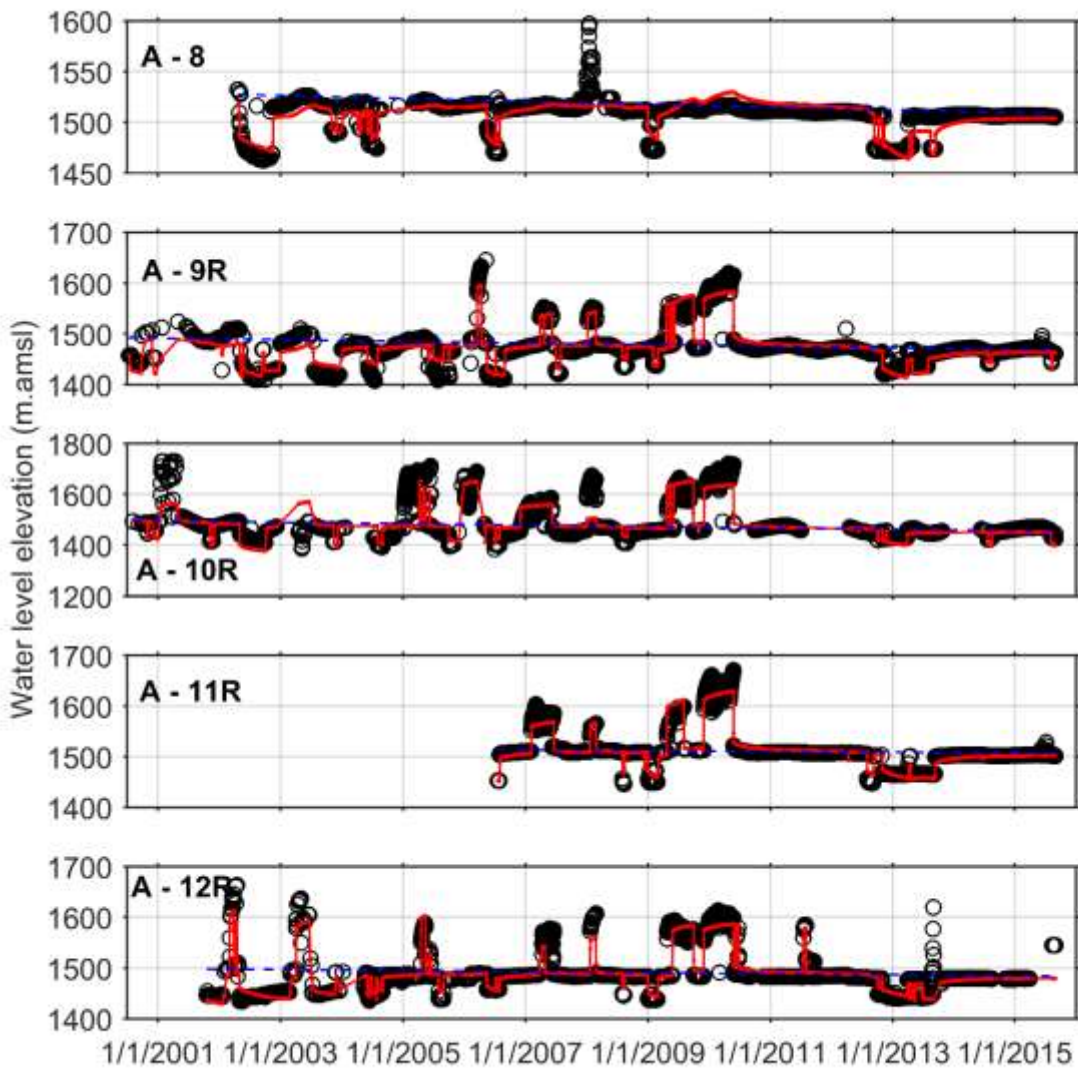


Fig. A6

Observed (black) and modeled (red) water levels and apparent recoverable water level (blue) for representative wells at the Arapahoe Aquifer.

Laramie-Fox Hills

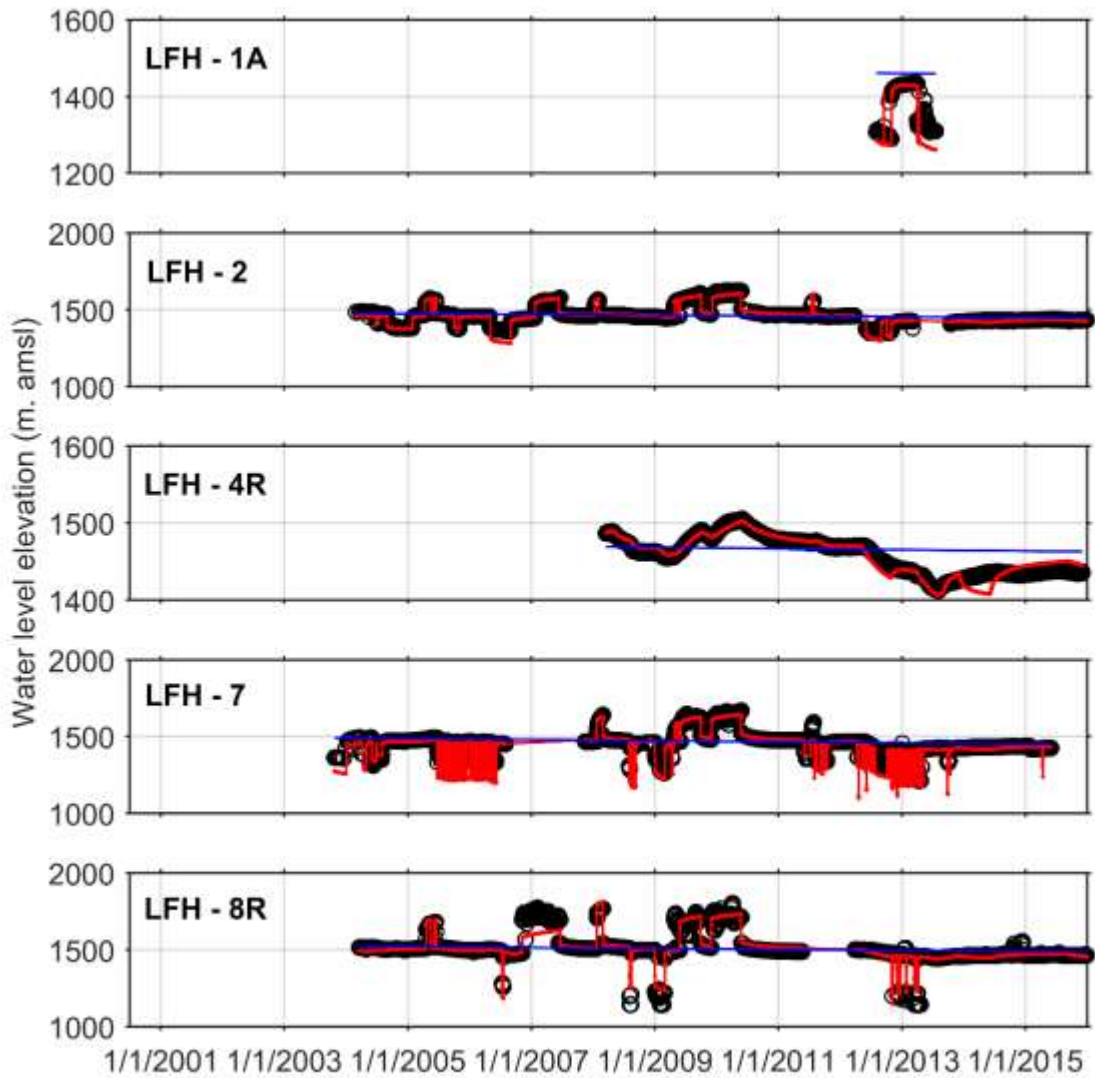


Fig. A7

Observed (black) and modeled (red) water levels and apparent recoverable water level (blue) for representative wells at the Larimer Fox-Hills Aquifer.

R² and NSCE values for the Denver and Arapahoe Aquifer wells

Table A4

Nash-Sutcliffe efficiency (NSCE) for Denver Aquifer wells

	NSCE
D4	-0.56
D8	0.61
D9	0.75
D10A	0.91
D11	0.81
D12R	0.90
D13	0.90
D14	0.94
D15	0.83
D16	0.50
D17	0.94
D18	0.95
D19	0.93
D20	0.93
TD5	0.90
TD6	0.97
TD7	0.75
TD8	0.82
TD10	0.91

Table A5

Nash-Sutcliffe efficiency (NSCE) for Arapahoe Aquifer wells

	NSCE
A1	0.47
A2	0.56
A3	0.68
A5	0.87
A6	0.79
A7	0.97
A8	0.61
A9	0.89
A10	0.64
A11	0.92
A12	0.81
A13	0.79

Absolut Value Error (AVE):

AVE is the mean of absolute difference between measured and modeled values and can be calculated as

$$AVE = \frac{\sum_{i=1}^n |O_i - M_i|}{n}$$

where O is the observed value, M is the modeled value and n is the number of points simulated.

Nash–Sutcliffe model efficiency coefficient (NSCE):

NSCE is a statistical technique that is used to measure the predictive power of hydrological models and can be calculated as

$$NSCE = 1 - \frac{\sum_{i=1}^n (M_i - O_i)^2}{\sum_{i=1}^n (O_i - \bar{O}_i)^2}$$

where O is the observed value, M is the modeled value, n is the number of points simulated, and \bar{O}_i is the mean of observed values.

Root Mean Square Error (RMSE):

RMSE is a standard deviation of residuals and can be calculated as

$$RMSE = \sqrt{\frac{\sum_{i=1}^n (O_i - M_i)^2}{n}}$$

where O is the observed value, M is the modeled value and n is the number of points simulated.